STHENURUS (MACROPODIDAE: MARSUPIALIA) FROM THE PLEISTOCENE OF LAKE CALLABONNA, SOUTH AUSTRALIA

RODERICK T. WELLS AND RICHARD H. TEDFORD

BULLETIN
OF THE
AMERICAN MUSEUM OF NATURAL HISTORY
NUMBER 225 NEW YORK : 1995

Recent issues of the *Bulletin* may be purchased from the Museum. Lists of back issues of the *Bulletin, Novitates,* and *Anthropological Papers* published during the last five years are available free of charge. Address orders to: American Museum of Natural History Library, Department D, Central Park West at 79th St., New York, New York 10024. TEL: (212) 769-5545. FAX: (212) 769-5009. E-MAIL: scipubs@amnh.org

STHENURUS (MACROPODIDAE: MARSUPIALIA) FROM THE PLEISTOCENE OF LAKE CALLABONNA, SOUTH AUSTRALIA

RODERICK T. WELLS
Department of Biology
Flinders University
Adelaide, South Australia

RICHARD H. TEDFORD
Chairman and Curator
Department of Vertebrate Paleontology
American Museum of Natural History

BULLETIN OF THE AMERICAN MUSEUM OF NATURAL HISTORY
Number 225, 112 pages, 36 figures, 27 tables, 1 appendix
Issued May 19, 1995
Price: $12.50 a copy

ISSN 0003-0090

CONTENTS

ABSTRACT

This study of the skeletal remains of three species of the extinct kangaroo *Sthenurus* (Sthenurinae: Macropodidae) from Lake Callabonna, northern South Australia, details the comparative osteology of these taxa and their functional, anatomical, and phylogenetic implications. Geological study of the locality assigns these fossils to the base of the Quaternary sequence in laminated clay and fine sands that are part of a unit correlated with the Millyera Formation of the Lake Frome area immediately south of Lake Callabonna. These deposits accumulated in a lake of variable salinity, several times the size of the present Callabonna playa. The plant remains associated with the Callabonna Fauna suggest a more arborescent flora than that near the present-day salina but one containing taxa that still exist in the surrounding region. These facts indicate a seasonal climate with fluctuating water table but a regionally more effective rainfall than at present. Direct C^{14} dating of wood from the *Sthenurus*-bearing deposits establishes an age beyond the limit of the radiocarbon method and regional geological correlations suggest a medial Pleistocene age within the span 0.2–0.7 Ma as most likely for the sthenurine kangaroos and associated large marsupials and ratite birds that constitute the Callabonna Fauna.

Like the other large-bodied vertebrates at Lake Callabonna, the *Sthenurus* species were mired in the clays while attempting to cross the floor of the lake during low-water or dry times. This mode of accumulation has yielded an unprecedented opportunity for comparative study of the remains of individual animals. Three closely allied sthenurine species coexisted at Lake Callabonna: a new giant taxon, *Sthenurus stirlingi,* a somewhat smaller *S. tindalei,* and the considerably smaller *S. andersoni.* Strong sexual dimorphism is shown by the larger taxa, resulting in size overlap between individuals, but morphological criteria identify the sexes and taxa involved. Comparative osteology of these *Sthenurus* species with *Macropus giganteus* emphasizes how different they are from the living gray kangaroo, especially in their short, deep skulls, long front feet with very reduced lateral digits, and the virtually monodactyl hind feet. These distinctions, and many others, limit functional analysis for lack of a closely comparable living model. We have nevertheless tried to gather the evidence into a coherent picture of *Sthenurus* as a living animal. The cheek teeth of these *Sthenurus* species fit the browsing grade of Sanson's (1978) model. The slender forelimbs are better fitted for feeding than locomotor function. These limbs could be raised above the head, and the hands, with their long phalanges and claws, could have grasped high vegetation. The vertebral column is more rigid than in living kangaroos and flexion is limited, but considerable extension of the anterior part of the body could have been retained as an important function in reaching for high browse. The pelvis is modified for flexion and adduction of the thigh, which would support a bulky animal while standing or elevating the body. The hind limb is more massive than in *Macropus,* but the elements are of similar proportion and there appears to be greater emphasis on the elastic properties of the tendons and ligaments to augment muscular action across joints, especially the knee and plantar parts of the pes. We conclude that species of *Sthenurus,* like other sthenurines, were bulky, browsing kangaroos that sacrificed quadrupedal or pentapedal movement for greater dependence on bipedal saltation and extension of the body and forelimbs for higher browsing. This diverse subfamily was a prominent element in Pleistocene faunas in Australia. Several taxa of comparable size were often found together which suggests partitioning of the browsing feeding mode—a broad niche that seems to contain few adherents among living large kangaroos.

INTRODUCTION

The "veritable necropolis of gigantic extinct marsupials and birds" (Stirling, 1894: 185) discovered in 1893 at Lake Callabonna, South Australia, represents a unique accumulation in Pleistocene lacustrine deposits (figs. 1, 2). The articulated skeletons of thousands of individual animals are scattered over much of the 50 km^2 of the present-day saltpan. The history of the discovery and exploration of this area is contained in the narratives of the five expeditions to Lake Callabonna over the past 100 years (Stirling, 1894 [reprinted with modification, 1900]; Brown, 1894; Fletcher, 1948; Stirton, 1954; Tedford, 1973; Rich, 1984). Only two of these parties made extensive collections: the original South Australian Museum work extending over 11 months in 1893, and nearly 80 years later in 1970, a joint Smithsonian Institution, American Museum of Natural History, and South

Australian Museum expedition (acronym: SIAM) spent 3 months working in the area. Although all parties secured remains of *Diprotodon,* the most common marsupial entombed, only the more protracted work collected other forms in any quantity. The results of the 1893 expedition enabled Stirling, with A. H. C. Zietz's assistance, to prepare descriptions of the previously unknown manus and pes of *Diprotodon* (1899), and to describe for the first time the dromornithid bird *Genyornis newtoni* (1900, 1905; Stirling, 1913a) and the skeleton of the giant wombat, *Phascolonus gigas* (Stirling, 1913b). The only other elements of the vertebrate fauna obtained in 1893 were remains of kangaroos that Stirling had hoped to delineate in a monograph following the publication on *Phascolonus.* He remarked that (of the kangaroos) "we have one small but very complete skeleton, and a large series of separate bones of several larger kinds, including a fairly complete skull, which has a length of 33.5 cm" (1894: 209). H. Y. L. Brown (1894: 7), upon seeing the foot bones of a kangaroo in the field at Lake Callabonna in June 1893, reported that "when placed in position [they] make the length of the foot 14 in." The skull and foot mentioned in these remarks are among the materials described in this paper as the remains of the largest species of *Sthenurus* yet discovered. We take great pleasure in naming this new species for Sir E. C. Stirling. In addition to *Sthenurus,* the 1893 collections contain the limbs of a large *Macropus,* probably *M. titan.*

Examination of the published narrative and records at the South Australian Museum, matching 1893 field photos to present terrain, and discovery of the 1893 campsite have assured confident identification of the site indicated in figures 2 and 4 as the campsite and the area nearby where the party, lead by A. H. C. Zietz in late 1893, obtained most of the material. The photos also identify SIAM sites 1 and 3 (figs. 2, 3, 5) and the terrain between as the area excavated by the party led by George Hurst earlier in 1893 for the South Australian Museum. Exploratory work by the University of California–South Australian Museum party in 1953 was conducted near the campsite and at site 1. Only *Diprotodon* was secured by that group.

The Smithsonian Institution–American Museum–South Australian Museum party worked SIAM sites 1 and 3, obtaining mostly articulated *Diprotodon* material and, exploring more widely on the lake floor, finally settled on SIAM site 4 to conduct its principal work. This site, about 5 km north of site 3, yielded a varied fauna from moist claystone above the groundwater level. It may be the site noted by H. Y. L. Brown (1894: 8) as "3 miles northwest of the locality first found" by the 1893 party. Nearly all the macropodid remains collected in 1970 were obtained at this site, including all of the *Sthenurus* material described in this paper. In addition to the two *Sthenurus* species, four partial skeletons of *Protemnodon* were obtained at site 4, a genus not represented in the 1893 collections. Curiously, no remains of the large *Macropus* encountered in 1893 were obtained by the SIAM group, but a partial skeleton and some isolated remains were found of an animal the size of the living *M. giganteus,* but still not identified. *Diprotodon,* represented by two size morphs (as mentioned by Stirling and Zietz, 1899: 3) and *Phascolonus,* were also found at site 4. Emus, similar in size to the living *Dormaius novaehollandiae,* were also found by the 1970 party in addition to, and often closely associated with, skeletons of *Genyornis newtoni.* Such differences in faunal composition are most likely due to chance, as the various sites from which collections have been obtained all seem to be located below the widespread selenite bed within the Millyera Formation (see discussion below). Therefore, we list Lake Callabonna Fauna as a composite of vertebrate species currently identified from these levels:

Class Aves
- Order Casuariiformes
  - Family Casuariidae
    - *Dromaius novaehollandiae*
  - Family Dromornithidae
    - *Genyornis newtoni*

Class Mammalia
- Infraclass Marsupialia
  - Order Diprotodonta
    - Family Diprotodontidae
      - *Diprotodon australis*
      - *Diprotodon* cf. *minor*
    - Family Vombatidae
      - *Phascolonus gigas*

Family Macropodidae
Macropus cf. *titan*
Macropus sp.
Protemnodon cf. *brehus*
Sthenurus andersoni
Sthenurus tindalei
Sthenurus stirlingi

METHODS AND ABBREVIATIONS

The primary purpose of this study is to describe the *Sthenurus* material now available from Lake Callabonna. Because these materials include some of the most complete skeletal remains of the genus, representing three closely allied species, we have adopted a format in which these materials are described and compared, with emphasis on the more complete new species. *Macropus giganteus* (specifically AMNH CA2390) and, where possible, *Procoptodon goliah* from Lake Menindee (Tedford, 1967) are compared with these large *Sthenurus* species. Materials are contrasted with a large living kangaroo and with the most derived sthenurine. The format of the comparative morphology section therefore differs slightly from the usual independent treatment of taxa; that is, descriptions and comparisons are combined in one section. The illustrations are also arranged in a comparative fashion. The systematic position of these forms and their amended diagnoses are treated separately for clarity in our conclusions on phylogeny and classification.

The anatomical terminology follows conventions used in the descriptive osteology of mammals as exemplified in the description of the skeleton of *Procoptodon* in Tedford (1967) and in compendia of anatomy of such mammals as the dog (Evans and Christensen, 1979). We illustrate features of the cranial anatomy (fig. 9) used herein. For convenience in comparisons, we have retained the serial designation of cheek teeth discussed and illustrated by Tedford (1966), rather than that of Thomas (1888) or that proposed by Archer (1978). We follow Flannery (1983) in most aspects of the nomenclature of dental morphology. Measurements, in millimeters, are given in the accompanying tables. Mensural reference points are indicated in the description of each dimension.

We use the following institutional abbreviations to indicate the sources of collections contributing to this study: AMNH, American Museum of Natural History; SAM, South Australian Museum; UCMP, University of California, Museum of Paleontology. Additional abbreviations include a system of denoting wear states of cheek tooth rows developed by Tedford (1966: 4–5). Millions of years ago is abbreviated Ma; yr BP refers to before present (1950) in the radiocarbon scale.

ACKNOWLEDGMENTS

This study would not have been possible without the labors of many people involved in collecting fossil vertebrates at Lake Callabonna. We are especially grateful for the companionship and diligent work of Clayton Ray, Robert Emry, and Frank Pearce of the National Museum of Natural History, and Paul Lawson and Neville Pledge of the South Australian Museum, whose efforts under trying conditions in the field in 1970 yielded the specimens described herein. Our efforts benefitted from the hospitality of Michael Sheehan of Moolawatana Station and his companions John Akbar, John Brown, and Jack and Iris Mobbs. Equally vital to this project has been the close interaction with the scientific illustrators, Lorraine Meeker and Chester Tarka, whose superb work documents the osteology of the taxa described in a way unmatched by words. Their assistance in the scientific study of these materials is gratefully acknowledged. In addition, the maps and geological section were skillfully prepared by Ray Gooris. Mr. E. S. Booth, grandson of Sir E. C. Stirling, contributed an important suite of documents and photographs taken on the SAM expedition of 1893 that helped relocate the sites worked by the museum party in that year. His help in historical matters is greatly appreciated, as is the assistance of personnel of the South Australian Museum in our research on the history of the discovery and first exploration of the Lake Callabonna fossil deposit. We are also indebted to Professors M. O. Woodburne, University of California, Riverside, and I. Gibbins, Flinders University of South Australia, for critical review of this work.

PHYSICAL SETTING AND GEOLOGY

Lake Callabonna is one of an arcuate chain of saltpans that lie at the foot of the coalesced alluvial fans extending eastward from the northern Flinders Ranges (fig. 1). It is joined to Lake Blanche to the north by the Moppacolina Channel, and a similar channel (Salt Creek) connects it with Lake Frome to the south. Although the bed of Lake Frome lies about 3 m below sea level, flow along Salt Creek is partially impeded by the youngest beach ridge on the eastern side of Lake Frome. This ridge forms a drainage divide, which partially isolates Lake Callabonna from Lake Frome. Only at lake-full time can this channel connect the lakes. Ancient gravel bars on the western side of Lake Frome and equivalents at Lake Callabonna indicate larger coalescence of these water bodies in the geological past. Accurate elevation data are lacking for lakes Callabonna and Blanche, but the lakes form the lowest part of the northern drainage basin and their floors probably approximate sea level. Creeks draining the northeastern side of the Flinders Ranges provide most of the water that reaches these normally dry saltpans. Heavy rains are needed to cause streams, such as Callabonna and Yandama creeks, that originate in the Barrier Ranges in New South Wales to flow through the interdune valleys of the Strezlecki dunefield to Lake Callabonna. The most important of these eastern streams is Strezlecki Creek, a distributary of Cooper Creek, which empties into the southern end of Lake Blanche during high floods in the Cooper. All of these drainageways were in operation during the several years of exceptional rainfall in interior Australia beginning in 1973, when Lake Callabonna and the other lakes in the system were filled. Normally in this region of low (100–125 mm/yr) and unreliable rainfall, the chains of lakes are saltpans and the surrounding plains and dunefields support a sparse vegetation.

The present-day arid environment is thus in distinct contrast with that of the Pleistocene, when the fossiliferous lacustrine deposits were accumulating at Lake Callabonna. Callen (1977: 153) and Tedford (1980) have discussed the late Cenozoic environment of this region and have correlated the fossiliferous deposits at Lake Callabonna with the Millyera Formation of Callen and Tedford (1976), which has its type section southeast of Lake Frome. This and other correlations of the Callabonna section with that in Lake Frome are discussed below.

STRATIGRAPHY

The stratigraphic record of Lake Callabonna is widely scattered among outcrops on the present saltpan floor and periphery. It has thus been difficult to relate the various facies distributed between lacustrine, fluviatile, strandline, and alluvial environments. The reconstructed cross section (fig. 4) correlates elevation data obtained by aneroid barometer with a series of measured sections that follows a northeast traverse across the central part of the saltpan shown on the geological map (fig. 2). This reconnaissance geological study of part of Lake Callabonna recognizes six major stratigraphic units exposed on the saltpan floor and immediate periphery.

The oldest unit exposed in the vicinity of Lake Callabonna crops out at the base of the escarpment 6 km southwest of the lake margin (northwestern part of the map area, fig. 2). These deposits are well-sorted, medium-grained, micaceous quartz sandstones with interbedded siltstones and claystones. The sandstones are thin to laminar-bedded and cross-strata are common. They have been stained and cemented with iron oxide. They contain silicified logs up to a meter in length and leaf impressions of angiosperms. Many approximately north–south faults cut these deposits, and drag folds are common superposed on a sequence that in general dips eastward at a moderate angle. We correlate these beds with the Eyre Formation of Wopfner et al. (1974), and although the sandstones are more persistently micaceous than seen in many Eyre Formation outcrops, such lithologies are recorded elsewhere in the basin. Seven kilometers to the northwest of this outcrop, a stratigraphic bore put down during the Mines Administration Pty. Ltd. exploration of uranium resources in the Callabonna Basin encountered over 100 ft of ferruginous sandy claystones with interbedded

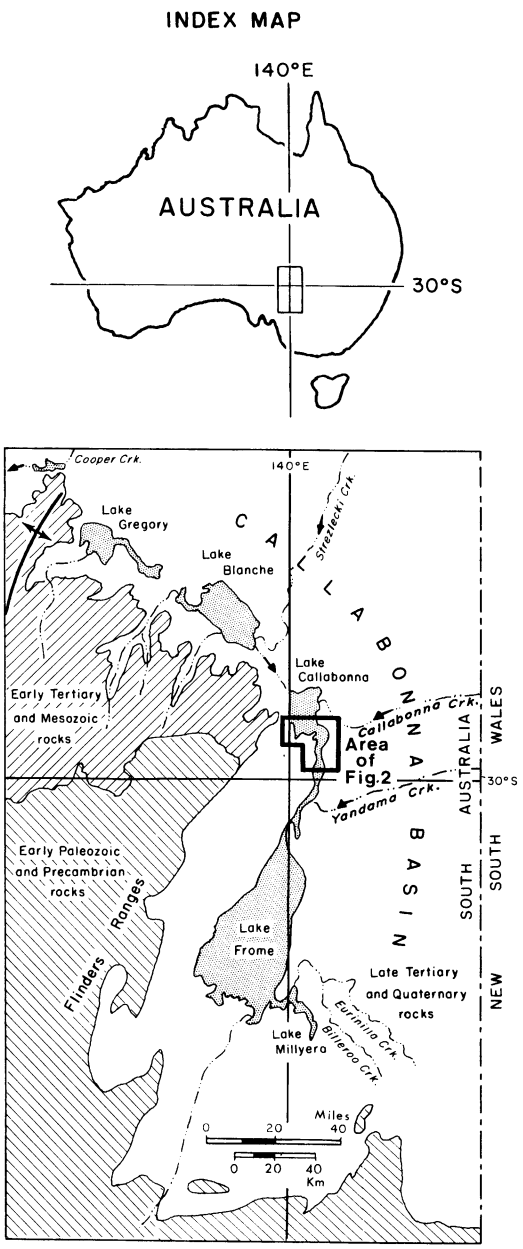

Fig. 1. Map showing the relationship of the study area of Lake Callabonna within the Australian continent and geographic features mentioned in the text. Lake Callabonna is one of an arcuate chain of salt pans that lie near sea level along the western side of the late Cenozoic Callabonna Basin in South Australia. These lakes are flanked by alluvium from the Flinders Ranges, whose elevations range from 500 to 3500 ft. To the north, a low divide formed by gently folded early Tertiary and Mesozoic rocks separates the Callabonna Basin from the Lake Eyre Basin. Cooper Creek breached this divide (shown in the northwest corner of the map) during the Pleistocene and entered the Lake Eyre Basin.

lignite that represent a finer-grained facies of the Eyre Formation. Contours drawn on the base of Eyre Formation that are taken from data obtained during the same exploratory work indicate thicknesses in excess of 165 m for the Eyre Formation in this area (Wopfner et al., 1974).

Unconformably overlying the Eyre Formation along the escarpment mentioned above are flat-lying sandstones and siltstones that lie on an erosion surface of 17 m or more of relief. The coarse sandstones have gritty textures and contain subangular polished quartz and claystone pebbles cemented with black iron oxide. These cross-stratified stream channel fills are interbedded with white-to-pink siltstones and finer sandstones containing ironstone nodules. At the top of the 23 m section of these rocks, white siltstone and fine sandstones bearing ironstone nodules are cemented with opaline or chalcedonic silica in large concretionary masses to form a silcrete that has been brecciated and recemented in places. These outcrops represent the fluviatile facies of the basal Namba Formation (Callen and Tedford, 1976). In the nearby Mines Administration bore mentioned of above, the Namba Formation is 30 m thick and is capped by opaline silcrete. The sequence encountered there includes medium-to-coarse quartz sands with polished grains interbedded with dark gray claystones.

In the escarpment section, the channel-filling sands grade laterally to black claystones with alunite(?) nodules. Similar rocks crop out on the floor of Lake Callabonna near site 4 (fig. 2), where they consist of black claystones with alunite(?) nodules, purple-weathering, dark gray, agrillaceous fine sandstone, and local channel-form bodies of well-sorted, medium-grained quartz sandstone with subrounded, polished grains frequently cemented with silica. Such rocks also crop out beneath the gravel bars on the western side of the lake and at shallow depth (2 m) between the gravel bars to the south. Aerial photo-

graphs of the northern part of the lake suggest a large area of outcrop of dark Namba Formation claystones on the floor of the deepest part of the saltpan.

On the western side of the lake, a few meters of red and green mottled claystones crop out beneath the older alluvium and overlying oldest gravel bar. Seven kilometers to the south, similar rocks form the upper 12 m of an east-facing gypcrete-capped escarpment. There they rest on gently west-dipping silicified and ferruginized Namba Formation. North of this outcrop, at the top of the escarpment referred to above, a few meters of carbonate-cemented gravels strongly cemented with gypsum may represent a correlative unit. These rocks are referred to the Willawortina Formation of Callen and Tedford (1976).

Within the perimeter of the lake, the Namba Formation is disconformably overlain by fine sands and laminated clays that constitute the *Diprotodon*-bearing unit, which is provisionally attributed to the Millyera Formation (sensu Callen and Tedford, 1976, including the Coomb Spring Formation of Callen, 1984). Where the contact can be seen near site 4 (fig. 2) on the eastern side of the lake, the basal Millyera Formation is a ferruginous fine sand containing black claystone clasts and quartz pebbles derived from the underlying Namba Formation. These basal sands may be greater than 2 m thick and contain lenses of greenish claystone that increase in frequency until claystone dominates the upper part of the section in which the fossil remains are found. Claystones form the upper 5 m of the Millyera Formation of the lake basin we have studied. The most fossiliferous interval, however, constitutes only the lower 2 m of this argillaceous member, which is overlain by a bed of large selenite crystals that crops out as a widely traceable, resistant unit that forms broad benches bordered by low erosional scarps (fig. 5). Laminated claystone alternating with laminae of fine sand characterize the fossiliferous unit, especially at site 4, where these beds form cyclic couplets of a few centimeters in thickness. Gypsum, in the form of small discoidal or "millet-seed" (Bowler and Teller, 1986) crystals, is abundant in these deposits, particularly in the sand laminae.

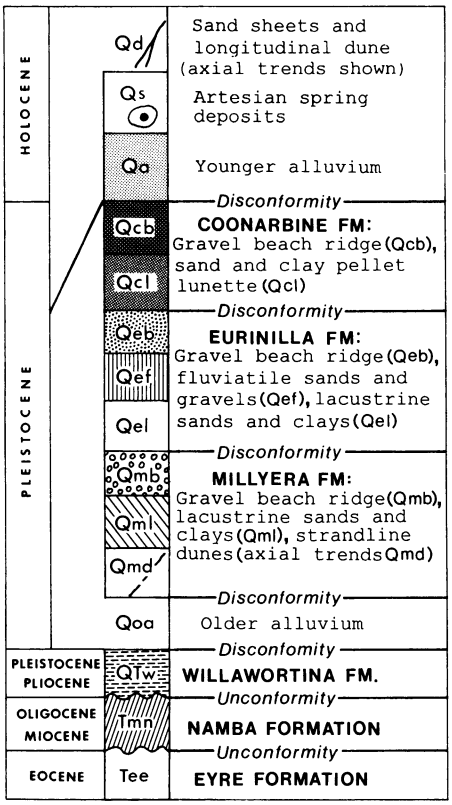

Fig. 2. Legend.

At site 4, the sand laminae, where etched out by deflation on the lake floor, show current ripples, desiccation polygons, and mammal trackways. Excavations revealed the extent to which these deposits have been deformed by the movement of heavy-bodied animals across wet sediments (fig. 6). Deformation of the sand and clay laminae through such bioturbation is common, and, in places, amounts to homogenization of an originally bedded sequence. This is exhibited in dramatic fashion in the proximity of the *Diprotodon* skeletons, where the animals churned the entrapping clays in their futile efforts to free themselves. Thin silty limestone or travertine lenses, often mudcracked, are also interbedded with the laminated clays. Trackways preserved in limestones were our first recognition of the presence of these unusual features (Tedford, 1973: fig on p. 349). Small fish (including articulated remains at site 1),

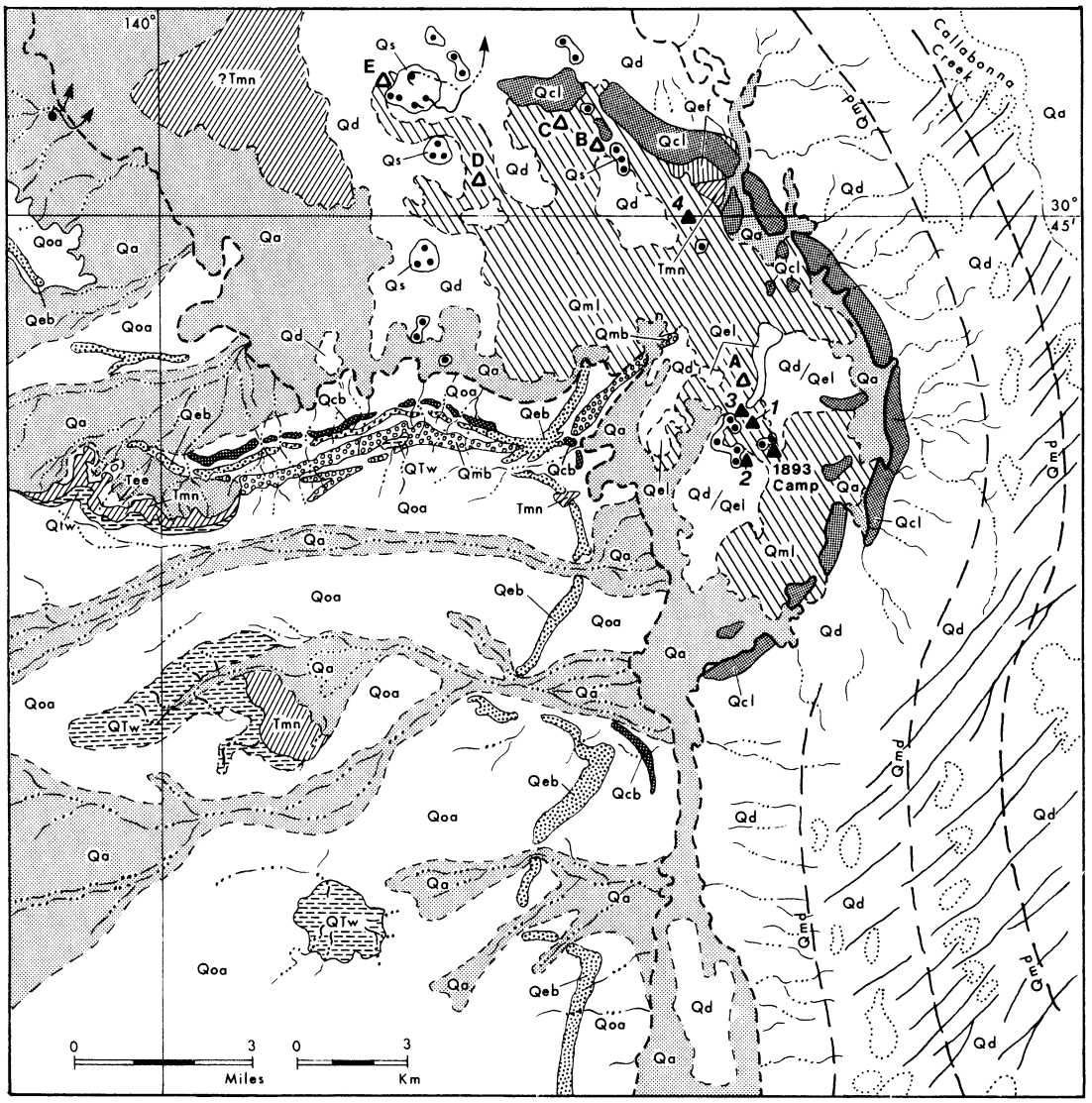

Fig. 2. Geological map of a part of Lake Callabonna and vicinity showing geologic and geomorphic units. The map was prepared from an enlargement of the Callabonna 4-mile sheet (1:250,000, SH54-6 Provisional Edition, Div. Nat. Mapping, Canberra, series R502, 1965) and the geology mapped by ground observation, aerial reconnaissance and photographs, and Landsat images. Numbered solid triangles indicate SIAM sites from which collections were secured; lettered open triangles indicate sites referred to in the Appendix.

gastropods (*Coxielladda*), beetle wing cases, ostracods, charophytes, abundant wood, twigs, *Callitris* cones, and pollen occur in the laminated deposits. Most of these remains occur below the selenite bed, but at site 3 and locality E, *Diprotodon* and other taxa were found in laminated clays above this unit.

We attributed the deeply dissected highest strandline gravel and sands exposed on the western shore of Lake Callabonna to the Millyera Formation. They also appear to form the eastern spit, where they extend into the lake and rest on the Millyera lacustrine deposits. These gravel bars are composed mostly of silcrete and quartz clasts in coarse sand that contains shells of *Coxielladda*. If these

Fig. 3. Aerial view looking south toward SIAM site 3 (at curve in the vehicle track at the left side of the view) and site 1. SIAM site 2 is just off the right edge of view in the middle distance. In 1893, fossils were collected within the area of white saline efflorescence between SIAM sites 1 and 3.

gravels approximate the highest shoreline of the Millyera Lake, the lake may have extended eastward to at least the 10 m contour. This would place the shoreline at about the limit of the well-defined arcuate claypan alignments that delimit the strandline dune system (see Landsat photos in Löffler and Sullivan, 1979: pl. 1; Callen, 1977: fig. 7).

In several places the older alluvium crops out beneath these high beach deposits. It is clear that the latter are derived from the alluvium. A calcareous paleosol is preserved at the top of the older alluvium in some places. Along the western margin of the lake, the older alluvium rests on the black claystones of the Namba Formation and consists of a basal gravel and sand with a red-brown clay matrix overlain by pebbly green-gray claystones that may grade laterally into the Millyera lacustrine deposits.

Disconformably overlying the Millyera Formation are fluviatile and lacustrine facies referred to the Eurinilla Formation, whose type section is also in the southern Lake Frome area (Callen and Tedford, 1976: fig. 1). Within the present lake basin, the Eurinilla Formation is represented by greenish-gray sandy clays, usually with a pebbly sand at the base that may be carbonate-cemented and may contain molluscs (*Coxielladda* at site 2). Clasts in these basal sands include quartz and travertine pebbles, as well as rounded fragments of bones and teeth (*Diprotodon* and *Protemnodon* could be identified). The sandy clays composing this facies are thin-bedded and are locally rich in charophytes and *Coxielladda*. Small rosettes of gypsum occur at various horizons, but are most abundant toward the top, where the rosettes may be concentrated, and platy gypsum is also present. At site 3 and vicinity, this gypcrete is overlain by a meter or two of loose pebbly sands bearing clasts of travertine, quartz, silcrete, dark rock fragments, jasper, and bone and eggshell fragments. We did not find autochthonous fossil vertebrates in this unit at Lake Callabonna, but Eurinilla Formation deposits in the Billeroo Creek drain-

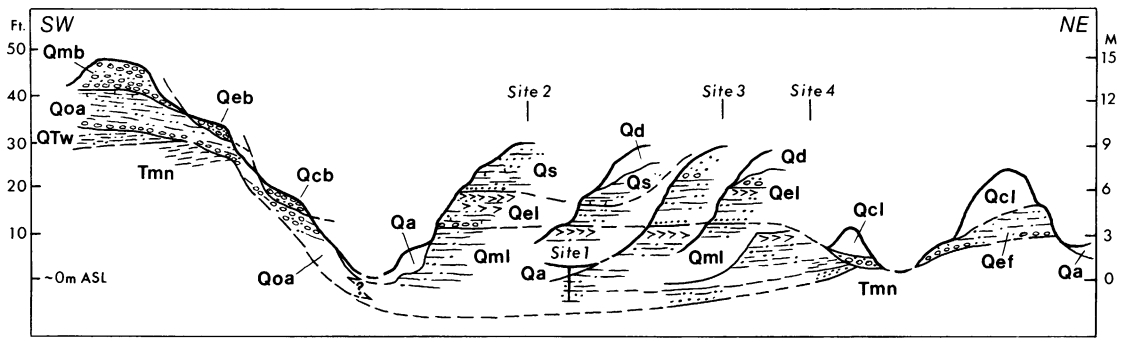

Fig. 4. Correlated columnar sections extend from the gravel beach ridge complex on the southwest shore of Lake Callabonna (left) eastward to sites 2 and 3 (fig. 2) and site 4 and the adjacent northern shore of the lake. Relative elevations were established by aneroid barometer (precision ± 2 m). Symbols are as defined in figure 2. Gypsum-indurated horizons are indicated by horizontal V, calcrete by inverted T, and travertine by the conventional symbol for limestone.

age, southeast of Lake Frome (fig. 1), have produced a Pleistocene fauna (Callen and Tedford, 1976; Williams, 1980) containing some of the taxa recorded from the Lake Callabonna Fauna, including *Sthenurus stirlingi.*

In the northern part of the mapped area, north of site 4, pebbly coarse sands cut into the Namba and Millyera formations represent a paleochannel fill. These deposits contain only silcrete, quartz, and quartzite clasts

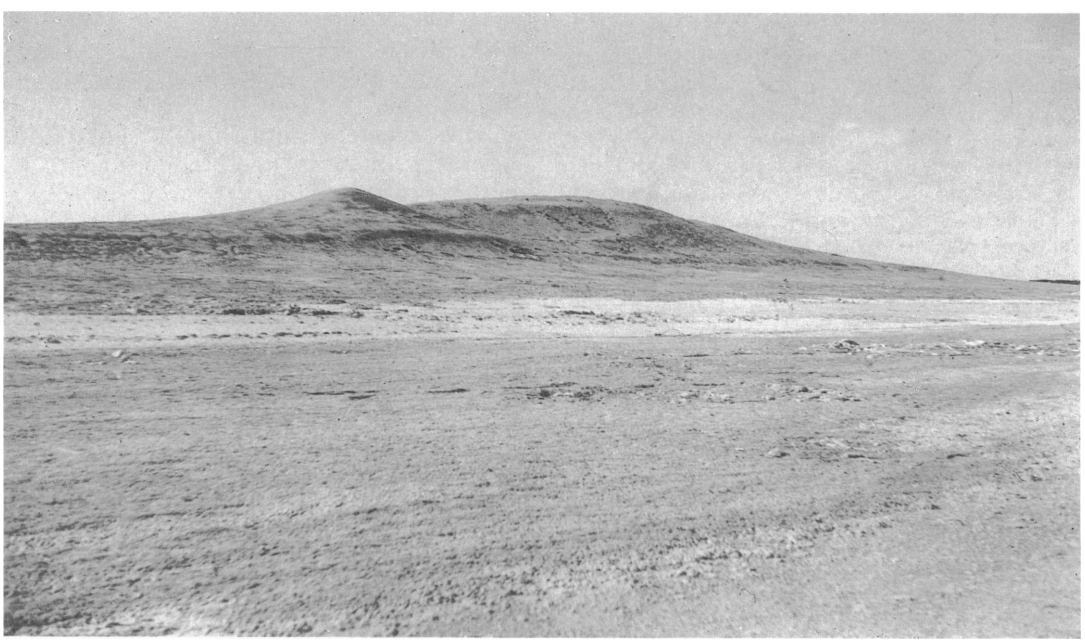

Fig. 5. View looking southeast at the bluff at SIAM site 3 in 1953. *Diprotodon* skeletons covered by saline efflorescence on the lake floor are at right of view. This is part of the area worked by the Hurst brothers early in 1893. The selenite unit within the Millyera Formation supports the bench at the left. The contact with the Eurinilla Formation is just above this level, and the latter unit forms the remainder of the hill (see diagrammatic section, fig. 4).

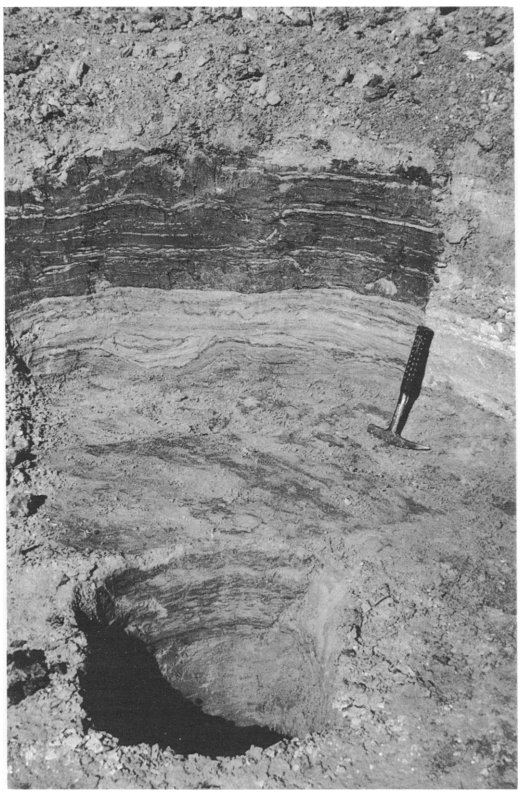

Fig. 6. Cross section of lower part of Millyera Formation at SIAM site 4 from which SIAM 50 (*Phascolonus gigas* partial skeleton) was obtained. Fossils were obtained from the laminated clays above the hammer handle (hammer 33 cm long). The laminated sands below clays are unfossiliferous and rest on black Namba Formation claystone (hand samples deposited to left of the pit). Note the contorted stratification, most of which represents vertebrate foot prints seen in cross section.

representing mature debris from the eastern side of the basin. The channel sands give way upward to gypsiferous, thin-bedded fine sands and clays of the lacustrine facies of the Eurinilla Formation. We also attribute to the Eurinilla Formation the higher of the two well-preserved gravel bars that skirt the western side of Lake Callabonna and extend discontinuously south to Lake Frome. At Lake Callabonna, these bars form the western gravel spits that extend to the lake floor, where they overlie the older alluvium. These gravels are composed mainly of silcrete, quartz, and dark metamorphic and plutonic rock clasts in very coarse sand matrix derived from the older alluvium on which these beach deposits rest. They lack molluscs and have no paleosols imposed on them. They correspond in elevation to a terrace cut across the flank of the Millyera strandline dune on the southeastern side of Lake Callabonna.

Equivalents of the Coonarbine Formation of the Lake Frome region (Callen and Tedford, 1976) are the youngest lacustrine deposits preserved within the Callabonna lake basin. They rest on the deeply dissected older Pleistocene deposits and include, as at Lake Frome, mainly strandline, aeolian, and artesian spring facies. We have not been able to separate a lacustrine facies from those deposited during the Holocene. The Coonarbine lake was confined to the limits of Holocene Lake Callabonna. Well-preserved beach-ridge gravels associated with this episode form the lowest tier of strandline deposits on the western side of the lake. They are composed of abundant milky quartz, silcrete, and dark metamorphic and plutonic rocks in a very coarse sand matrix. Green-gray clay lenses are present. No paleosols were developed on these beach ridges. The ridges correspond in elevation with the lowest terrace surface imposed on the Millyera strandline dunes on the southeastern side of Lake Callabonna.

The arcuate eastern shore of Lake Callabonna is rimmed by an eroded lunette. The easternmost, and more continuous, line of dunes is formed of cross-bedded tan sands. A lower clay pellet and quartz sand dune forms the discontinuous innermost lunette remnant. Part of the blanket of tan sands on the floor and perimeter of Lake Callabonna may have been initiated during deposition in the Coonarbine Formation and reworked into younger land forms.

Natural artesian mound spring deposits are a prominent feature on the floor of Lake Callabonna. Older mounds larger than those still active are found within the linear trends of the active mounds. Near site 2 and locality E, these extinct mounds intrude the Millyera and Eurinilla formations. The latter deposits in turn include travertine beds that indicate a long history of spring activity. These older mounds imply greater discharge than the active springs and may correspond with the Coonarbine lacustrine episode.

The deep dissection of the lake floor prior to deposition of the Coonarbine Formation was most likely accomplished by deflation, as there are limited avenues for effective transport of sediments from the basin by fluviatile means. We equate this major deflation with the erosion of the Millyera strandline dunes and the formation of the sief dune system so conspicuous in the present landscape.

Holocene deposits at site 2 include brown argillaceous sands or sandy clays lacking gypsum nodules. These are interbedded with thin travertine and intruded by natural artesian spring heads. The springs built silty clay mounds with travertine carapaces. Mound springs are abundant at Callabonna, as shown on figure 2, and most represent Holocene phenomena. At site 2 a cormorant nesting site was found in which bird skeletons, eggs, guano, and fish remains occurred in silty sands interbedded with travertine from a nearby extinct spring head. In more recent times, red-brown sandy clays and gravel deltas have been deposited on the lake floor from the streams on the western side of the basin. These clays, and the abundant *Coxielladda* contained in them, are now being reworked into red-brown clay pellet dunes near site 3.

STRUCTURE

The Quaternary succession at Lake Callabonna is flat-lying and displays no obvious structural deformation. Alignments of mound springs in the area mapped (fig. 2) suggest control by fractures reaching the artesian aquifers beneath the lake. No displacements of the Quaternary section could be detected on the lake floor. A major northerly oriented chain of prominent springs extends through the middle of the lake at the western edge of the mapped area, and the springs at sites 1–4 and to the north seem to indicate a northwesterly trend. These alignments are more or less in agreement with the trend of structural lineaments mapped by Firman (1974) for this part of South Australia.

Tertiary rocks exposed in escarpments southwest of Lake Callabonna indicate significant faulting and associated folding of the Eocene Eyre Formation and the less severe deformation of the unconformably overlying late Oligocene or early Miocene Namba Formation. Structures in the Eyre Formation seem to have approximately north–south orientations in accord with the trend of the central mound-spring system of the lake. Western dips in the Namba Formation appear to reflect local events (perhaps drag folding associated with faulting) that cut across the regional eastward dip into the Callabonna Basin.

GEOLOGICAL HISTORY

A remarkable aspect of the Quaternary lacustrine sequence in the Lake Callabonna area is that it is so thin. We record 10 m near sites 1–3 (fig. 4), and the maximum may not exceed this thickness by very much. This is surprising in that Lake Callabonna is the focus of an important part of the present drainage of the central Lake Frome region. Much of the Quaternary history of the area is probably represented by the disconformities that break the stratigraphic column. The sedimentary succession preserved has been correlated with that worked out for the Lake Frome area by Callen and Tedford (1976). The sedimentary environments delineated by those authors and later reviewed for the Millyera Formation and other units by Callen (1977, 1984) are broadly those indicated by the evidence at Lake Callabonna.

The Millyera Formation was deposited in a lake basin that probably extended much farther east than the present confines of Lake Callabonna. The presence of older Cenozoic rocks along the western shore of the present saltpan and a beach ridge attributed to the Millyera lake suggests that the western boundary of this lake basin is approximated by the modern shoreline. The Millyera Formation exposed on the present lake floor represents quiet-water lacustrine and marginal lacustrine facies, with the basal sands implying shallower water than the succession of argillaceous sediments that follow. Cyclic, thin couplets of rippled fine sand and laminated clays within the lower part of the more argillaceous member reflect episodic deposition. This can be related to changes in water level in the lake. Longer periods of higher water tables are represented by laminated clays. These periods alternate with shorter intervals of shallow water, which are indi-

cated by ripple-marked fine sands or dry surface conditions that occurred with deposition of interstitial evaporites and drying and cracking of surface deposits. A more protracted deep lake phase is indicated by the widespread unit of large twinned selenite crystals that punctuates the lacustrine facies of the Millyera Formation. Abundant trackways also indicate that the lake floor was occasionally dry enough to be crossed by large marsupials and birds. Salinity-tolerant gastropods, ostracods, and charophytes plus interstitial displacive gypsum and salt also indicate that the waters of this Millyera lake were saline much of the time. Abundant plant macrofossils contained in these sediments, however, suggest a climate with more rainfall than occurs presently. In addition to the native pine cones (*Callitris*) noted by Stirling (1894) and ourselves, Dr. G. Singh (Department of Biogeography and Geomorphology, Australian National University, personal commun. 1972) examined the pollens from clays surrounding a eucalypt branch used for radiocarbon determination (I-5479, Buckley, 1973, date beyond the range of the radiocarbon). His preliminary identifications from this single sample suggest a somewhat richer flora for the surrounding area during deposition of the Millyera Formation. Tentative assessment of the vegetation includes a saltbush-dominated savanna with scattered wattle, she-oak, and native pine crossed by eucalpyt-lined water courses. Such a flora would require a somewhat higher precipitation and/or lower evaporation rate than is present in the Lake Callabonna area today. These results agree with the geological indications of a mostly positive water balance broken spasmodically by more arid intervals.

Association of the highest gravel bar on the western side of the lake with the Millyera Formation implies the presence of a large lake that would have extended eastward to near the limit of the strandline dunes, which are marked by aligned claypan chains in the Strezlecki Desert. The regression of the Millyera lake is marked by these strandlines. A final stage in this drying is probably represented by the depth of incision of stream courses entering the lake from the east. Much of the upper part of the Millyera Formation must have been removed by such fluviatile scour and deflation prior to the Eurinilla phase of deposition.

If we have properly associated the suite of facies with the Eurinilla Formation, it represents the return to deeper water lacustrine conditions in a somewhat more permanent system localized within the perimeter of the present lake. A sand- and gravel-filled shallow stream course on the eastern side of the basin represents the early phase of filling of the Eurinilla lake. This may represent part of the history of Callabonna Creek as it worked its way through the transverse dunes during the regression of the Millyera lake. There are few evaporites in the Eurinilla Formation except the small gypsum rosettes and plates. These are especially frequent near the top of the section. However, the lack of an aquatic fauna beyond the eurytopic *Coxielladda* suggests that the lake waters were not fresh enough to support a diverse molluscan assemblage. The gravel bar (fig. 2) developed on the older alluvium on the western side of the basin records a high stand of this lake and corresponds to a terrace cut into the Millyera strandline dune, which limits the basin to the east.

The sands and gravels that cap the Eurinilla Formation outcrops on the lake floor may represent fluviatile deposits spread across the floor of the drying Eurinilla lake. Subsequent to this event, deep dissection of the lacustrine deposits took place. Most of the Eurinilla Formation was removed, as was at least half the Millyera Formation. Much of this denudation was undoubtedly accomplished by aeolian activity, but part may have been removed southward to Lake Frome through Salt Creek before scour reached the water table. The initiation of sief dunes, largely derived from the Millyera strandline dunes, seems to be correlated with this episode of severe denudation of the floor of Lake Callabonna.

When the water table again rose, lacustrine conditions were restored to Lake Callabonna partly because southward drainage through Salt Creek was now impeded by growth of the lunette at the northeastern edge of Lake Frome. The fresh-looking lowest gravel bar is attributed to the Coonarbine Formation; it records the level of a lake within the confines of present Lake Callabonna. Quartz sand

and clay pellets formed a lunette on its eastern margin. Continued development of the longitudinal dunes of the Strezlecki Desert immediately east of Lake Callabonna seems related to these younger events at the lake. At Lake Frome the Coonarbine Formation also includes extensive gypsum lunettes that record the arid phase of the last glacial, which is so widely documented in southeastern Australia (17,000–20,000 yr BP, Bowler, 1976; Callen et al., 1983).

Since the deposition of the Coonarbine Formation, Lake Callabonna has remained a playa or ephemeral lake under an arid climatic regime, subject to rare inundations such as occurred in the 1970s; mostly, however, it has been subjected to aeolian deflation that has continued to scour the Quaternary sequence to the present water table over large parts of the lake floor. Thin sedimentary blankets on the present lake floor, which were contributed by brief episodes of sedimentation, are slowly being reworked into aeolian land forms under the present dry, windy climate.

Two radiocarbon dates have been reported (Buckley, 1973) for the Coonarbine Formation at Lake Callabonna. Both dated the same event, the water bird nesting locality at site 2, and yielded similar dates based on charcoal (2375 ± 95 yr BP) and egg shell (2080 ± 100 yr BP)—about 2000–3000 yr BP. We now regard these deposits as associated with artesian spring mounds that formed islands during a late lake-full phase in the Holocene history of this basin.

CORRELATION AND AGE

In the discussion above we have proposed a correlation of the lithostratigraphy exposed at Lake Callabonna with presumed equivalents described by Callen and Tedford (1976) from the same basin, but at the southeastern part of the Lake Frome playa. Callen (1984) described a new unit, the Coomb Spring Formation, based on beds at the top of the Millyera Formation type section (units 5–7 of Callen and Tedford, 1976). He regards the new unit as representing a separate lacustral phase from the Millyera. The Coomb Spring lake is smaller than the Millyera, being approximately the same area as the present Lake Frome playa, and its sedimentary record is dominated by sands from fluviatile and aeolian sources. What we have identified as Eurinilla Formation at Lake Callabonna perhaps should be correlated with the Coomb Spring Formation. The Eurinilla equivalent may be absent or represented within the fluviatile and aeolian deposits identified as the Coonarbine Formation at Lake Callabonna. The latter deposits are the only ones at the lake that include a lunette related to the lake perimeter. At Lake Frome, extensive gypsum, quartz, and clay pellet dunes fringing the eastern side of the lake are regarded as Eurinilla Formation. A higher water table there may have favored lunette development at that time.

Regional stratigraphic work is needed between lakes Frome and Callabonna to resolve these correlations. Nevertheless, the evidence for three successive lacustrine events at Lake Callabonna seems secure and these should represent coeval events in the adjacent Lake Frome area. In a review of radiocarbon dates from various units in the Lake Frome area, Callen et al. (1983) concluded that the Coonarbine Formation accumulated during the last lacustral period, 30,000–45,000 yr BP. They also speculated that the underlying Eurinilla Formation accumulated at least 95,000 yr BP, probably during the penultimate lacustral phase 125,000–200,000 yr BP. The Coomb Spring and Millyera formations represent previous lacustral phases during the Brunhes Chron (Callen, 1984: 169) whose maximum age would be 0.7 Ma.

This chronology receives some support from extensive thermoluminescence dating of Quaternary deposits in the adjacent Lake Eyre Basin (Nanson et al., 1992). Major fluviatile episodes supportive of lacustral conditions in Lake Eyre are found equivalent to the last two interglacials (oxygen isotope stages 5 and 7) and the stage 3 subpluvial. These are dated approximately 200,000–250,000, 80,000–120,000, and 35,000–55,000 yr BP, respectively, which correspond well with the estimates of the ages for lacustral events in the Callabonna Basin.

Regardless of the precise correlation of the unit containing the Callabonna fauna, it is evident from the proposed chronology that the assemblage of organisms obtained from

the *Diprotodon*-bearing beds are of significant antiquity and belong to some period within the 0.2–0.7 Ma span. The vertebrate fauna obtained from the Eurinilla Formation at Billeroo Creek southwest of Lake Frome (Williams, 1980), although more diverse than that from Lake Callabonna, includes the same or closely comparable taxa. These faunas from successive stratigraphic units suggest stability in faunal composition in the Lake Frome area during the medial to late Pleistocene interval.

TAPHONOMY

All specimens representing the genus *Sthenurus* so far obtained at Lake Callabonna have been represented by partial or nearly complete skeletons. The sole individual representing *S. andersoni* (SAM P13672–3) was obtained at site 1 near the camp of the Zietz party in 1893, and the same area produced the skull and mandible of *S. stirlingi* (SAM P12882) and associated limbs of the same taxon (SAM P13936–8, P13940) obtained by the Hurst party earlier in 1893. The *S. stirlingi* material represents at least two individuals, as there is an isolated metatarsal IV (SAM P13939) that also belongs to this taxon from that site.

The *Sthenurus* material obtained by the 1970 expedition all came from site 4 and includes four individuals of *S. tindalei* and six of *S. stirlingi* (including the type specimen). These individuals were represented by many articulated elements, usually the hind limbs and especially the hind feet (fig. 7) and parts of the caudal vertebral column. At this site the laminated fossiliferous clays varied from 0.5 to 1.5 m in thickness (thickest in the western part of the site). We found that the skeletal elements of a single individual could be scattered throughout the local thickness of these clays. The hind limbs, especially the feet, were usually the more deeply buried. Cross sections of the clay unit revealed by the walls of our excavations showed contorted sand laminae, most often convex upward (fig. 6), that when exposed at the surface proved to be mammal trackways. In some areas the clays were intensely churned over many square meters, as was dramatically indicated by the sand laminae that were contorted, broken, and often tilted vertically. All fossil remains in these zones were similarly churned with the sediments. Intense bioturbation by the heaviest bodied animals (*Diprotodon*) must have been responsible for much of the disarticulation and deep burial of remains of the smaller forms such as *Sthenurus*. In the case of the type specimen of *S. stirlingi,* the skull and articulated mandible were nose down in the sediments and the cranium was forced into the nasal cavity. The anterior part of the skeleton was partially articulated and the pelvis and hind limbs were separated from the rest and from each other by a short distance; the hind limbs were increasingly articulated down to the feet (fig. 7). This specimen was one of the better articulated ones and suggests partial disarticulation before burial, coupled with compression through trampling by other taxa. In some cases broken bones were found in situ, further indicating scattering by predators scavenging the exposed carcasses. Some bones were cracked from prolonged exposure to the air, especially a skull and mandible of *S. stirlingi* (AMNH 117496) whose cranium had been broken away. Field evidence suggests entrapment of large-bodied animals in fluid clays. In the case of kangaroos, the hind limbs and feet were initially buried and were thus most often preserved in articulated fashion; the upper part of the body may have been exposed and was occasionally scavenged and disarticulated. The bones were cracked by longer exposure, possibly being aided by crystallization of salts in the efflorescent zone of the lake floor, as is the case of the fossil bones exposed on the present playa surface. The taphonomic evidence indicates short-term fluctuations of the water table in this part of the Callabonna Basin in Pleistocene time, possibly representing seasonal wet-dry cycles punctuated by more protracted events.

An unusual aspect of the preservation of organic remains at Lake Callabonna is the existence of skin and hair impressions or re-

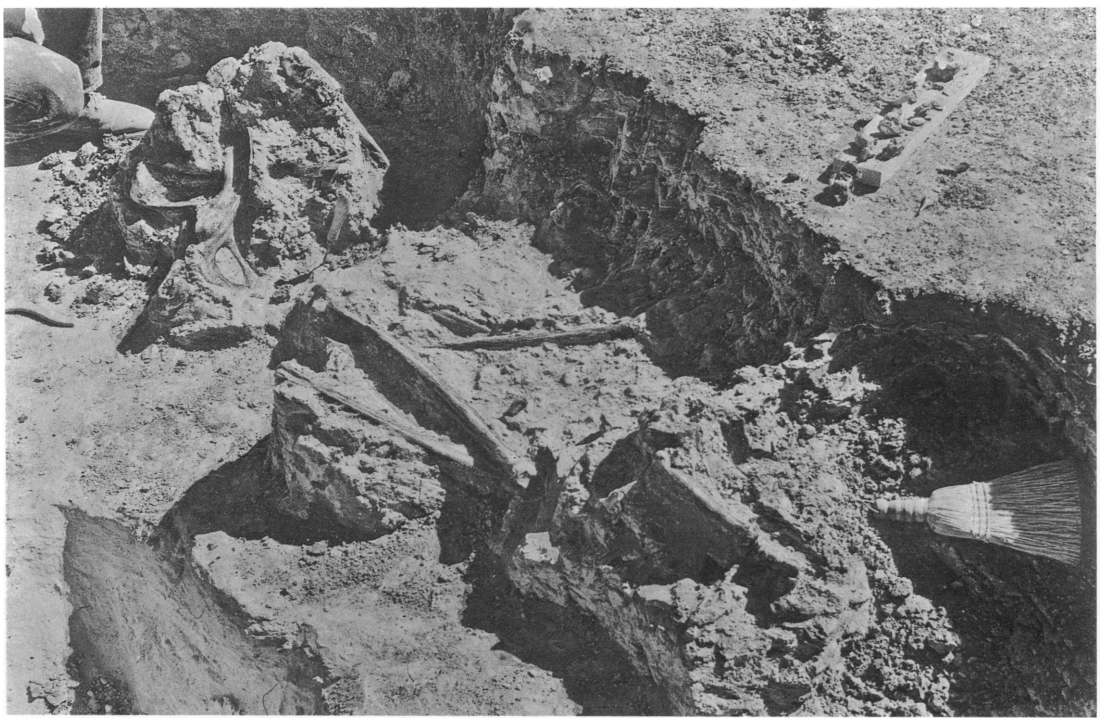

Fig. 7. Hind limbs of the holotype of *Sthenurus stirlingi* (SAM P22533, SIAM 62) in situ, SIAM site 4. The pelvis and femora are in the block in the upper left, the tibiae-fibulae in the center, and hind feet in the lower right view. The bones are semi- to fully articulated and lie at the base of the laminated clays. The underlying sands are exposed in the pit in lower left.

placements by microcrystalline gypsum and calcite. In the case of the *Sthenurus* material, we encountered an individual of *S. tindalei* (AMNH 11797) whose caudal vertebrae were partially articulated and were surrounded by replacements, probably void fillings, of the caudal skin by microcrystalline gypsum. Impressions of hair of the tail in the same material were also found. This material allows some aspects of the external morphology of the tail integument to be described, as reported below.

SYSTEMATICS

INFRACLASS MARSUPIALIA
ILLIGER, 1811

ORDER DIPROTODONTIA OWEN, 1866

SUPERFAMILY MACROPODOIDEA
GRAY, 1821

FAMILY MACROPODIDAE GRAY, 1821

SUBFAMILY STHENURINAE
(GLAUERT), 1926

In a previous review, one of us (Tedford, 1966) presented a list of characters (op. cit.: 7–10) that he believed to be diagnostic of the subfamily Sthenurinae (Glauert), 1926. Among the features noted, the following seem to constitute the more important synapomorphies uniting the genera *Sthenurus, Simosthenurus,* and *Procoptodon* as a monophyletic group within the Macropodidae: skulls brachycephalic with deep, broad rostra; very brachycephalic species with remarkably short, wide, and deep skulls with basicranium elevated well above palatal plane; zygomatic process of squamosal deep;

masseteric process of zygoma very robust; large palatal vacuities, narrow palatine bars; external auditory meatus very long, ventrally keeled and strongly sutured to squamosal; upper incisors form narrow, V-shaped group viewed ventrally; I3 with high crown elongate posteriorly without lateral grooves; P3 with high lingual crest extending full length of tooth and connected to labial or main crest by transverse laminae; lower jaws strongly sutured, often ankylosed at symphysis in adults, boss often formed at union; horizontal rami deep and thick, depth at symphysis not appreciably shallower than beneath cheek teeth; mandibular or posterior mental foramen on labial side of mandible beneath cheek teeth; lower incisor with short crown, and sharply produced dorsal margin; p3 with labial crest; permanent premolars, erupt late in ontogeny, usually after eruption of M4; front foot with digits I and V greatly reduced, elongate metacarpals II–IV and long curved ungule phalanges; hind foot with digits II–III, V reduced to vestiges, distal end of metatarsal IV wide, phalanges broad; proximal phalanx with lateral scars on midshaft for sesmoid ligaments.

Additional synapomorphies listed in Flannery (1983) included: occlusal surface of central upper incisor short, not broad and bladelike as in macropodines; upper molars with postlink present on rear face of hypoloph; in anterior upper molars postmetacrista continues lingually across hypoloph and terminates nearer occlusal edge than posthypocrista, providing overlap of these structures; enamel completely encircles crown of i1; lower molars with well-developed premetacristid that usually contacts paracristid (forelink). These features and the others listed above enabled Flannery to demonstrate that the subfamily included the fossil genus *Troposodon* Bartholomai, 1967, as well as the living banded hare wallaby, *Lagostrophus* Thomas, 1887, the most plesiomorphic member of the group.

The sthenurines are the sister-taxon of the macropodines because they share strongly bilophodont cheek teeth, absence of a posthypocristid, and pedal features pointed out by Flannery (1983). This relationship is expressed by uniting the sister-taxa as subfamilies of the family Macropodidae. In turn, these forms are grouped into the superfamily Macropodoidea with the rat kangaroos (Potoroidae) through such synapomorphies as the wide masseteric canal in the mandible, enlargement of the forestomach for ruminant-like digestion, and modifications of the limbs and axial skeleton for saltatorial locomotion. The potoroids (including the subfamily Hypsiprymnodontinae) show unique union of the squamosal and frontal bones on the side of the cranium, a vaginal caecum (anterior vaginal expansion; see Rose, 1978, for review of this character), and other features reviewed by Flannery et al. (1983), which are summarized and extended by Archer (1984).

We agree with Flannery (1983) that *Procoptodon* and *Simosthenurus* are sister-taxa united by the following synapomorphies: markedly short and deep skulls with basicranial planes strongly elevated with respect to palatal plane; very deep squamosal process of zygoma; masseteric process of zygoma very well developed, vertically dependent and formed jointly by jugal and maxillary; lower jaws ankylosed, very thick and deep. In contrast, the genus *Sthenurus,* although united with *Procoptodon* and *Simosthenurus* by the synapomorphies characterizing the subfamily Sthenurinae, possess few autapomorphies. The cheek tooth dentition in *Sthenurus* is high-crowned and has better-developed midlinks than in *Simosthenurus* and primitive (sensu Sanson, 1978) macropodines, and in this sense approaches *Procoptodon.* We regard this as a case of parallel development of high-crowned, better-linked teeth in those sthenurines (as in some macropodines), possibly in response to the selection pressures postulated by Sanson (1978). We thus place more emphasis on the complex of skull features uniting the brevirostrine sthenurines. The very close morphologic resemblance between all the species of *Sthenurus* sensu stricto reinforces the shared-derived cheek tooth features in indicating their monophyly.

Sthenurus Owen, 1873

Five species have been described and grouped into the genus *Sthenurus* in the restricted use advocated in this paper. There is a sixth species represented by two rami in the older Queensland Museum collections. These rami were most likely collected from the Pliocene Chinchilla Sand of the western Darling

Downs. They were described by Bartholomai (1963: 58–59) and later studied by Tedford, who agrees with Bartholomai that a distinct taxon is represented. One of these rami (QM F813) preserves the p3, and its morphology closely resembles that of *S. andersoni* in having the posterolabial crest fused to the anterior cusp, the junction of which is marked by a shallow groove. Both rami contain molar teeth markedly smaller than *S. andersoni* or *S. atlas*; however, like these late forms, they show high crowns, strong links, and few crenulations on the lophids. A well-developed premetacristid is present. We designate this taxon informally as *Sthenurus* species in the following discussion.

Phylogenetic analysis (fig. 8) shows *Sthenurus* as a monophyletic assemblage of species defined by the possession of high-crowned cheek teeth with well-developed links and the absence of enamel on the lingual face of the lower incisor. These features parallel those of more advanced macropodines, but are combined with the characteristic union of forelink (paracristid) and premetacristid of the sthenurines.

The form of the p3 serves to separate *Sthenurus atlas* and *S. notabilis* from the rest of the genus (fig. 8). In these species, the form of this tooth is thought to represent the derived condition in which the posterolabial crest is isolated from the anterior cusp by a deep narrow groove that may extend nearly halfway down the crown. Other *Sthenurus* species have strong union of the posterolabial crest with the anterior cusp, and this is the condition in all other sthenurines. Tedford (1966: 26) discussed the relationship of *S. notabilis* to *S. atlas*: the two species are primarily distinguished by size (*S. notabilis* being larger) and by the relatively smaller size of p3 relative to the cheek teeth in *S. notabilis*.

Sthenurus andersoni, S. tindalei, and *S. stirlingi* have a greatly reduced or absent premetacristid, which represents a reversal of the condition that otherwise is characteristic of sthenurines. *Sthenurus andersoni* is the smallest taxon, but is otherwise plesiomorphic as far as comparison is possible. The larger species are united as sister-taxa in sharing unique separation of the premaxilla from the nasals by interposition of a process of the maxillary. In addition, *S. stirlingi* has a prominent lingual groove on I3 that is unknown in other taxa.

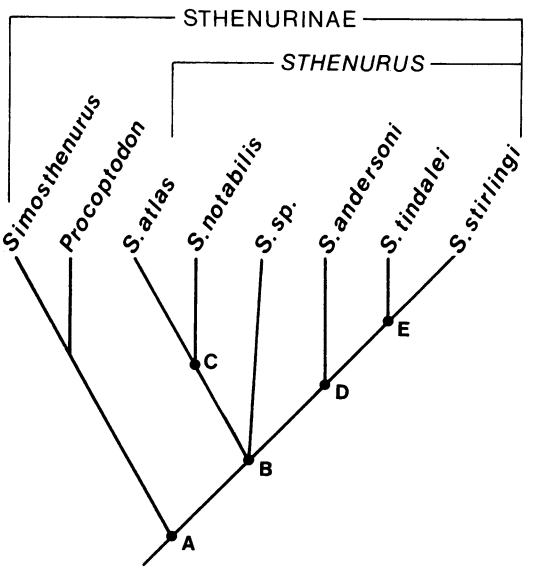

Fig. 8. Cladogram showing the relationships of the *Sthenurus* species discussed in the text. Node A, sthenurine synapomorphies detailed in the section on systematics; node B, high-crowned cheek teeth with well-developed links and enamel lacking on lingual face of lower incisor; node C, p3 with posterolabial cusp separated from anterior cusp by deep cleft; node D, premetacristid greatly reduced or absent; node E, larger taxa distinguished by separation of premaxilla and nasal bones by a maxillary process.

The chinchilla taxon occupies a trichotomous position with regard to the named taxa in that it appears to be a plesiomorphic *Sthenurus* species in all available features of the dentition, especially the union of posterolabial crest with anterior cusp on p3. This form approximates a stem-species in the phylogeny of *Sthenurus*.

The above data yield the following revised diagnosis of *Sthenurus* Owen, 1873: relatively dolichocephalic skull, proportions more macropodine-like than in other sthenurines; palatal and basicranial planes nearly approximating one another; mandibular rami weakly ankylosed; relatively narrow, shallow symphyseal union not extending significantly behind genial pit; lower incisors spatulate, procumbent; upper and lower premolars nar-

row for their length, length greater than any molar, more trenchant in form than in other sthenurines; third upper premolars always with posterolabial cusp; molars higher crowned than in other sthenurines, lacking conspicuous crenulations on loph(id)s, midlinks low, but consistently present; lower molars relatively narrow for their length with well-developed forelink and midlink; metatarsal IV long and slender.

Sthenurus contains the following species: *S. atlas* (Owen), 1838 (genotypic species); *S. andersoni* Marcus, 1962; *S. notabilis* Bartholomai, 1963; *S. tindalei* Tedford, 1966; *S. stirlingi,* new species; and *Sthenurus* sp. Bartholomai, 1963: 58–59.

CALLABONNA *STHENURUS*

The three species of the extinct macropodid genus *Sthenurus* described in this paper are made known on the basis of relatively complete and associated skeletal remains. These are the first descriptions of the postcranial remains other than metatarsals attributed to the genus. This unprecedented situation has provided new morphologic evidence relevant to questions of relationships and function in comparison with other taxa contained in the Macrpodidae.

Sthenurus andersoni Marcus, 1962

HOLOTYPE: Left ramus lacking ascending portion, root of lower incisor, p3, part of alveolus and anterior root of m1, m2–4 complete (II-MBB), AM MF 946. Bingara Fauna, New South Wales.

PARATYPES: Include left and right jaw fragments and isolated teeth of the upper dentition from the type locality (Marcus, 1962).

REFERRED SPECIMENS: In addition to the jaw and maxillary fragments already referred to this species by Bartholomai (1963) and Tedford (1966), a partial skeleton (SAM P13672 jaw, P13673 skull and postcranials) from Lake Callabonna, South Australia, is also assigned to this taxon. This specimen is contained in the collections of the South Australian Museum and is presumed to be that referred to by Stirling (1894: 209): "of fossil kangaroos we have one small but very complete skeleton." This skeleton includes the anterior portion of the skull including left and right I1.2.3, P3, M1.2.3.4 (IV. L+L+LL) premaxillary, maxillary, nasals, frontals, jugals, and exoccipital fragment; the mandible, less the right and left ascending rami but including right i1–p2 and fragmentary m1.2.3 (IV. L+L+LL) and left i1 fragmentary p3, m1.2.3.4 (IV. L+L+LL); portions of cervicals 5, 6, and 7; thoracic vertebra 1 and centra 2 to 8 inclusive; lumbar vertebra 3 and centra of 2, 4, 5, and 6; fragmentary sacrum and pelvis including right epipubic fragment; caudal vertebrae 1 to 17 inclusive plus three intervertebral chevrons; right and left femora, tibiae, and fragmentary fibulae; left and right tarsi, metatarsi IV, and fragmentary metatarsi II, III, and V, proximal, medial, and distal phalanges IV; rib fragments and sternubrae; proximal portions of left scapula; right and left humeri, ulnae, radii; partial right carpus including scapholunar, trapezoid, magnum, unciform, and cuneiform; partial left carpus comprising scapholunar and unciform fragments; fragmentary right metacarpals I to V and left metacarpals I to III; left and right proximal, medial, and distal phalanges II and III; two distal phalanges I; proximal and medial and a single distal V. The above-listed postcranials were included in the 1893 Lake Callabonna collection in the South Australian Museum in trays marked "Kangaroo L. Callabonna" or "small Wallaby." Although the skull and jaws were located elsewhere in the collection and attributed to another collector, recovery of matching jaw fragments from the trays with the skeleton confirmed their association.

Marcus's (1962) original diagnosis was based on characteristics of the jaw and lower dentition. Tedford's (1966) revised diagnosis included features of the upper dentition. The advanced tooth wear in P13672/P13673 has eliminated reference to some of those species characters. The following criteria have been used to refer this individual to *S. andersoni*: long slender lower jaw; procumbent lower incisors, smaller in cross section than in *S. atlas*; P3p3 within the size range of *S. andersoni* (Table 5) and of similar form; M1–4m1–4 protoloph (id), metaloph, and hypolophid

widths fall within the size range of *S. andersoni*; lower molars and upper M1.2 slightly shorter than the smallest *S. andersoni* (a condition attributable to the advanced state of wear); and M3.4 within the size range of this species. The left m3 retains vestiges of the enamel crown, suggesting a U-shaped median valley, an incipient midlink, an anterior cingulum approximately half the width of the tooth, and no evidence of a posterior cingulum. Enamel crowns are preserved on M3.4, the median valley is U-shaped, there is no forelink, the anterior cingulum is well developed and extends the full width of the tooth, there is no midlink, and a weak posthypocrista ("postlink" of Tedford, 1966) descends labially from the "hypocone" (metaconule) to the base of the metacone.

Sthenurus tindalei Tedford, 1966

HOLOTYPE: Fragmentary skull containing the broken right I1–3, left I1–2, nearly complete left I3, complete little worn (II. LMEB) cheek teeth of both sides, SAM P138201. Lake Menindee, New South Wales.

REFERRED SPECIMENS: In addition to the jaw fragments tentatively identified with the holotype (Tedford, 1966: 26) from Lake Menindee, New South Wales, the following materials are attributed to four individuals of this taxon from Lake Callabonna (site 4), South Australia: AMNH 117491 (field number SIAM 35), skull lacking lambdoidal region of cranium has full, but well worn, dentition (IV. L+L+LM), and associated skeletal elements including: partial vertebrae, ribs and clavicle, parts of right manus, left ulna, proximal end right fibula, and parts of right pes (probably male, as discussed below). AMNH 117492 (field number SIAM 40), nearly complete skeleton too badly fractured by salt crystallization and matrix shrinkage to enable preparation of all its elements. Bones successfully prepared include: badly fragmented skull lacking most of dentition and left zygoma, right ramus with nearly complete cheek tooth dentition (/II. LMEU) (probably female). AMNH 117493 (field number SIAM 54), complete skull and mandible of a young individual with early wear but adult dentition (II. LMEU/II. LMBU) and associated partial skeleton including: partial vertebral column, ribs and sternubrae, pelvis, right epipubic, partial femora and fibulae, tibiae, right and left pes, distal ends scapulae, clavicles, right humerus, both radii and ulnae, partial right and left manus (probably female). AMNH 117499 (field number SIAM 84), palate and mandible of a young individual with early wear, but adult dentition (III. LMEU/III. LMEU) and associated partial skeleton including: parts of the cervical, thoracic, sacral and caudal vertebral column, partial ribs, sternubrae and clavicle, left pelvis, left femur, left tibia, fragment of left fibula, fragments of the pes, left scapula, left humerus, left ulna, fragments of a left radius and manus (probably male).

SPECIFIC DIAGNOSIS: The following revised diagnosis takes into account the more complete material from Lake Callabonna herein referred to *S. tindalei*. Reference to this taxon was established by direct comparison of a cast of the type with the Callabonna material.

Somewhat smaller than *S. stirlingi* (about 15% smaller in length of molar teeth) but significantly larger than other described species; skull form more as in *S. atlas*, relatively dolichocephalic for Sthenurinae; cranium significantly elevated above palatal plane only in older individuals; premaxilla excluded from contact with nasals as in *S. stirlingi*; palatal vacuity reaches junction of M1–P3; mandible with procumbent incisor as in *S. andersoni*; I3 lacks lingual groove; P3 about the same length and morphology as in *S. stirlingi*, but narrower, differs from other species in having lingual crest crossing anterior end of labial crest to merge with anterior cingulum; upper molars narrower relative to length than in *S. stirlingi* and likewise lack forelink, have weak midlink, and have well-developed posthypocrista; lower incisor crown narrow, shallow, and short, rather like *S. andersoni*, not broad and wide as in *S. stirlingi*; p3 longer than any molar and nearly length of that of *S. stirlingi*, but narrower, with labial crest united at rear of anterior cusp rather than at anterior end as in *S. stirlingi*; lower molars narrower for their length than in *S. stirlingi*, weak links and proportions as in smaller *S. andersoni*.

Sthenurus stirlingi, new species

ETYMOLOGY: For Sir Edward C. Stirling (1848–1919), Director of the South Austra-

lian Museum, 1895–1913, prominent Australian biologist who, with his assistant A. H. C. Zietz, first collected and described the fossil vertebrates of Lake Callabonna.

HOLOTYPE: SAM P22533 (field number SIAM 62), skull and mandible of a young adult (II. MEBU/II. MEBU) and most of the associated postcranial skeleton including: complete cervical, most of thoracic, lumbar, and caudal vertebrae and caudal haemal arches, complete pelvis, sternubrae and ribs, partial epipubic bones, complete femora, tibiae, fragments of fibulae, complete right and left pes, clavicles, scapulae, humeri, radii, ulnae, most of both mani (thought to be male according to criteria discussed below).

REFERRED SPECIMENS: From Lake Callabonna we record the following remains of nine individuals identified as *S. stirlingi*: AMNH 117494 (field number SIAM 59), part of lambdoidal crest of a skull, but no other cranial remains, one thoracic vertebra, median part of the caudal column and some haemal arches, left rib fragments, femora, tibiae, fragments of both fibulae, parts of both pes, scapulae fragments, fragments of distal end of right humerus, left humerus and radius, fragments of both ulnae, parts of both manus (probably male). AMNH 117495 (field number SIAM 78), skull fragments including fragments of a left premaxillary and maxillary and anterior zygoma, parts of the right maxillary, but no mandible, juvenile individual, P2 Dp3 M1–4, P3 calcified, unerupted (III. BBUUU), parts of cervical, thoracic and caudal vertebrae, right ischium and ilium, right epipubis, right femur, right tibia, parts of right pes, ribs, and scapula (sex unknown). AMNH 117496 (field number SIAM 79), skull (lacking most of cranium) and mandible of an old individual , teeth badly fractured and broken (IV. L+L+LL/IV. L+L+LL), parts of the cervical, thoracic, lumbar, sacrum and anterior part of caudal column, haemal arches, ribs, clavicles, sternubrae, pelvis, left epipubis, femora, tibiae, fibulae, both pes, left scapula, left humerus, radii, ulnae, most of left manus and parts of the right (thought to be female). AMNH 117497 (field number SIAM 81), right ramus and badly fragmented left maxillary and premaxillary of a young individual with early wear (/III. LMME) and associated partial skeleton with a cervical vertebra, some lumbars, sacrum, and caudal vertebra; ribs, sternubrae, pelvis, right femur, distal end left femur, both tibiae and fibulae, parts of both hindfeet, partial radii, ulnae and front feet (probably male). AMNH 117498 (field number SIAM 83), weathered fragment of left ramus with m1–4 of old individual (L+L+LL), and associated skeletal fragments: cervical fragment, rib fragments, sternubrae, most of right femur, proximal part of right tibia, distal end right fibula, distal end right humerus, distal ends right ulna and radius, metacarpals (apparently male). SAM P12882, crushed skull and jaws of an old individual (presumed male) with broken incisors and worn but complete cheek tooth row (IV. L+L+LL/IV. L+L+LL). SAM P13936, complete right and distal three-fourths of left tibia and proximal parts of associated fibulae; P13940, right femur; P13937, right pes; P13938, left pes; all are of comparable size and probably belong to a single individual, presumably that seen in the field by Brown (1894: 7). SAM P13939, left metatarsal IV.

SPECIFIC DIAGNOSIS: Largest known species of *Sthenurus,* approximately 15% larger in molar length than nearest-sized and contemporary *S. tindalei,* I3 deeply grooved lingually; skull differs from *S. tindalei* in more elevated basicranium relative to palatal plane, greatly inflated nasofrontal area; mandible with relatively shorter diastema than in *S. tindalei,* symphysis more upturned and mandibular foramen visible above masseteric crest when mandible is viewed laterally; P3 broader, but nearly same length as in *S. tindalei*; lower incisor notably less procumbent than in *S. tindalei*; p3 shorter for its width than in *S. tindalei,* but otherwise of similar morphology.

COMPARATIVE MORPHOLOGY

In the following, the skeleton of *S. stirlingi* is compared with material attributed to *S. tindalei* and *S. andersoni* from Lake Callabonna, and with living *M. giganteus.* In all cases, semi-articulated skeletons of individuals were available for the fossil taxa so that the association of elements of the skeleton was either known directly or could be inferred

by articulation and comparison with *Macropus*. Individuals of *S. stirlingi* and *S. tindalei* broadly overlapped in size, but the bones of these taxa could be distinguished morphologically in most cases, as indicated in the discussions below. Within each taxon the range in postcranial skeleton size corresponds to that observed in larger living Macropodidae in which sexual dimorphism is particularly marked. These *Sthenurus* species also appear to be dimorphic, and we have tentatively assigned each individual to its purported sex as indicated in the description of the material above. In the following comparative study we will discuss intraspecific (sexual) as well as interspecific characters in the larger forms.

SKULL (table 1, figs. 10–13): The large dolichocephalic skull of *S. stirlingi* is distinguished from the contemporaneous *S. tindalei* by the more elevated position of the braincase and the greatly inflated nasofrontal region. These general features, as well as others mentioned below, also characterize the skulls of purported females of *S. stirlingi* (e.g., AMNH 117496), which are no larger overall than males of *S. tindalei* (e.g., AMNH 117491). In *S. stirlingi,* the palatal aspect of the premaxilla is broader relative to its length than in *S. tindalei* and bears a V-shaped array of robust incisors. The anterior portion of the premaxilla, as in *S. tindalei,* ascends obliquely in a smooth, continuous line from the I1 alveolus to meet a small anterior dorsal process of the maxilla (fig. 13), thus excluding the contact of the premaxillary and nasal bones. In *S. andersoni* and other dolichocephalic forms (*S. atlas* and *Macropus giganteus*), as well as brachycephalic forms (*Simosthenurus occidentalis* and *Procoptodon goliah*; Tedford, 1966), the premaxilla extends dorsally to make the usual lateral contact with the nasals (fig. 13). The diastema of *S. stirlingi* is approximately 30 percent of the palatal length. It is intermediate between that of *S. tindalei* (37%) and the brachycephalic *P. goliah* (25%). Unlike *S. tindalei,* but similar to *S. andersoni,* the palate is markedly deflected ventrally relative to the occlusal plane of the molars. The incisive foramina, which are deep and narrow at the premaxillary–maxillary suture, flare anteriorly. They extend to a line opposite the posterior border of the I3 alveolus as in *S. andersoni.* The palatine vacuities are short relative to those of *S. tindalei.* They extend posteriorly from a line opposite the protoloph of M2 to the weak palatine bars opposite the metaloph of M4. A similar condition prevails in *S. andersoni.* The palate is concave in both transverse and longitudinal planes, a condition similar to that in *S. andersoni* and *M. giganteus. Sthenurus stirlingi* differs from the other taxa in that the cheek tooth row curves medially, both anteriorly and posteriorly, from a line tangential to the labial side of the molars at the anterior edge of the masseteric processes. The row also curves dorsally anterior to this line, as in *Macropus.* The maxillary is constricted above the root of P3 to form a deep buccinator fossa containing the infraorbital foramen. In *S. andersoni* and *S. tindalei* the infraorbital foramen lies above P3, behind the buccinator fossa and higher on the maxillary, as in *Macropus.* The maxillary, which is convex in midlateral aspect, joins dorsally with the anteriorly tapering nasals to form a long, ventrally curved tubular rostrum. The anterior ends of the nasals taper to fine points that overhang the narial opening as far forward as the incisor alveoli, as in *S. andersoni.* The high vaulting of the frontals above the orbits is continuous, with the line of the rostrum giving a domed appearance to the forehead—a feature not evident in other dolichocephalic sthenurines. The postorbital constriction forms a line above the posterior end of the palate as in *M. giganteus.* Behind this line the cranium narrows to a single sagittal crest supported by the parietals. In *S. tindalei,* both females (AMNH 117493) and apparently males (judging from the posterior part of the dorsal cranial surface in AMNH 117499) have parasagittal crests that converge posteriorly but do not meet to form a single crest. The zygomatic arch of the *S. stirlingi,* even in females, is deeper than in *S. tindalei,* with approximately equal contribution from the squamosal and the jugal. The laterally and distally flared masseteric processes lie at the jugal root of the arch opposite the protoloph of M3. They are formed largely from the maxillary with some lateral buttressing by the jugal, and although far more pronounced than in other members of the genus, they are not as robust as those of brachycephalic forms of comparable size (e.g., *Procoptodon*). The deep orbits have a broad

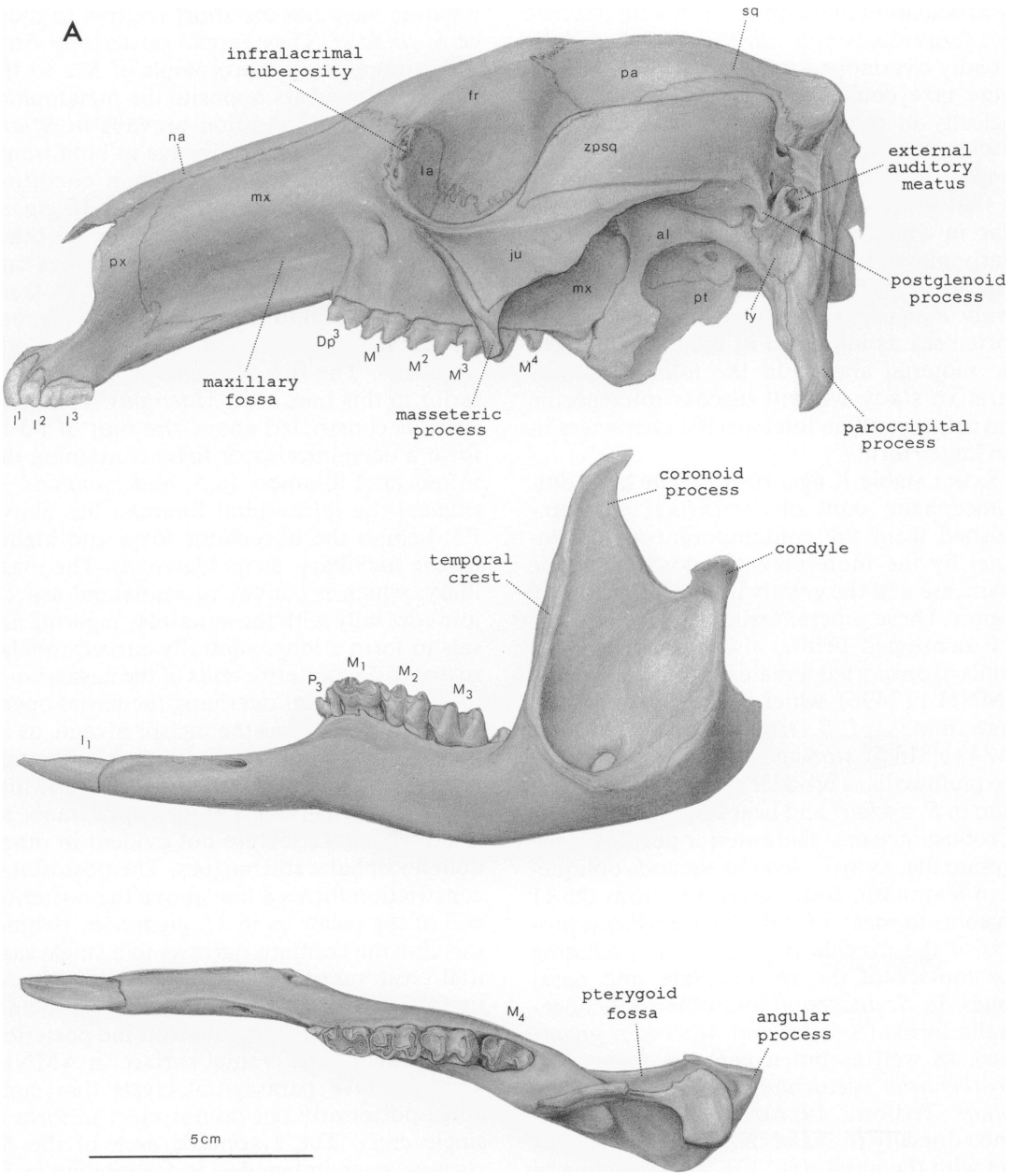

Fig. 9. Cranial anatomical features and nomenclature using skulls and mandibles of male and female *Macropus giganteus*. **A,** Lateral view of male skull (AMNH 66174); lateral and occlusal view of left ramus. **B,** Lateral view of female skull (AMNH 42905); lateral and occlusal view left ramus. **C,** Dorsal view of skull; male left, female right. **D,** Posterior view of skull; male left, female right. **E,** Palatal view of skull; male left, female right. Abbreviations for cranial bones: al, alisphenoid; bo, basioccipital; bs, basisphenoid; ex, exoccipital; fr, frontal; ip, interparietal; ju, jugal; ma, mastoid; mx, maxillary; na, nasal; pa, parietal; pl, palatine; pt, pterygoid; px, premaxillary; so, supraoccipital; sq, squamosal; ty, tympanic; zpsq, zygomatic process of squamosal. Serial designations of incisors (I), premolars (P), deciduous premolars (Dp), and molars (M) follow Tedford (1966).

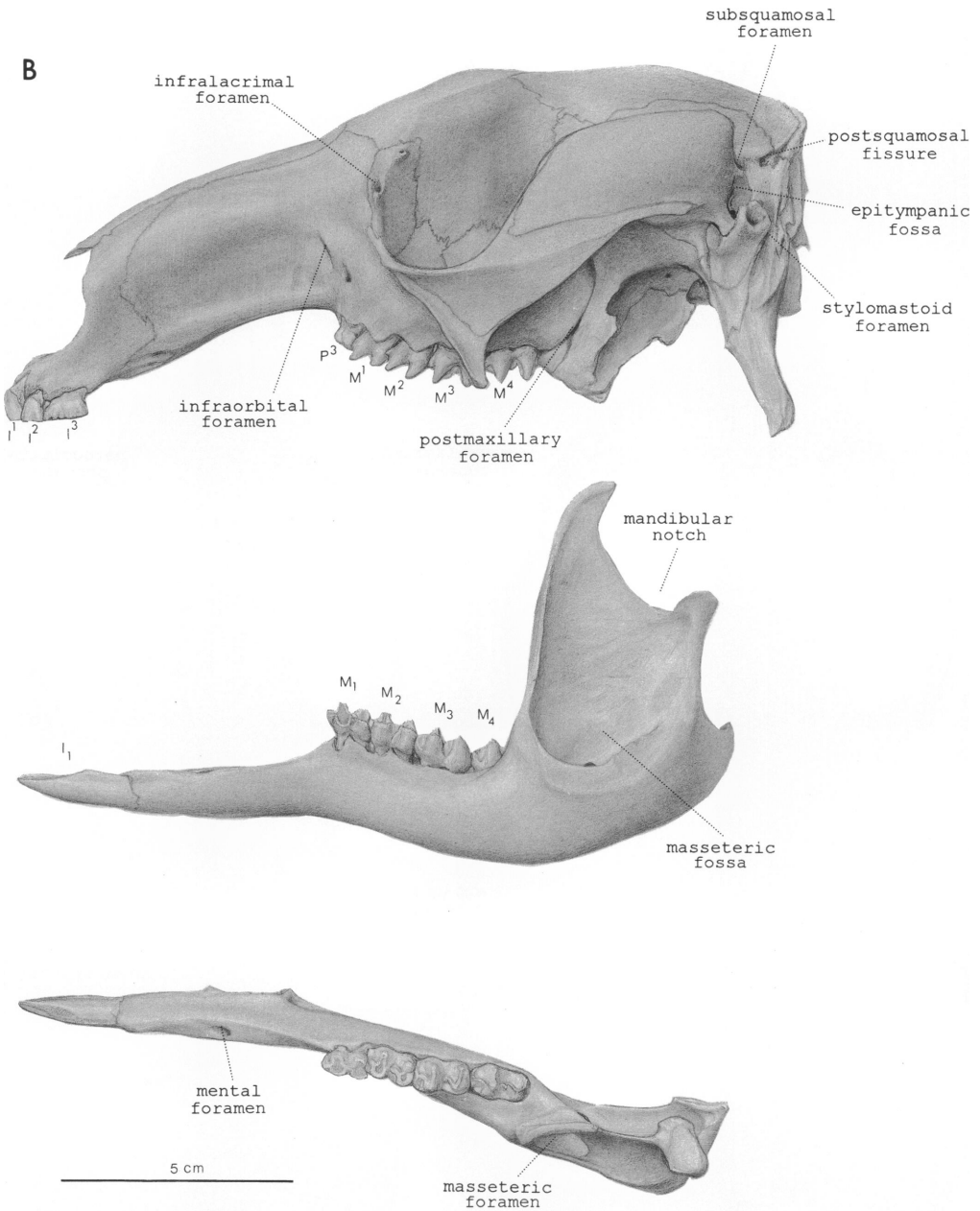

Fig. 9. Continued.

rim bound by the jugal and lacrimal. In ventral aspect the orbit forms a shelf that protrudes laterally beyond the blade of the zygomatic arch. The anterior border of the orbit lies opposite the protoloph of M2 as in *S. tindalei*. In *S. andersoni* this border lies opposite the protoloph of M1. The lacrimal in *S. stirlingi* appears to be narrow and confined to the rim of the orbit; it bears two small foramina separated vertically by a small rugose tuberosity.

The cranial portion of the skull is missing from the *S. andersoni* specimen. In *S. stirlingi* the squamosal process of the zygomatic arch

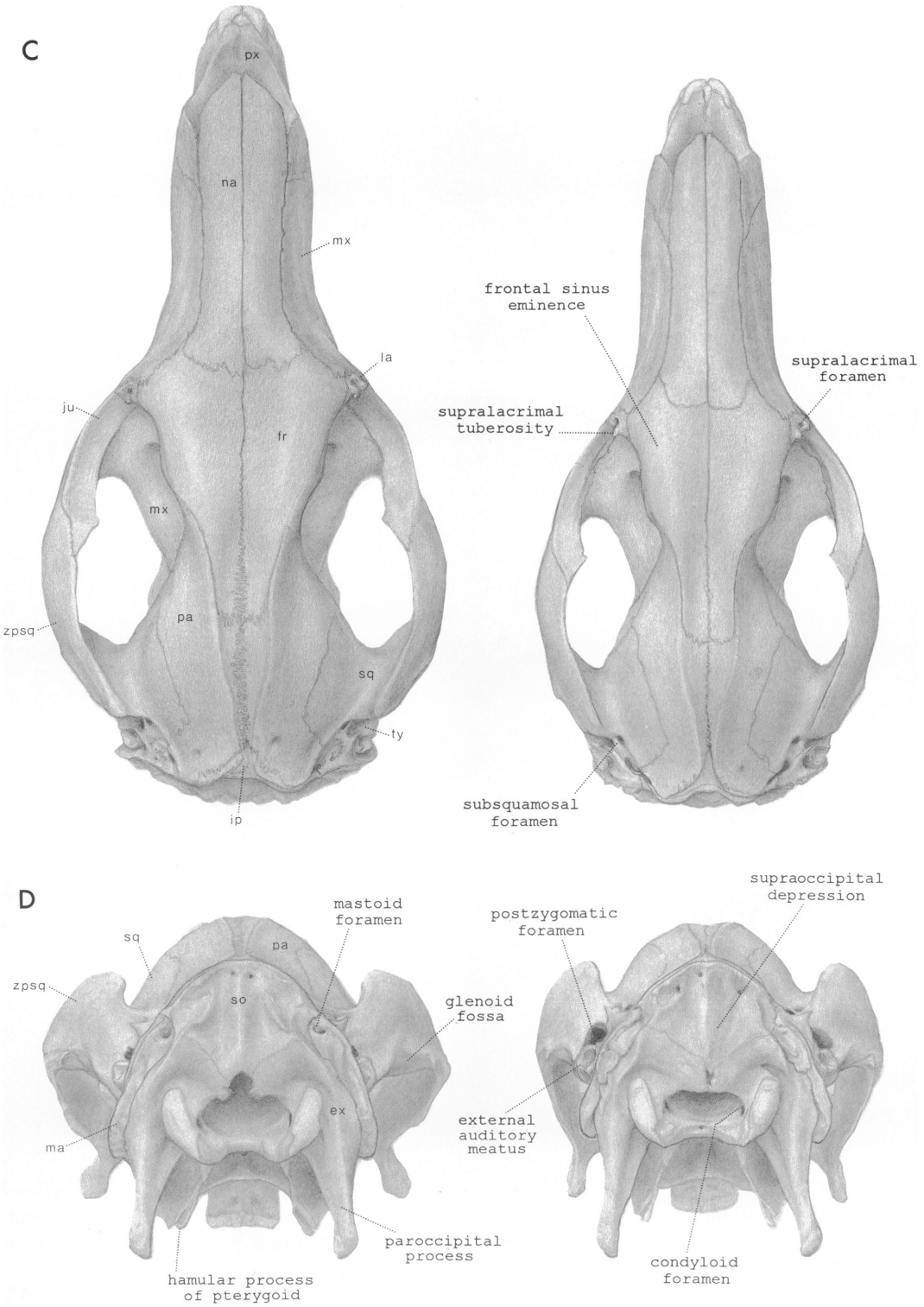

Fig. 9. Continued.

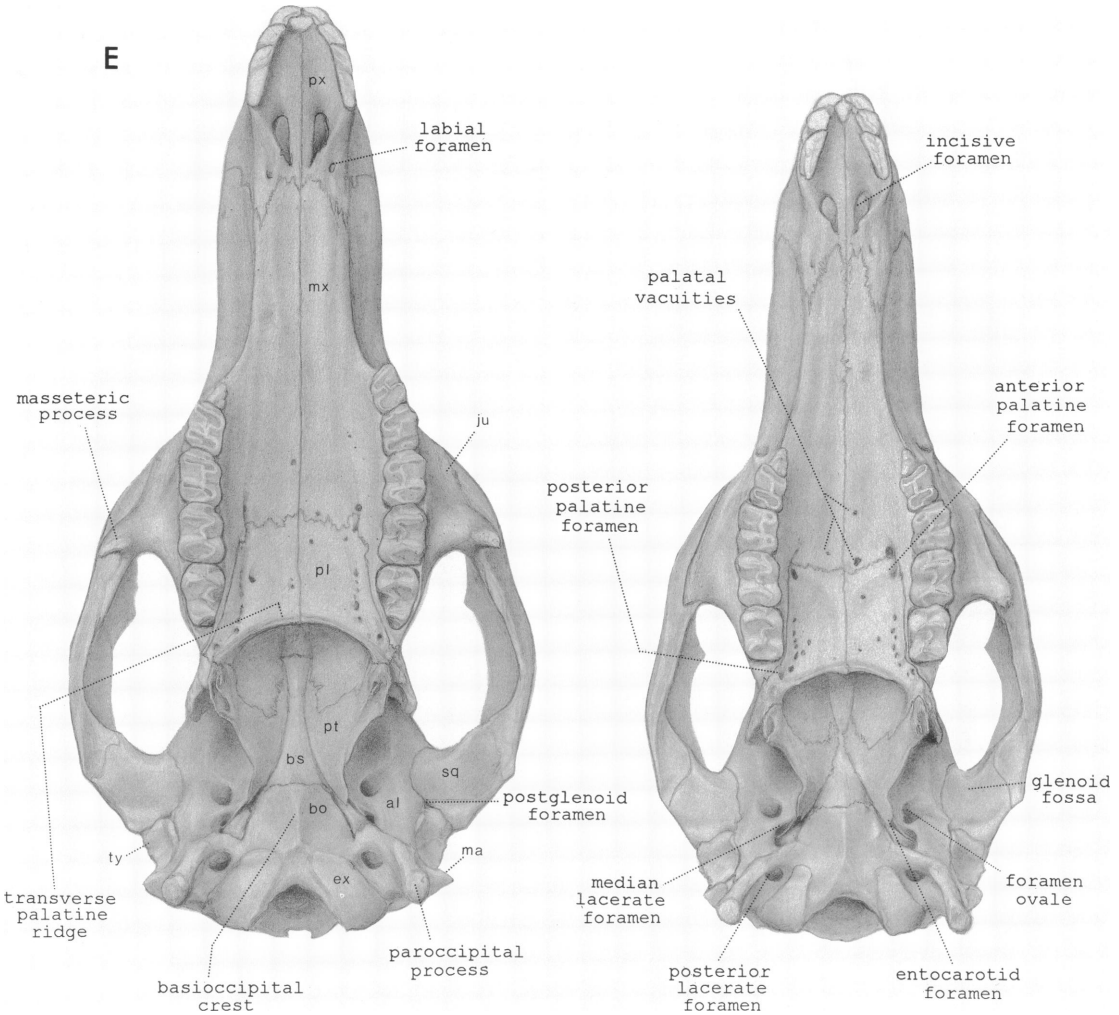

Fig. 9. Continued.

extends posteriorly to form the mastoid–squamosal crest. Anteriorly, the squamosal extends to the posterodorsal border of the alisphenoid, and dorsally it extends to the posteroventral border of the parietals. A large oval postsquamosal foramen occurs in the squamosal near the dorsal union of the zygomatic arch with the temporal crest. The glenoid fossa arises solely from the squamosal. It is flat dorsally, narrow and gently convex posteriorly, which more closely resembles that in *S. tindalei* than *P. goliah*. The ectotympanic arises medially at the alisphenoid bulla and extends laterally as an expanding subangular thick-walled tube. A weak crest occurs on the posteroventral border of the ectotympanic. Anteriorly, a strong crest is continuous with the postglenoid process of the squamosal. There are two postglenoid foramina. The long paroccipital processes curve gently lateromedially from the base of the exoccipitals to the level of the occlusal plane. They are buttressed anteromedially by the alisphenoid bulla and posterolaterally by the mastoid. The broad supraoccipital is flanked by the mastoid and abuts the exoccipital ventrally. The wide ovate foramen magnum is flanked by broad occipital condyles. The articulating surfaces of the condyles are directed more ventrally than in *M. giganteus*, which

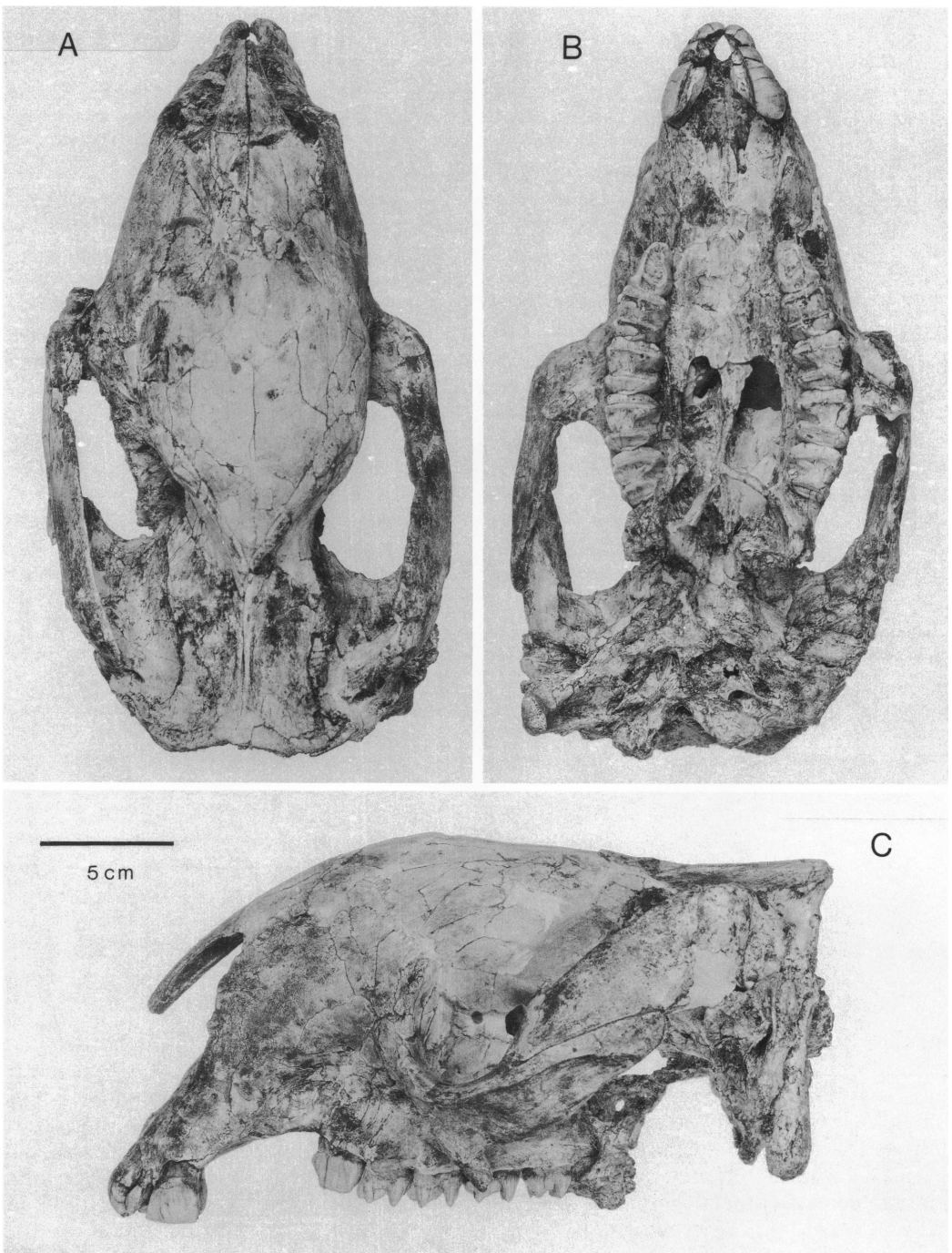

Fig. 10. *Sthenurus stirlingi,* holotype skull, SAM P22533. **A,** Dorsal view; **B,** palatal view; **C,** lateral view (reversed).

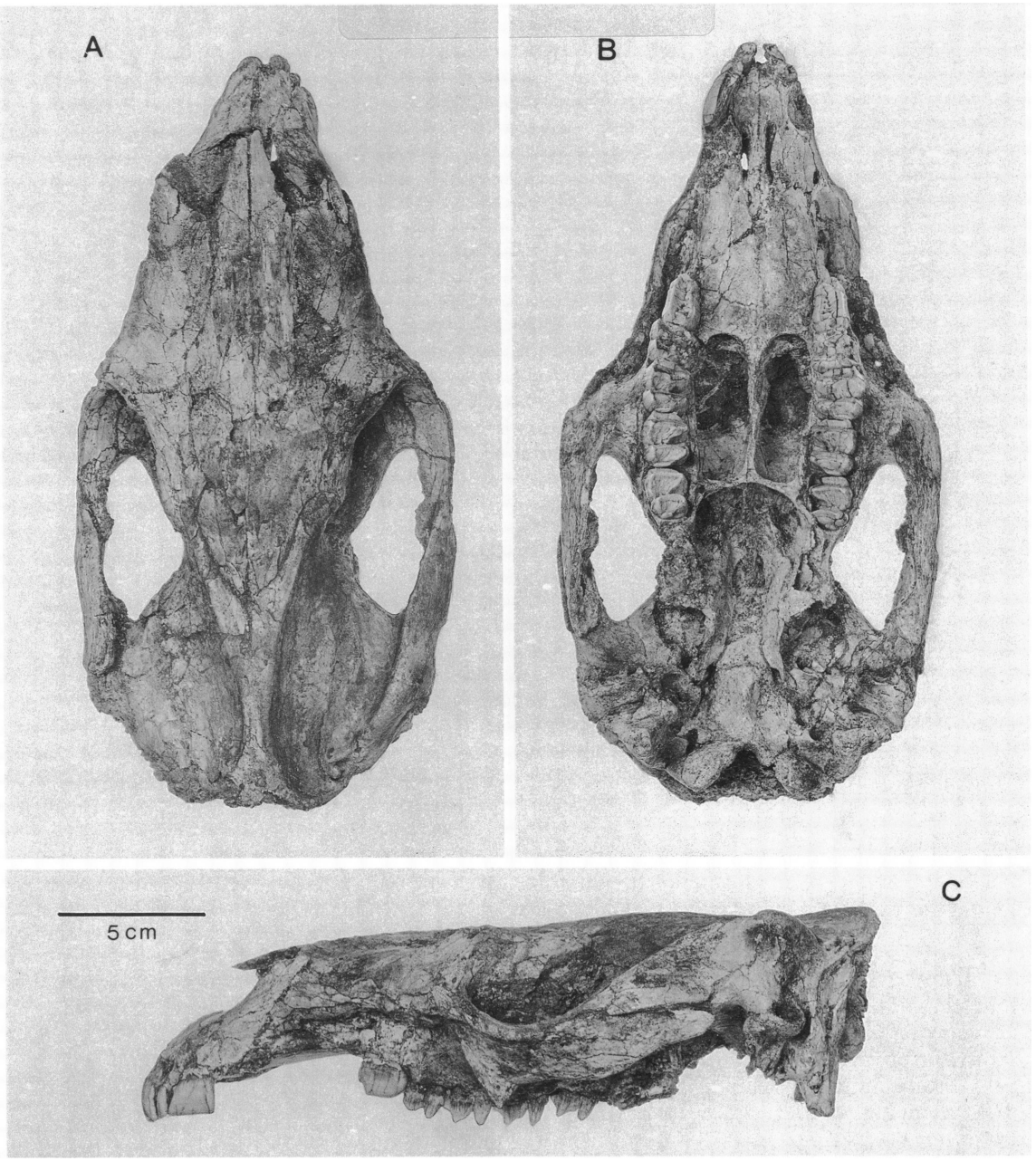

Fig. 11. *Sthenurus tindalei,* referred skull from Lake Callabonna, AMNH 117493. **A,** Dorsal view; **B,** palatal view; **C,** lateral view (reversed).

closely approximate those in *P. goliah.* The single or double condylar foramen is close to the anterolateral lip of the condyles.

The posterior lacerate foramen occurs on the medial aspect and at the base of the paroccipital process. It is surrounded anteriorly by the posteroventral wing of the alisphenoid and dorsally by the exoccipital. The basioccipital abuts the exoccipital posteriorly. Its forward extent in this specimen is concealed, along with the entocarotid canal, beneath the crushed remaining portion of the basisphe-

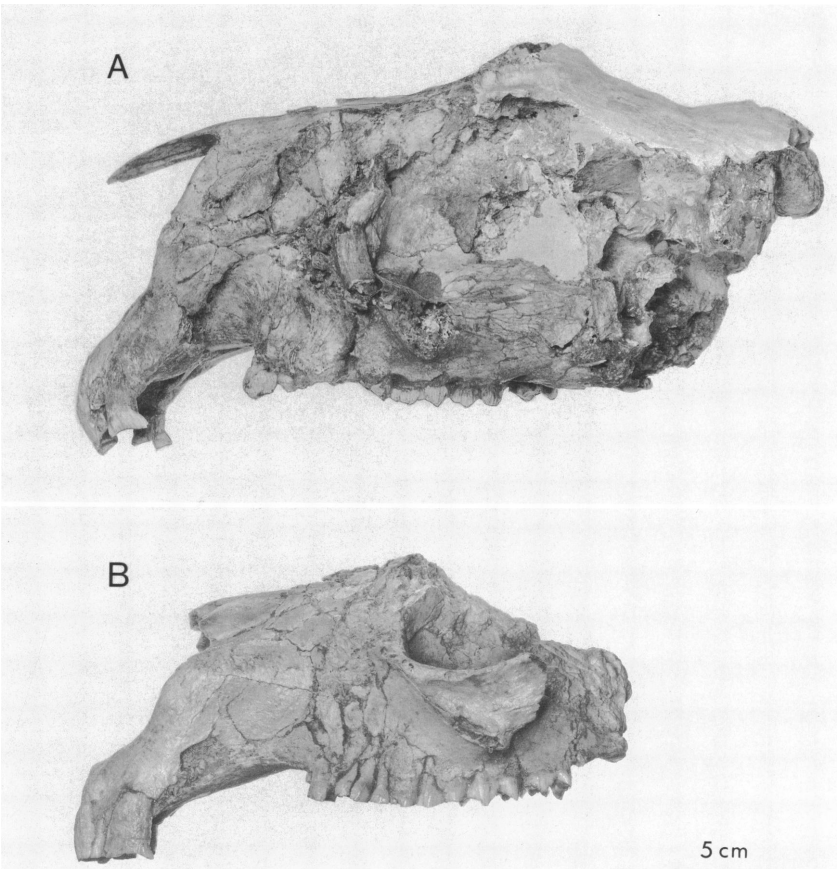

Fig. 12. *Sthenurus tindalei,* referred male skull fragments, AMNH 117491. **A,** Lateral view (reversed). *Sthenurus andersoni,* referred, anterior part of skull from Lake Callabonna, SAM P13672. **B,** Lateral view of skull (reversed).

noid. It appears to lack the prominent ventral keel of *P. goliah* and to be more like *Simosthenurus occidentalis* or *S. brownei* in form.

Only the crushed left anterolateral portion of the basioccipital is visible. It appears to form the medial border of a common fossa containing the petrosal, the opening to the eustachian canal, and presumably the median lacerate foramen and posterior opening of the carotid canal. The opening to the posterodorsally directed foramen ovale lies at the medial aspect of the alisphenoid bulla. Portions of the left and right pterygoids remain attached to the pterygoid process of the palatine, indicating a deep pterygoid fossa. Their contact with the alisphenoid has been severed by distortion of the cranium. Ventrally, the palatine is pierced by the two large palatal vacuities separated and bounded posteriorly by thin transverse palatine bars. Dorsally, the palatine extends into the postorbital region of the skull. At its contact with the ventromedial border of the orbit it abuts the large maxillary foramen, posterior to which it is perforated by the sphenopalatine and orbitopalatine foramina. A similar condition appears to prevail in *S. tindalei* (AMNH 117491, SIAM 35). Details of the postorbital portion of the palatine in the specimen of *S. andersoni* have been obscured because of deformation of the skull.

Upper Dentition (tables 2, 3, 5; figs. 13, 15A–H): The upper incisors of *S. stirlingi* are more robust and higher-crowned than those

of *S. tindalei.* They increase in size in the order I2 I1 I3. They form a V-shaped array as in *S. andersoni,* thereby differing from the more curved array of *S. tindalei.*

I1 is subtriangular in section as in *S. tindalei* and *S. andersoni.* It extends anteriorly beyond the premaxilla, curving ventrally and medially. Its outer enamel surface protrudes below the occlusal plane of the remaining incisors.

I2, as in the other dolichocephalic sthenurines, is much smaller than I1. Its crown is subrectangular in section, with enamel restricted to the labial surface.

I3 is exceedingly large and robust, even in females (e.g., AMNH 117496). Its broad crown tapers to a point posteriorly. It is deeply grooved on the anterolingual surface, which produces a marked lingual ridge. The crown is surrounded by enamel. The I3 in *S. tindalei* is not as broad anteriorly and shows only a shallow groove on the anterolingual surface. There is no evidence of a groove in the subrectangular and well-worn I3 of *S. andersoni.*

The P2 and Dp3 of *S. stirlingi* are represented by broken teeth in the juvenile (AMNH 117495), but enough remains to provide the following information on their morphology: The P2 is shorter than Dp3 or M1, and like the P3, consists of two components, a labial crest composed of two compressed cusps joined into a linear ridge and a lower lingual crest that passes obliquely forward from the posterior end of the tooth to merge with the anterior cingulum. The occlusal outline is wedge-shaped. The valley enclosed by these crests is crossed by two low transverse ridges originating from the bases of the principal cusps of the labial crest. There is no posterolabial cusp on the labial crest as in the P3. Dp3 is similar in all respects to M1 except that the protoloph is narrower than the metaloph.

The P3 of *S. stirlingi* is larger than that of *S. tindalei, Simosthenurus pales,* or *P. goliah.* Morphologically it is almost identical to that of *S. tindalei.* It is subtriangular in occlusal view, long, broad, and high-crowned (maximum labial crown height, SAM P22533: 14.1 mm). The labial crest is high and narrow and parallels the longitudinal axis of the tooth. A number of weak ridglets descend the labial side of the crown to the margin of the labial crest. The posteriormost of these ridglets is larger than the others and forms a posterolabial stylar cusp (Tedford, 1966: fig. 3). A similar feature occurs in the holotype of *S. tindalei* and in two of the three individuals of that species from Lake Callabonna in which the P3 is preserved. The labial and lingual crests enclose a deep median valley. The valley is bridged posteriorly by a strong transverse ridge ascending posteromedially from the labial ridge to the posterior end of the lingual crest, and anteriorly by a ridglet arising from the anterior aspect of the lingual crest. As in *S. tindalei,* the lingual crest is lower than the labial crest and extends the full length of the tooth, curving posterolabially to meet the labial crest and descending anteriorly to merge with the low anterior cingulum that crosses the anterior end of the labial crest as in *S. tindalei.* A number of transverse laminae arise from the lingual crest, but they do not bridge the median valley.

The upper molars of *S. stirlingi* are high-crowned and morphologically similar to those of *S. tindalei,* although they are broader both absolutely and relative to length. The molars increase in length in the order M1 M4 M2 M3. As in *S. tindalei,* the lingual and labial faces of the lophs are convex such that the enamel surface protrudes beyond the alveolar margins. The cheek tooth row is more strongly curved than in *S. tindalei* so that the lophs, when projected, converge lingually to a focus on the masseteric process of the opposite side. The posterior side of the V-shaped median valley is far steeper than the anterior side; the valley is closely labially by a bladelike crest (postparacrista) that arises below the apex of the paracone. The median valley deepens lingual to the weak midlink. The midlink arises from the central part of the protoloph and merges with the postprotocrista. A few low crenulations occur on the posterior surface of the protoloph at the midlink. Comparable structures are more numerous in *S. tindalei* and cover most of the posterior surface of the protoloph and metaloph. A well-developed anterior cingulum extends across the base of the protoloph, curving sharply posteriorly to join the crest of the protoloph at the paracone. A low crest (posthypocrista of Flannery, 1983) arises from the apex of the metaconule ("hypocone") and curves dorsally in

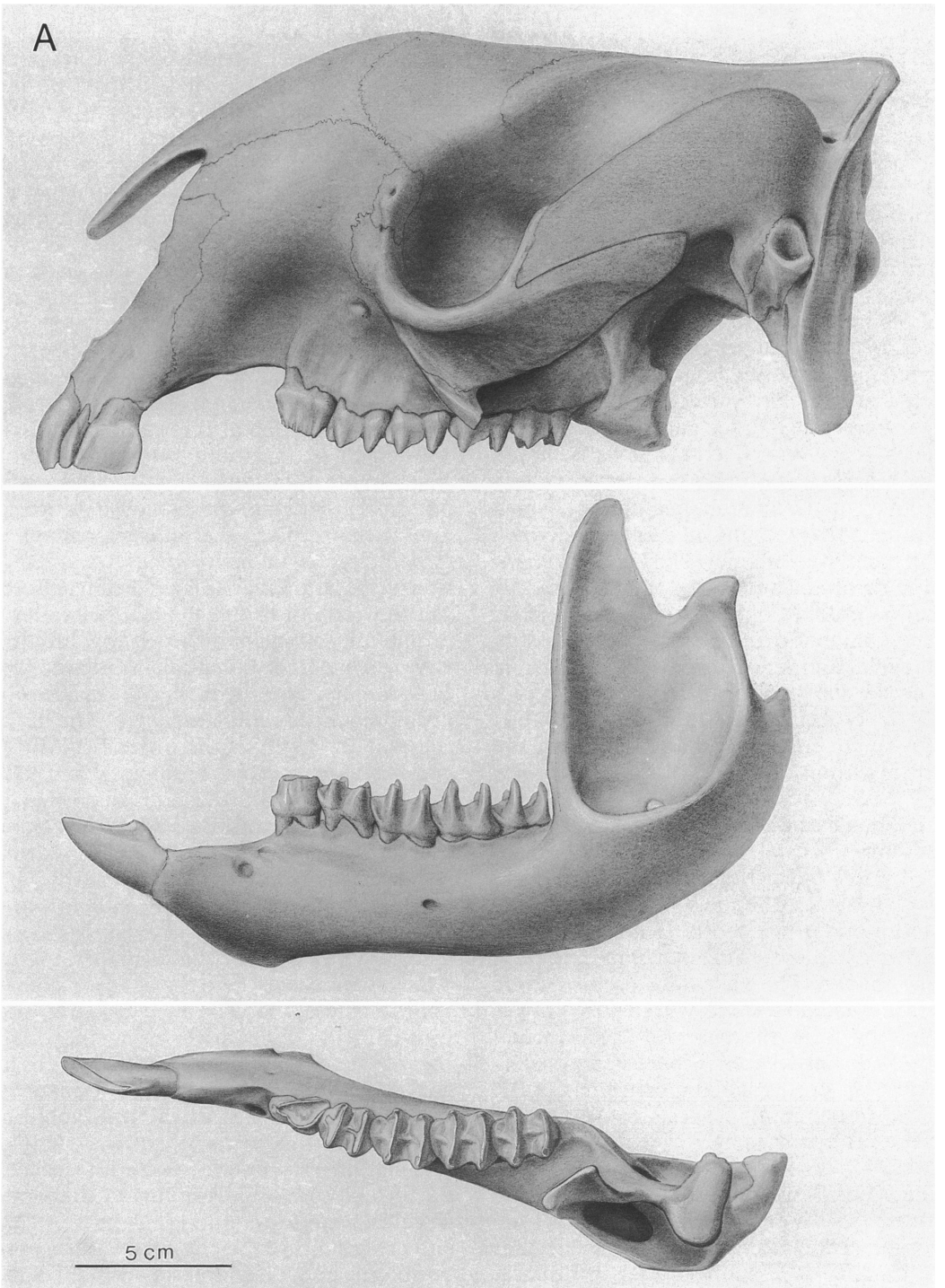

Fig. 13. Reconstructed skulls and rami of *Sthenurus stirlingi* and *S. tindalei* based on all available remains from Lake Callabonna. **A,** *S. stirlingi* lateral view of skull, lateral and occlusal view of ramus; **B,** *S. tindalei* lateral view of skull, lateral and occlusal view of ramus; **C,** *S. stirlingi* dorsal view left, *S. tindalei* dorsal view right; **D,** *S. stirlingi* posterior view left, *S. tindalei* posterior view right; **E,** *S. stirlingi* ventral view left, *S. tindalei* ventral view right.

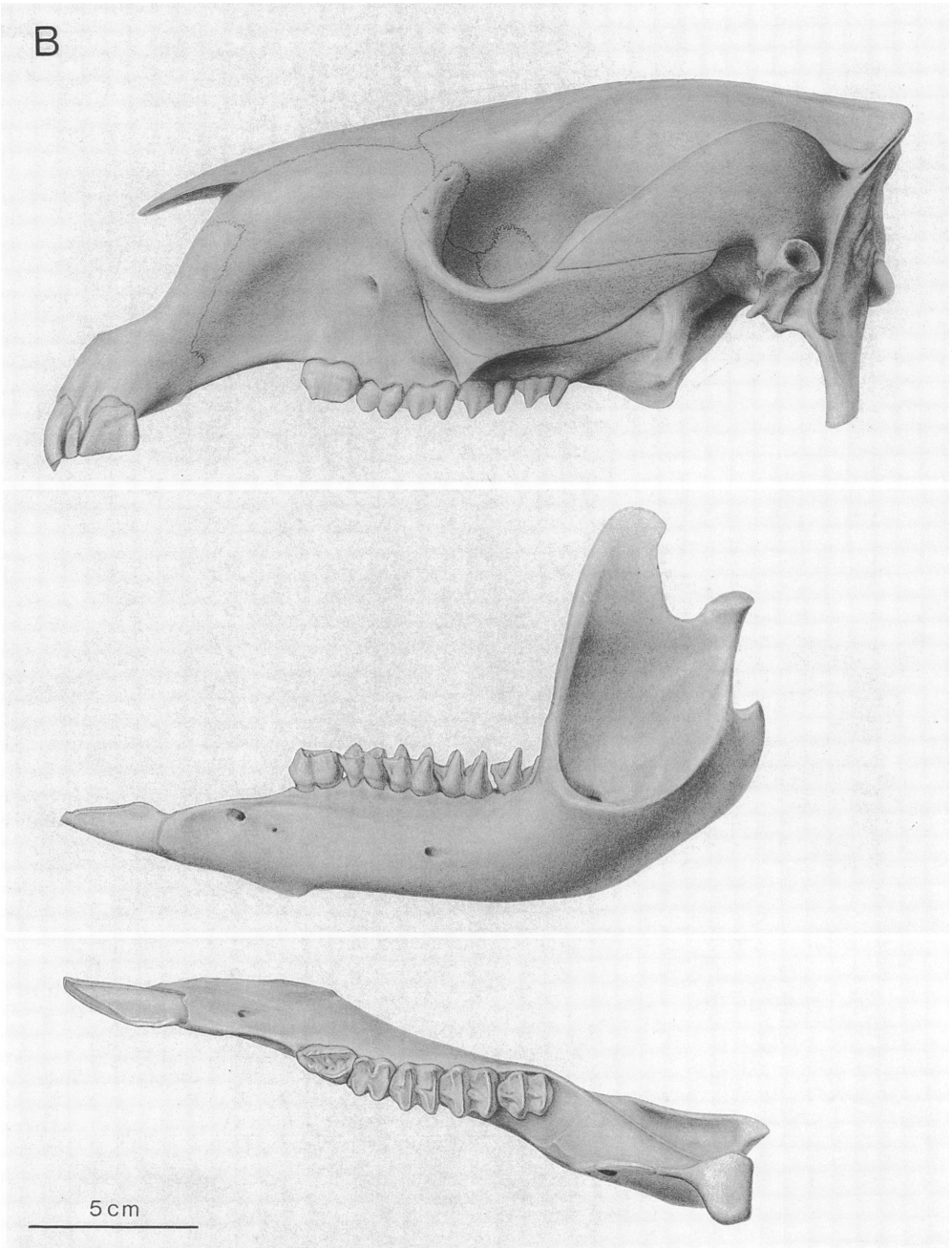

Fig. 13. Continued.

a gentle arc to the posterolabial base of the metaloph. This does not join the very weak postmetacrista. There is no postlink (sensu Flannery, 1983). All these features are similar to those in *S. tindalei* except that a distinct, but short, posterior cingulum occurs in that taxon.

LOWER JAW (fig. 14): The body of the mandible of *S. stirlingi* is long and slender; the ratio of the depth below anterior root m4 to

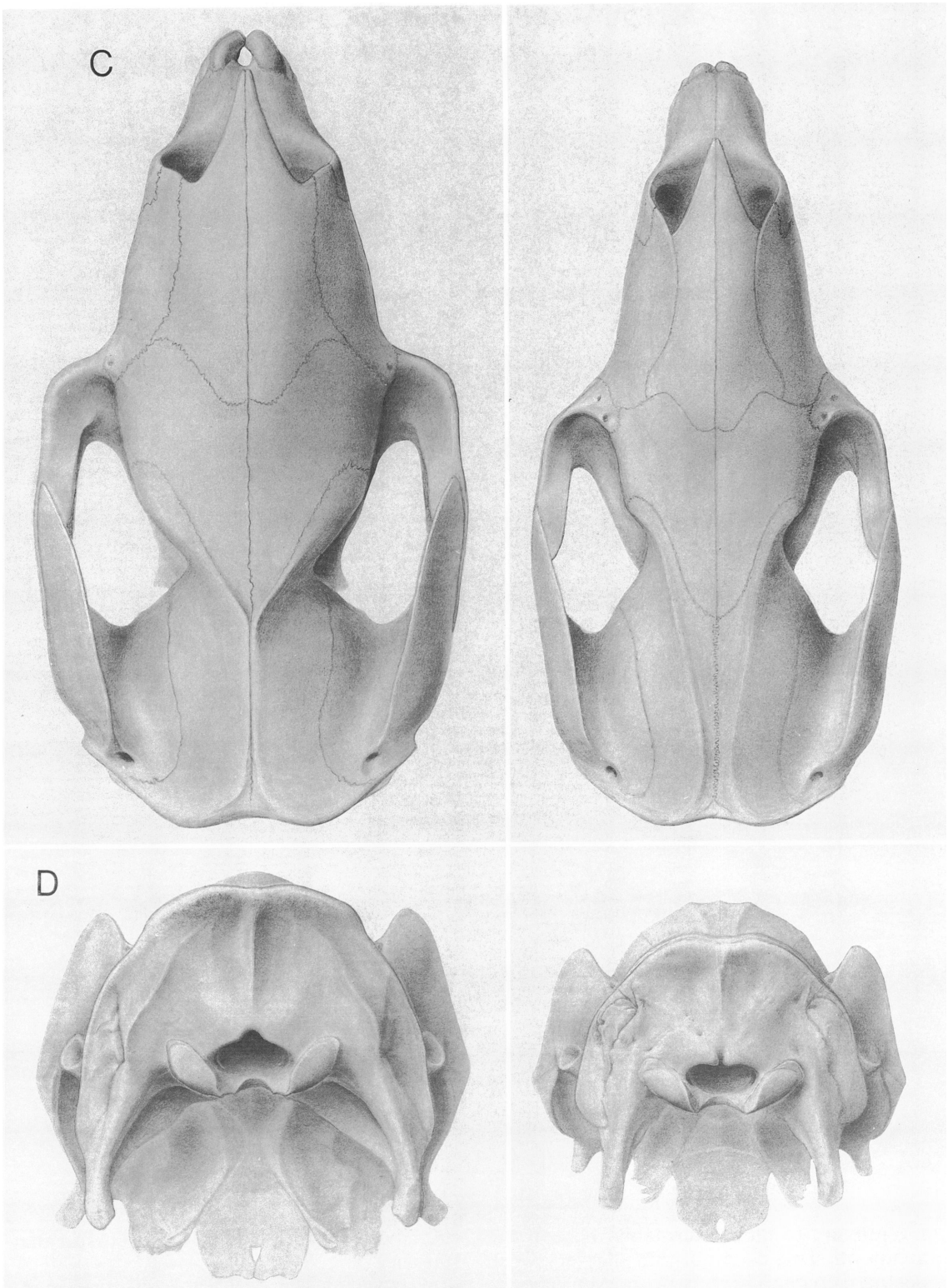

Fig. 13. Continued.

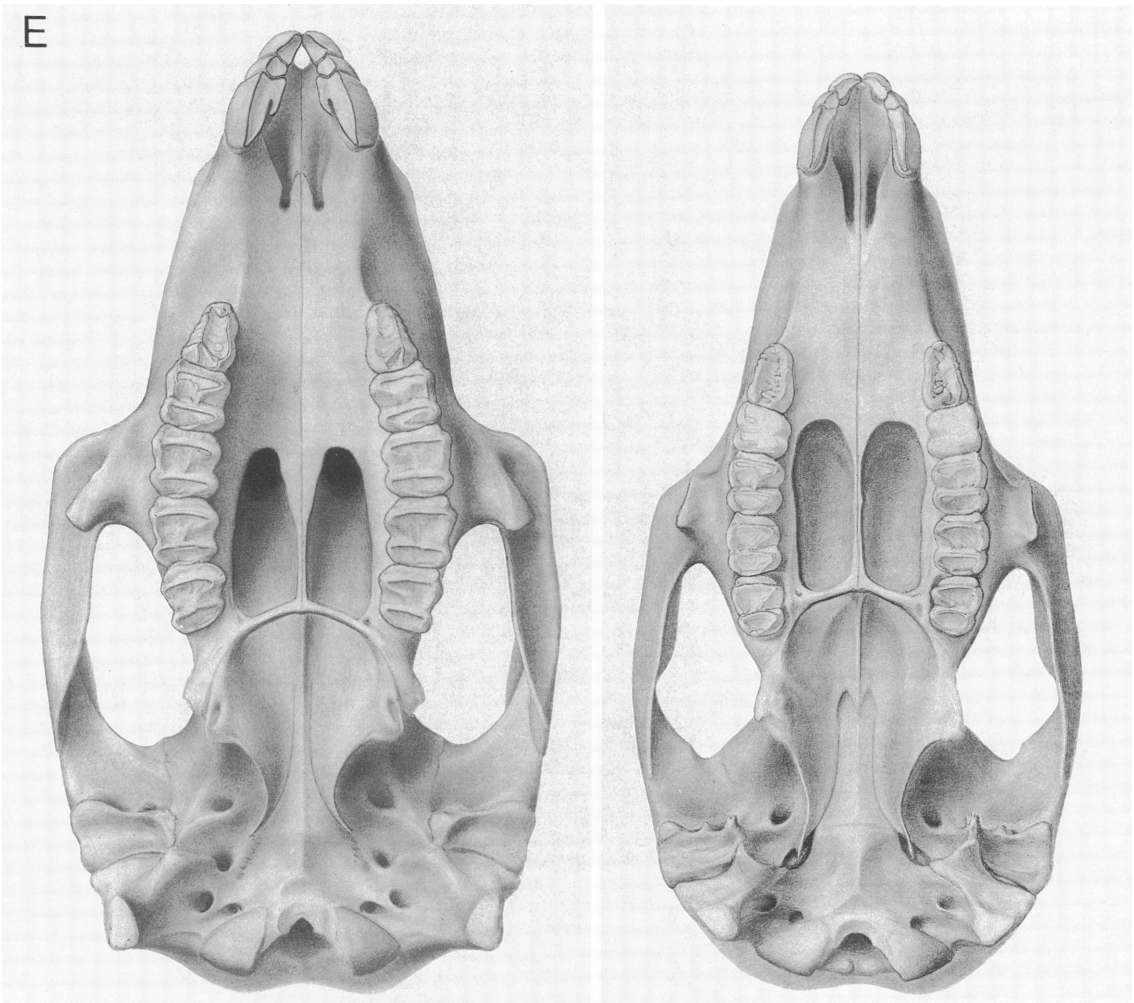

Fig. 13. Continued.

the total length ramus is 0.19, which is identical to adult *S. tindalei* (0.19) and differs markedly from the browsing forms such as *Simosthenurus occidentalis* (0.25), *Simosthenurus brownei* (0.30), and *P. goliah* (0.23). The symphysis extends posteriorly and ventrally just beyond the single genial pit to a point below the posterior root of p3. The i3–p3 diastema is 34.0 mm, which is shorter relative to the length of the mandible (ratio of 0.16) than in *S. tindalei* (0.20), and shows greater affinities with brachycephalic forms such as *P. goliah* (0.16), *S. brownei* (0.18), and *S. occidentalis* (0.14). The large mental foramen is positioned anterior to p3 and just below the dorsal margin of the diastema. The buccinator muscle scar arises dorsoposterior to the mental foramen and extends as a shallow groove posteroventrally to below the posterior root of m1. An anteriorly directed mandibular or posterior mental foramen (Tedford, 1966, 1967) lies in the midlateral aspect of the mandible below the posterior root of m2. The molar tooth row is more strongly convex labially than in *S. tindalei,* and the occlusal plane is rotated ventrolingually posteriorly and ventrolabially anteriorly. The anterior root of the ascending ramus lies behind m4 as in *S. tindalei* and *S. andersoni,* a more posterior position than in

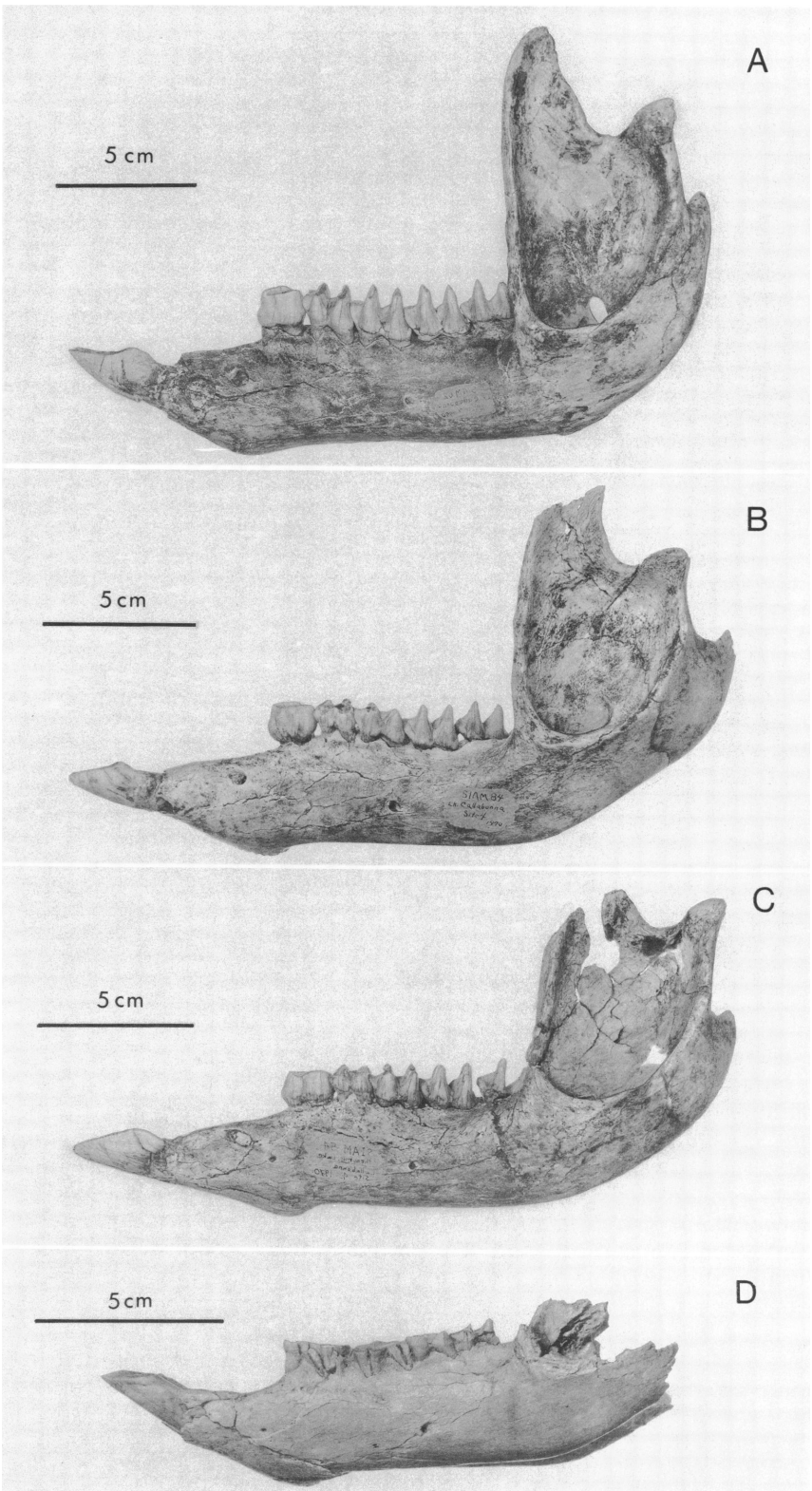
A
5 cm
B
5 cm
C
5 cm
D
5 cm

the adult brachycephalic sthenurines. The anterior edge of the ascending ramus forms a right angle with the horizontal axis of the mandible in the Callabonna taxa. The masseteric crest is strongly developed and extends from the temporal ridge to the neck of the condyle, reaching as low as the level of the m4 alveolar margin where it forms the lateral border of the large elliptical masseteric foramen. The masseteric canal does not appear to invade the body of the mandible, but lies adjacent to the inferior dental canal. The dorsal border of the large mandibular foramen extends to the level of the occlusal plane of m4 and, unlike *S. tindalei* and *S. andersoni,* is clearly visible above the ventral margin of the masseteric crest. A long narrow digastric sulcus arises ventromedially below the posterior root of m3 and passes posteriorly beneath the angle of the jaw. This sulcus is broader and shallower in *S. tindalei* and *S. andersoni* than in *S. stirlingi.* The digastric process forms a medially directed ventral lip of the digastric sulcus. The angular process arises from the posteromedial aspect of the mandible and sweeps dorsally in a smooth arc to a point below and posterior to the condyle. It encloses the broad and deep angular fossa that holds the pterygoid musculature. The articulating surface of the condyle is broad laterally, tapers medially, and is tilted anteromedially. Medially, the condyle of *S. stirlingi* bears a process that descends anteriorly and merges with a crest, enclosing a fossa medial to the neck of the condyle. The crest, but no corresponding fossa, is found in *S. tindalei.* The height of the condyle above the ventral border of the ramus relative to the length of the jaw (ratio 0.54) is similar to that of *S. tindalei* (0.50) and differs from the more elevated position in brachycephalic forms such as *P. goliah* (0.82), *S. brownei* (0.68), and *S. occidentalis* (0.63). The tall bladelike coronoid process is deflected posteromedially and is curved posterodorsally at its distal end.

LOWER DENTITION (tables 4, 5; figs. 13, 14, 15I–N): The lower incisor of *S. stirlingi* lies at an angle between 30° and 40° to the axis of the mandible, similar to *S. andersoni, Simosthenurus occidentalis,* and *Simosthenurus brownei* and markedly different from the very procumbent 10–30° of *S. tindalei.* The long scalpriform crown is more similar in form and wear pattern to that of *S. occidentalis* than that of *S. tindalei.* Enamel is absent on the lingual faces of the incisor in early wear in *S. stirlingi* as in other species of *Sthenurus* and *Macropus.*

The p3 of *S. stirlingi* is proportionally a shorter and broader tooth than that of *S. tindalei.* It is high-crowned (maximum labial crown height, SAM P22533, SIAM 62: 11.5 mm). The smooth lingual face of the crown is formed by a relatively straight lingual crest lying obliquely to the axis of the mandible and parallel with the sagittal plane. The labial crest descends anteriorly and joins the lingual crest at the anterior cusp. It is markedly convex labially over the posterior two thirds of the tooth. The labial and lingual crests enclose a broad median valley. Anteriorly, a small ridglet arises from the lingual crest and extends partway into the valley; posteriorly, the valley is obstructed by a medial eminence arising from a transverse ridglet. The posteromedial opening of the median valley is a prominent feature of both *S. stirlingi* and *S. tindalei.*

The high-crowned lower molars of *S. stirlingi* are morphologically similar to those of *S. tindalei.* They are much broader relative to length than those of *Simosthenurus occidentalis, S. brownei, S. pales,* or *P. goliah.* They increase in size in the order m1 m4 m2 m3 and are all essentially similar in structure. They have nearly straight lophids with convex labial and lingual surfaces that protrude beyond the alveolar margin. As in the upper molars, the lophids of the lower molars of *S. stirlingi* converge slightly medially in contrast with the parallel lophids of *S. tindalei.* A broad

←

Fig. 14. Lower jaws of *Sthenurus stirlingi,* **A,** holotype, SAM P22533 (reversed); *S. tindalei,* **B,** male, AMNH 117499, and **C,** female, AMNH 117493 (reversed); and *S. andersoni* **D,** SAM P13672. (All to same scales as corresponding skulls, figs. 10–12.)

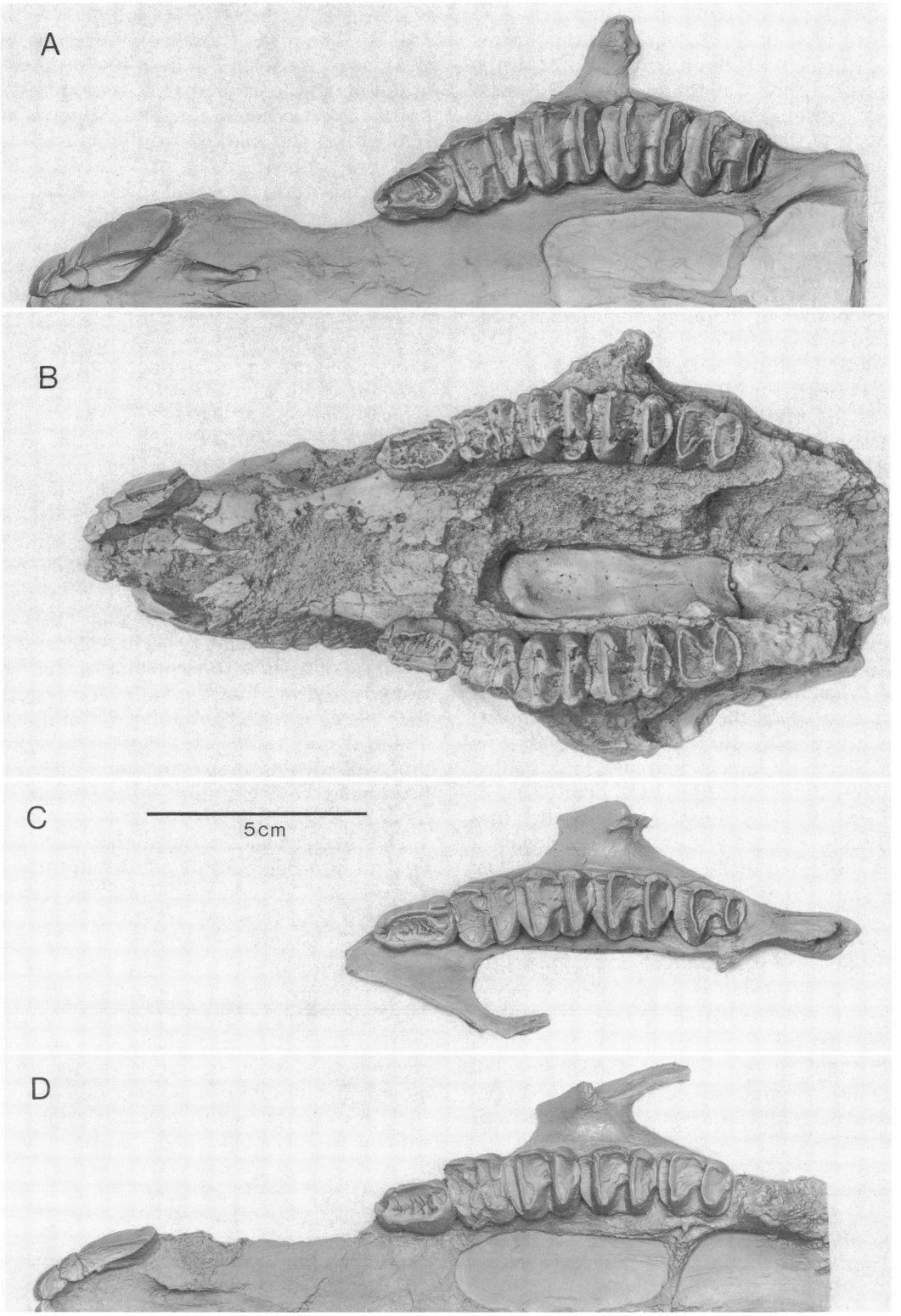
A
B
C
5cm
D

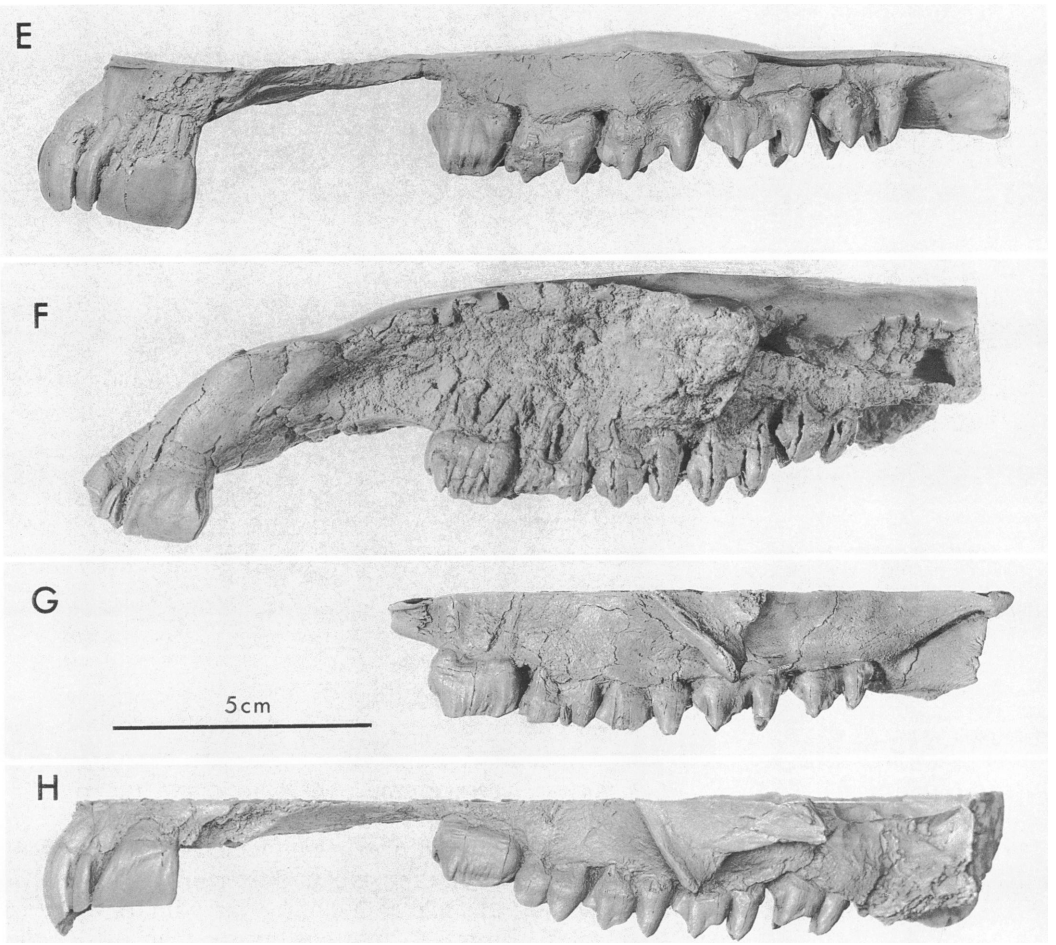

Fig. 15. Continued.

anterior cingulum extends from near the lingual base of the protolophid to the midline of the tooth where it is intersected by a narrow forelink; labial of the forelink it forms a broad shelf that tapers and curves ventrally to the anterolabial corner of the lophid. The forelink, although weak, forms a sharp crest that originates medially and ventrally of the protoconid, arching lingually and ventrally to cross the anterior cingulum in the midline of the tooth. There is no premetacristid, a feature also lacking in *S. tindalei* and weakly developed in *S. andersoni.* A weak midlink arises just below the crest of the hypolophid labial to the midline and descends to meet the posterior face of the protolophid in the midline of the tooth. A low posterior cingulum extends across the base of the crown. As in *S. tindalei,* no crenulations can be detected on the anterior faces of the lophids.

←

Fig. 15. Upper dentitions, occlusal and lateral views. *Sthenurus stirlingi,* **A, E,** SAM P22533; *S. tindalei,* **B, F,** holotype, SAM P138201, **C, G,** AMNH 117499, and **D, H,** AMNH 117493 (reversed). Lower dentitions, occlusal and lateral views. *Sthenurus stirlingi,* **I, L,** holotype, SAM P22533; *S. tindalei,* **J, M,** AMNH 117499, and **K, N,** AMNH 117493 (reversed).

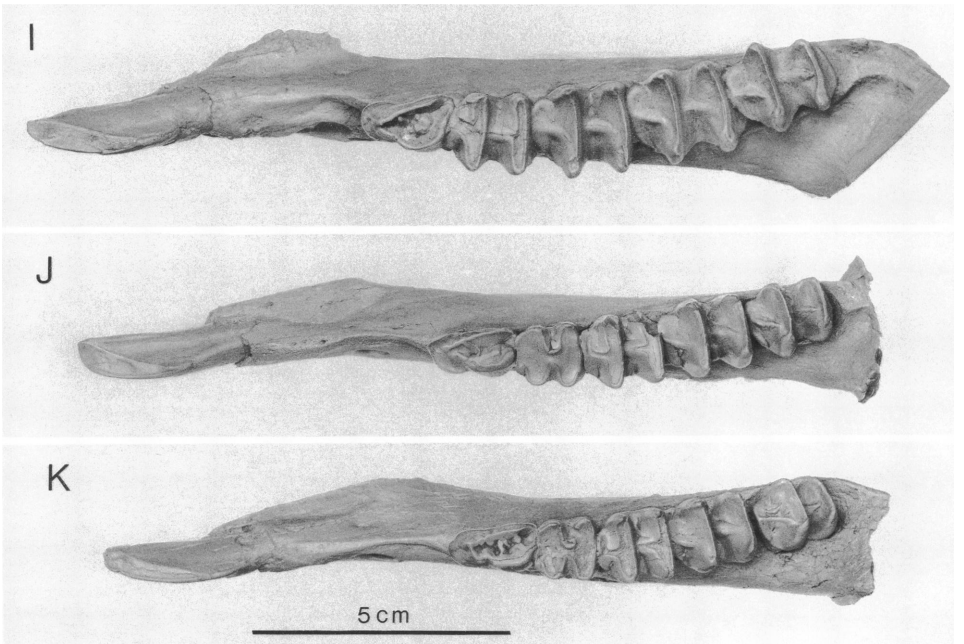

Fig. 15. Continued.

ATLAS (table 6; fig. 16A–D): Atlas vertebrae of *S. stirlingi* (SAM P22533, AMNH 117496) and *S. tindalei* (AMNH 117493) are compared with those of *M. giganteus* (AMNH 2390). The vertebrae of both sthenurine species are similar in form and size in the females of *S. stirlingi* (AMNH 117496) and *S. stirlingi* (AMNH 117493). They are proportionally shorter, broader, and more dorsoventrally flattened than in *M. giganteus*. Unlike adult *Macropus*, the ventral arch is not closed by the neurapophyses as they extend only marginally beyond the medial border of the condylar cusps. The diapophyses are expanded at their distal ends; they are more robust in *S. stirlingi* and *S. tindalei* (even in females) than in *Macropus* and are deflected more caudally.

AXIS (table 6; fig. 16E–I): Only the caudal portions of the neural arch and the left pleurapophysis are missing from the male *S. stirlingi* axis (SAM P22533). An axis of a female (AMNH 117496) lacks parts of the neural arch and both pleurapophyses. The female *S. tindalei* axis (AMNH 117493) comprises a centrum and odontoid process, but a male (AMNH 117499) lacks only the anterior process of the neural arch and the right zygapophysis and pleurapophysis. The neural arch in *S. stirlingi*, which is thickened anteriorly and tapers posteriorly, is proportionally higher and narrower, with the apex rising more steeply posteriorly than in *M. giganteus*. The neural arch does not extend as far over the cranial and caudal articular surfaces of the vertebral body as it does in *M. giganteus*. The slender pleurapophyses extend more laterally and caudally than in *M. giganteus*. The large prezygapophyses completely cover the forepart of the centrum on either side of the relatively broad odontoid process. The axis in *S. tindalei* suggests a similar morphology to that of *S. stirlingi*, differing only in the slightly shallower and more elongate centrum and larger prezygapophyses.

CERVICAL VERTEBRAE (table 7; fig. 17): Cervical vertebrae 3–7 are present in *S. stirlingi* (SAM P22533). Only the 5th and 7th cervical vertebrae (AMNH 117491 and AMNH 117499, respectively) are preserved in *S. tindalei*. Fragmentary 5th and 6th, and nearly complete 7th of *S. andersoni* (SAM P13673) are available. These vertebrae, with their remarkably short, almost platycoelous centra

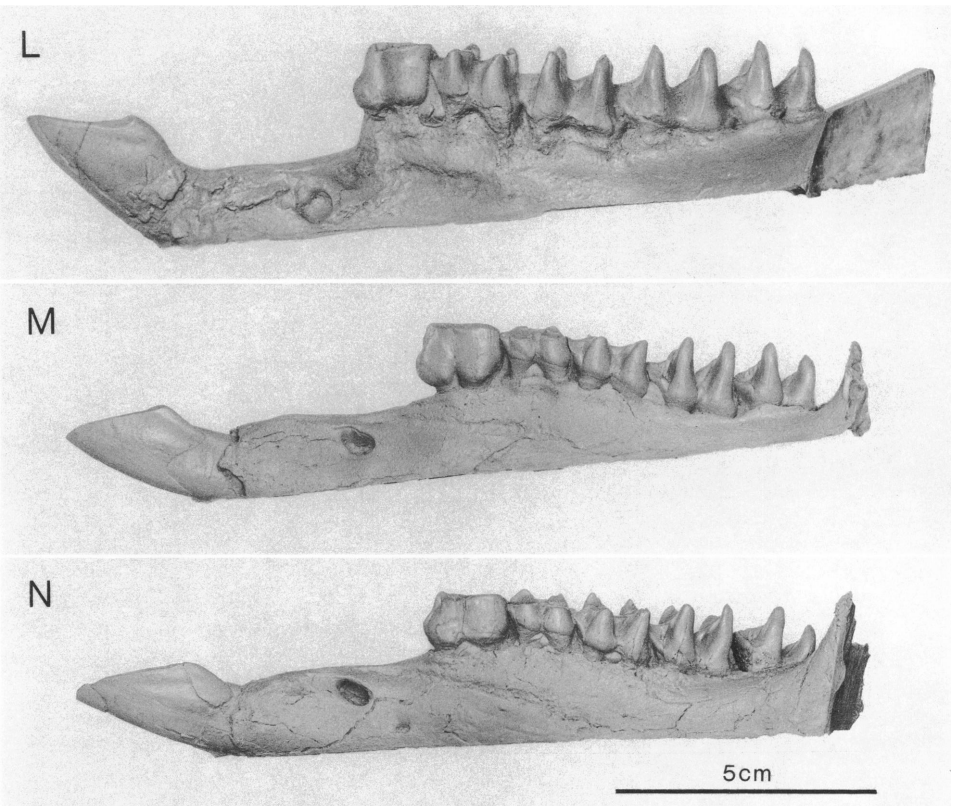

Fig. 15. Continued.

and their slender neural spines, are similar to those of *P. goliah* (Tedford, 1967: fig. 22). They are easily distinguishable from the long, procoelous, low-crested cervicals of *Macropus* species. The resulting cervical column is relatively short, as in the rat-kangaroo (*Bettongia* sp.). The neural arch is narrow and vaulted, enclosing an almost triangular neural canal. The neural spines are relatively short and slender. The spine of cervical 3 is the highest, with gradual decreasing height to cervical 7. The more robust neural spines of cervicals 3 and 5 have slightly inflated rugose areas on the posterior aspect of the apex that serve as sites of attachment for the supraspinous ligaments.

The pleurapophyses are long and slender; those of cervicals 3, 4, and 5 are deflected caudally, whereas those of cervicals 6 and 7 project laterally, almost at right angles to the sagittal plane. Weak parapophyses extend anteriorly as narrow flanges from the base of the pleurapophyses of cervical 5 and develop into large oval rugosities on cervical 6. They are absent from cervicals 3, 4, and 7. The 6th cervical vertebra of *S. tindalei* is essentially similar in form to that of *S. stirlingi,* but, as with the axis of this species, the centrum is slightly shallower and not as wide. The 5th, 6th, and 7th cervical vertebrae of *S. andersoni* are essentially similar to those of *S. stirlingi* and *S. tindalei,* differing only in the knoblike form of the distal pleurapophysial processes of the 7th cervical vertebra.

THORACIC VERTEBRAE (table 8; figs. 18, 19): Thoracic vertebrae numbers 1–4 and fragments of 11 and 12 (SAM P22533), 1, 2, and 5 (AMNH 117496), and 5 (AMNH 117494) represent *S. stirlingi.* Vertebrae 4–8 and 10–13 (AMNH 117493) and 4–6, 9, and 13 (AMNH 117499) represent *S. tindalei.* Most are complete but for the tips of the neural spines. *S. andersoni* is represented by a complete 1st thoracic and fragmentary centra of

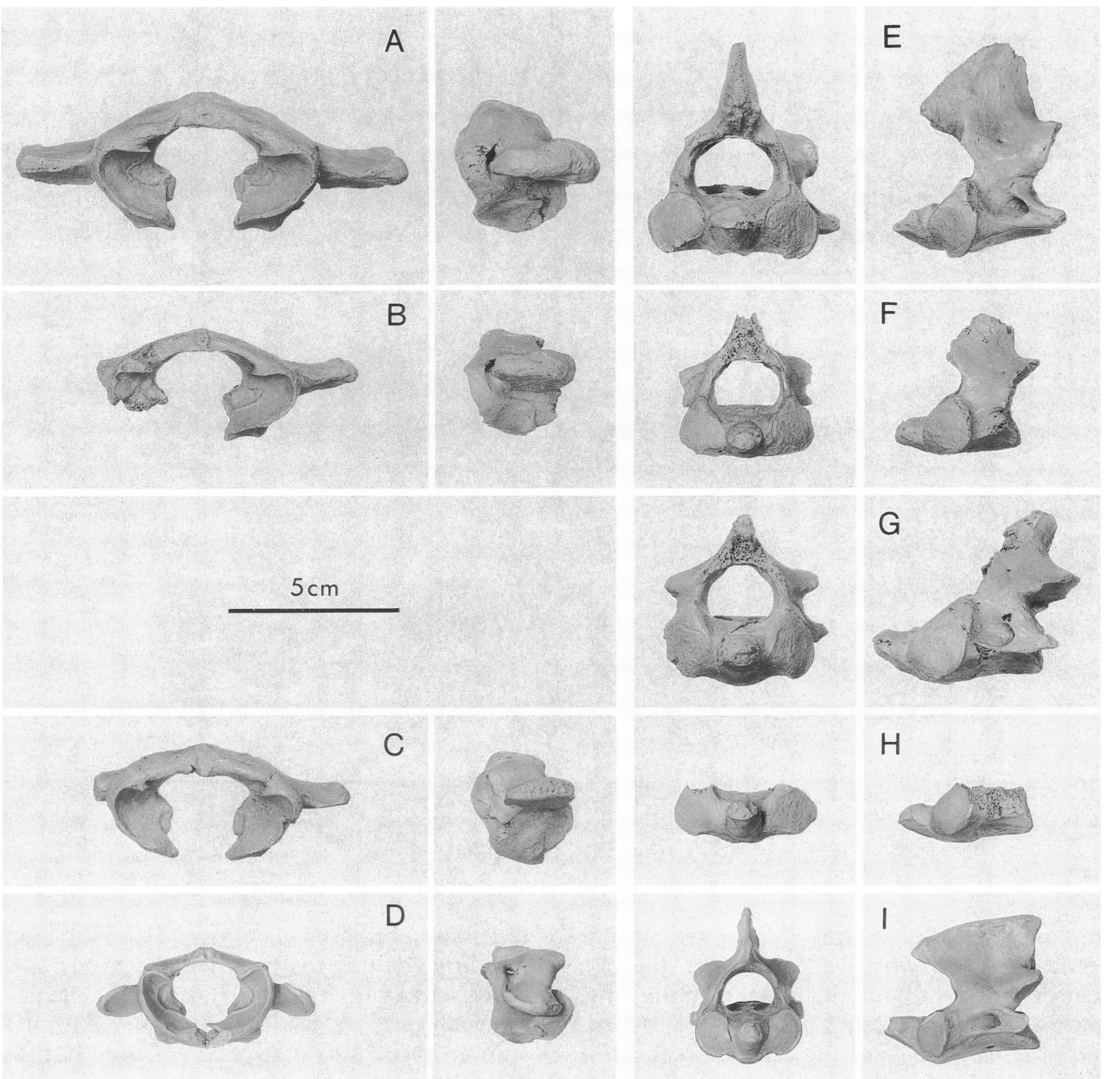

Fig. 16. Comparative anterior and lateral views of the atlas (left) and axis (right) vertebrae, respectively, of *Sthenurus stirlingi,* **A, E,** holotype, SAM P22533 (reversed), and **B, F,** AMNH 117496; *S. tindalei,* **G,** AMNH 117499, **C,** AMNH 117493 (reversed), and **H,** AMNH 117493; and *Macropus giganteus,* **D, I,** AMNH 2390.

2–4 and 6–8. As in *P. goliah* (but unlike *M. giganteus*), the thoracic centra of all three sthenurine species are short and deep and very slightly opisthocoelous. Similarly, the centra of the 1st and 2nd thoracics lack the midventral keel of *M. giganteus.* The pre- and postzygapophyses are relatively small compared with those of *M. giganteus.* The neural spines, where preserved, are proportionally similar in height to those of *M. giganteus,* but do not taper distally. As in the latter species, the neural spine of the 2nd thoracic vertebra in *S. stirlingi* (SAM 22533) is the tallest. In all preserved thoracic vertebrae, both the anterior and posterior aspects of the base of the neural arches are deeply excavated where they attach to the axial musculature, similar to those described for *P. goliah* (Tedford, 1967). The thoracic vertebrae of *S. stirlingi* may be distinguished from those of *S.*

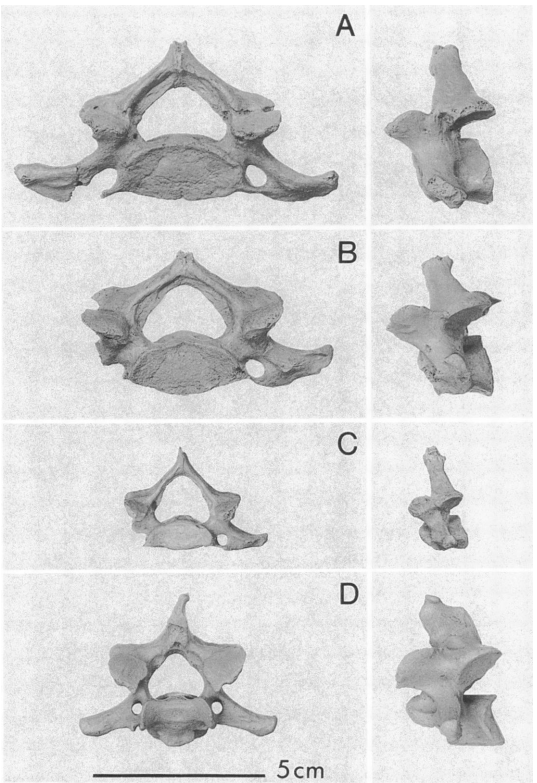

Fig. 17. Comparative anterior and lateral views of the 7th cervical vertebra of *Sthenurus stirlingi,* **A,** holotype, SAM P22533; *S. tindalei,* **B,** AMNH 117499; *S. andersoni,* **C,** SAM P13673 (reversed); and *Macropus giganteus,* **D,** AMNH 2390.

tindalei based not only on size but also by the more posteriorly directed neural spines. This posterior declination is also pronounced on the 1st thoracic, the only spine preserved in *S. andersoni.* A short, broad metapophysis first appears on the 11th thoracic or anticlinal vertebra in *Macropus.* Indeed, in *Macropus* species, the anticlinal vertebrae are easily distinguished by the reinforcement of the prezygapophysial process by the adjacent metapophysis to provide a buttress against posterior movement of the proceeding postzygapophysis. In *M. giganteus* and *M. rufa,* the anticlinal vertebrae were thoracics 10 and 11; in *M. robustus,* they were 9 and 10. The anticlinal vertebra is the 2nd lumbar in *S. stirlingi* and the 1st lumbar in *S. tindalei.* In neither case is there any modification of the zygapophyses (as seen in *Macropus* species). In these sthenurines, metapophyses first appear on the 11th thoracic and increase dramatically in size in both the 12th (SAM 22533; AMNH 117493) and 13th (AMNH 117493) thoracics. There is no caudal costal fovea and only a very small cranial one on the 13th thoracic vertebra (AMNH 117493). Beyond the 4th thoracic the transverse processes are short, blunt, and rounded; they also lack the well-developed rim to the costal fovea that occurs in *M. giganteus.*

LUMBAR VERTEBRAE (table 9; fig. 20): Matching the articular surfaces of the centra suggests the presence of six lumbar vertebrae in both sthenurine species. Lumbars 1–4 and 6 (SAM P22533) and centra of 4 and 6 (AMNH 117496) are present in *S. stirlingi,* 1, 2, and 4–6 (AMNH 117493) in *S. tindalei,* and centra of 2–6 in *S. andersoni.* The lumbar series of both sthenurine species are morphologically similar in their almost platycoelous centra; they differ markedly from those of *Macropus* in the vestigial nature of the diapophyses and almost total absence of anapophyses. The exceedingly long metapophyses are deflected more medially than in *M. giganteus* and they do not show the marked serial reduction in size passing posteriorly. Sufficient neural spine is preserved in the 6th lumbar of *S. stirlingi* to indicate a reduction in size over those preceding it. A foreshortening of the ventral border of the 2nd lumbar vertebra in *S. stirlingi* is responsible for arching of the backbone about this point. This is considered the anticlinal vertebra, although the neural spine is deflected caudally, as occurs in all lumbar vertebrae of this species. In *S. tindalei,* the lumbar vertebrae form a gentle arc and there is no distinctive bend at the 2nd lumbar, as in *S. stirlingi.* Furthermore, the neural spines (except the 6th) appear to extend approximately at right angles to the axis of the centrum. In *S. andersoni,* the lumbar series forms a gentle arc, as in *S. tindalei.* The neural arch, pre- and postzygapophyses, and proximal fragments of the diapophyses are preserved only on lumbar 3; they are similar in form to those of *S. stirlingi.*

In the three sthenurine species, the proportionally longest centrum occurs at the 4th lumbar vertebra. The arc formed by the axes of the distal lumbar centra is not continuous

with the axes of the centra of the sacrum, as in *M. giganteus* (fig. 36).

SACRUM (fig. 21): The sacrum of *S. tindalei* (AMNH 117493) consists of two fused platycoelous vertebrae as in *S. stirlingi* (AMNH 117496) and *S. andersoni.* The sacrum is relatively broader and shorter than in *M. giganteus.* In *S. stirlingi* and *S. tindalei* both the pre- and postzygapophyses are proportionally smaller and more widely spaced than in *M. giganteus.* These structures are not preserved in the *S. andersoni* specimen. Only the damaged bases of the neural spines remain in the two larger species; these are proportionally shorter than in *Macropus.* The large sacroiliac connection in *S. stirlingi* and *S. tindalei* extends more dorsally and its anterior edge is inclined more steeply (75°) to the axis of the sacrum than in *M. giganteus* or *S. andersoni* (45°). This may be a function of size, as similar changes in proportion were observed in larger richochetal rodents (Hatt, 1932).

The sacrum of *S. stirlingi* is similar to that of *S. tindalei,* but the caudally deflected neural spine of the 6th lumbar suggests a more rigid sacrolumbar connection in the former species than in either *S. tindalei* or *M. giganteus* due to the closer juxtaposition of the adjacent neural spines. In *S. tindalei* the neural spine of the 6th lumbar is deflected more anteriorly than in *S. stirlingi*; in combination with the relatively reduced metapophyses, it suggests a more flexible sacrolumbar ligamentous connection in this species.

CAUDAL VERTEBRAE (table 10; fig. 22): Caudal vertebrae 3–14 (AMNH P22533) and 1–7 and ?12 (AMNH 117496) represent *S. stirlingi,* and 2–5, 7–16, and ?20 (AMNH 117493) represent *S. tindalei.* Vertebrae 1–17 of *S. andersoni* were recovered. In both large sthenurine species the centra increase in length up to the 9th caudal, beyond which they decrease to the tip of the tail; however,

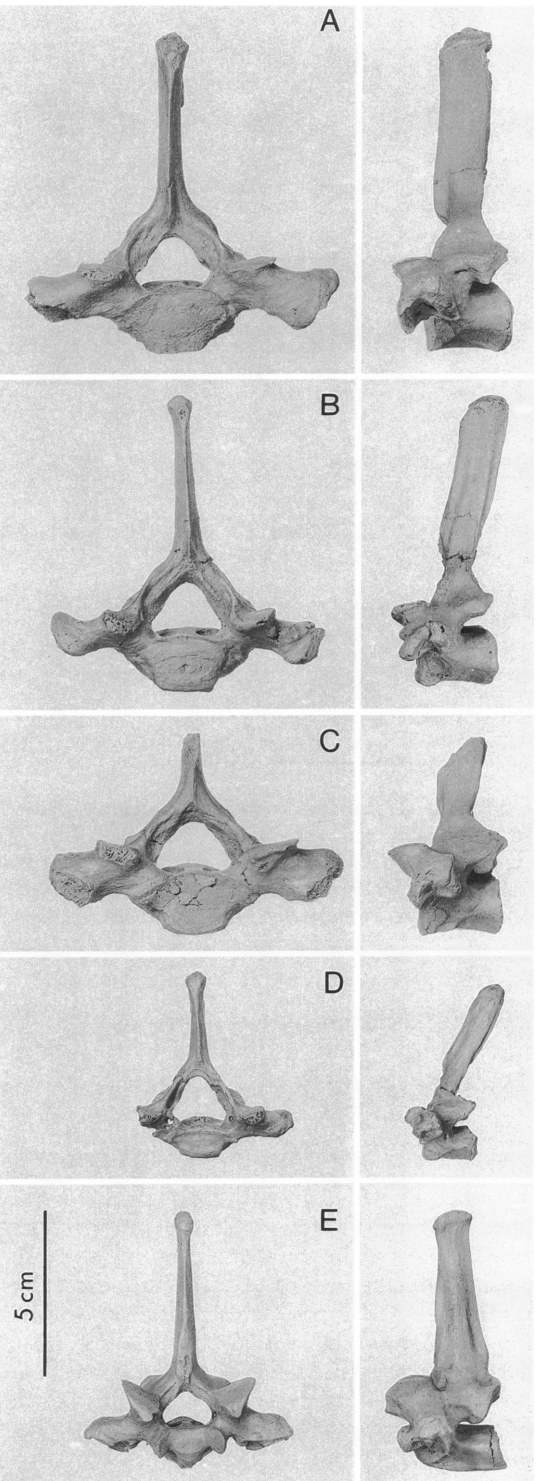

→

Fig. 18. Comparative anterior and lateral views of the first thoracic vertebra of *Sthenurus stirlingi,* **A,** holotype, SAM P22533, and **B,** AMNH 117496 (reversed); *S. tindalei,* **C,** AMNH 117499; *S. andersoni,* **D,** SAM P13673; and *Macropus giganteus,* **E,** AMNH 2390.

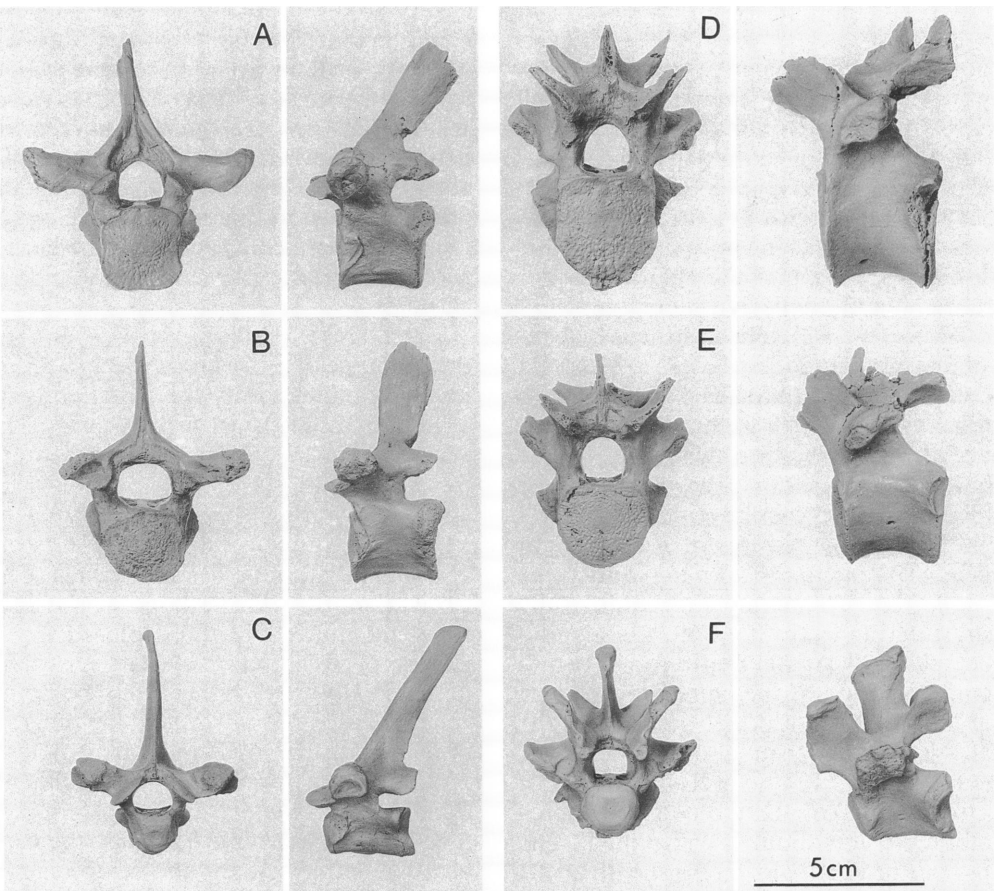

Fig. 19. Comparative anterior and lateral views of the 4th (**A–C**) and 12th (**D–F**) thoracic vertebrae of *Sthenurus stirlingi,* **A,** holotype, SAM P22533 (reversed); *S. tindalei,* **B,** AMNH 117499; *Macropus giganteus,* **C,** AMNH 2390; *Sthenurus stirlingi,* **D,** holotype, SAM P22533; *S. tindalei,* **E,** AMNH 117493 (reversed); and *Macropus giganteus,* **F,** AMNH 2390.

in the smaller *S. andersoni,* the 6th caudal is the largest. In *S. stirlingi* the caudal centra have proportionally greater dorsoventral diameters than in the other macropodid species examined. Prezygapophyses project anteriorly from the metapophyses of the first five caudal vertebrae as in *M. giganteus.* The neural arches are short and broad, and, like *P. goliah* (Tedford, 1967), lack a neural spine and have rugose areas both anteriorly and posteriorly for insertion of the axial musculature. The first five caudals are similar in both large sthenurine species and are easily distinguished from those of *Macropus* by their relatively short centra and distinctive diapophyses. The diapophysis of the 1st caudal (AMNH 117496) of *S. stirlingi* and *S. andersoni* extends the full width of the centrum and projects posterolaterally as a ventrally deflected slender spine. The diapophysis of the 2nd caudal in the larger species, as well as that of the smaller *S. andersoni,* arises just posterior to the anterior edge of the centrum, extends to the posterior edge, and projects laterally and ventrally. Distally, the tip is deflected ventrally and in the larger species carries a large anteriorly directed, transverse dorsal facet. The diapophysis of the 3rd caudal in *S. stirlingi* and *S. tindalei,* which is slightly narrower than that of the 2nd, sweeps posterolaterally to terminate in an expanded posteroventrally deflected process similar to that of *M. giganteus.* Only the proximal portions of these vertebrae are preserved in *S.*

andersoni. The diapophysis of the 4th caudal in the larger species is essentially similar to that of *M. giganteus,* whereas that of the 5th sweeps posterolaterally to terminate in a small transverse process, rather than in a lateral one. The diapophyses of the 4th and 5th caudals are not preserved in *S. andersoni.* All caudals beyond the 5th are similar to those of *M. giganteus,* differing only in the relative length of the centra and the slightly shorter and more laterally deflected metapophyses.

CHEVRONS (fig. 23): The distinctive chevrons of the 1st to 2nd (SAM P22533, AMNH 117496), 2nd to 3rd (AMNH 117496) 5th to 6th, 6th to 7th, and 7th to 8th (SAM 22533) caudals of *S. stirlingi* are available. Of the remaining caudal series, five chevrons for SAM P22533 and three chevrons for AMNH 117496 were recovered for *S. stirlingi,* eight (AMNH 117493) for *S. tindalei,* and three for *S. andersoni.* They are morphologically similar, differing from those of *M. giganteus* in their relatively greater depth to width and the reduced nature of the hemal spines.

TAIL INTEGUMENT: Associated with the partially articulated caudal vertebrae of *S. stirlingi* (AMNH 117497) were fragments of skin impressions in light blue-gray microcrystalline gypsum about 1–2 mm thick. The impressions originally formed a sheath about the tail, but when excavated were found to be broken and disoriented in situ, suggesting their formation soon after burial, with disturbance occurring during bioturbation of the sediments. The thinner skin impressions preserve the best surface detail, including the pattern of squamation and unfilled holes that represent hairs. This allows the morphology of the skin surface to be described. Impressions of the skin surface reveal imbricate rows of scales, roughly rectangular in shape (2.5–3.5 mm long and 1.5–1.8 mm wide), apparently forming annulations encircling the tail. Hairs, all of similar diameters, were bundled in units of three to six and protruded between the rows of scaly annulations. A few impressions of the shafts of the tail hairs themselves indicate lengths of more than 32 mm.

Direct comparison in the field between these impressions and the surface of the caudal skin of a red kangaroo (*Megaleia rufa*) showed close correspondence in all respects. This observation is reinforced by Semichon's (1926) study of the caudal skin of the same living taxon. The hair bundles do not consistently include a larger central follicle, at least at the surface, as Hardy (1947) also observed in *Macropus giganteus* and as seen in Semichon's description of the red kangaroo. Judging from the long ("guard") hair impressions, the tail may have had a relatively long coat more comparable to the euro kangaroo (*Osphranter robustus*) than the red kangaroo.

RIBS: Thirteen ribs from the right side of the holotype of *S. stirlingi* (SAM P22533) are nearly complete; only the distal ends of the 11th and 12th ribs are broken away. The rib cage in *S. tindalei* is less well represented, but for AMNH 117493 parts of the 1–4, 6–11, and 13 have been identified, and for AMNH 117499 a complete 1st rib and parts of ribs 2, 4, 6, and 12 have been identified. The 1st rib is a short, massive bone whose proportions are much like those of *Macropus giganteus.* The capitulum is relatively small and flattened dorsally, rather than being hemispherical as in *Macropus,* and the tuberculum is also relatively small and narrow and more cyclindrical in form. The succeeding ribs in *Sthenurus* have more anteroposteriorly flattened bodies than in *Macropus,* the capitula bear flat epiphyses, and the tubercula are relatively smaller throughout, even on the 13th rib. The ribs also have rather flat facets confined to the dorsal margin and lack the groove that occurs around the anterior margin of the tuberculum in *Macropus.* The sulcus that occurs on the posterior surface of the neck in *Macropus* is very shallow or lacking in the sthenurines compared here. In all these features the ribs resemble those of *Procoptodon goliah* as described by Tedford (1967).

CLAVICLE AND STERNEBRAE (fig. 24): Compete clavicles are present for *S. stirlingi* (SAM P22533; AMNH 117496) and *S. tindalei* (AMNH 117493) in addition to specimens (AMNH 117481, SIAM 35; AMNH 117499, SIAM 84) of the latter species showing the lateral end of most of the shaft. The sthenurine clavicles are more robust that those of *M. giganteus*; they are ovoid in cross section, whereas those of *M. giganteus* tend to be more flattened and straplike. In both the sthenurines and *M. giganteus* the anterior third of the clavicle is moderately convex at the ster-

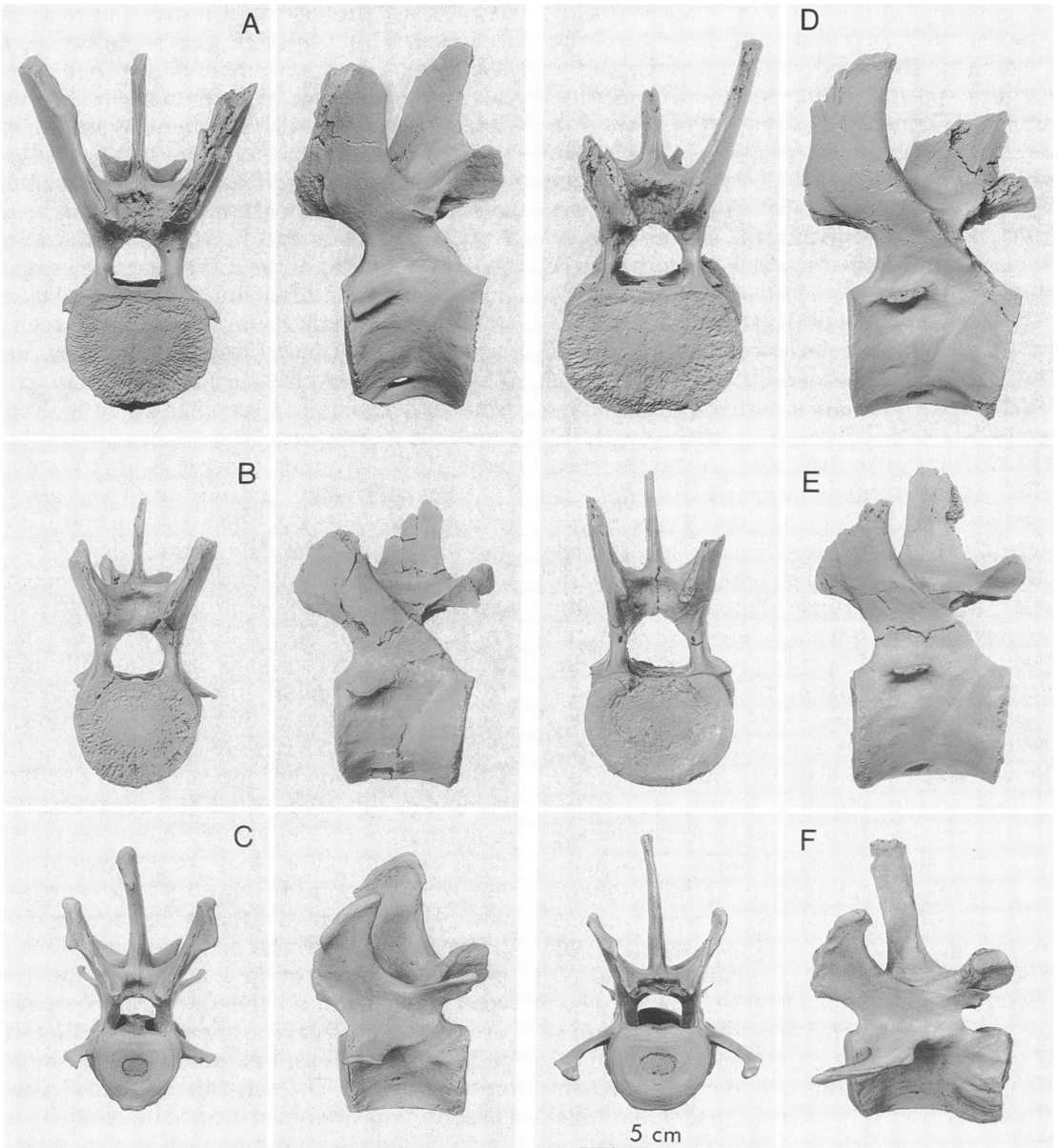

Fig. 20. Comparative anterior and lateral views of the 2nd (**A–C**) and 4th (**D–F**) lumbar vertebrae of *Sthenurus stirlingi,* **A,** holotype, SAM P22533 (reversed); *S. tindalei,* **B,** AMNH 117493; *Macropus giganteus,* **C,** AMNH 2390; *Sthenurus stirlingi,* **D,** holotype, SAM P22533; *S. tindalei,* **E,** AMNH 117493 (reversed); and *Macropus giganteus,* **F,** AMNH 2390.

nal end. In contrast, the lateral two thirds of the sthenurine clavicle is more markedly concave forward than in *M. giganteus,* thereby allowing passage over the coracoid process of the scapula during elevation of the forearm. Indeed, in general form, the sthenurine clavicles more closely resemble those of man than those of *M. giganteus.* Within the sthenurines the differences between species are more subtle. The degree of curvature of the lateral two thirds of the clavicle is greater in *S. tindalei* than in *S. stirlingi.*

A pronounced tubercle on the apex of the concave inferior surface of the sthenurine clavicle marks the point of attachment of the coronoid portion of the coracoclavicular ligament. This tubercle is more pronounced in *S. stirlingi* than in *S. tindalei.* Although the sample is small, *S. stirlingi* clavicles are larger than those of *S. tindalei.* We attribute the differences in size within the species sample to sexual dimorphism, which is more clearly evident in other elements of the forelimb.

The six elements of the sternal column are fully represented in the holotype of *S. stirlingi* (SAM P22533). A manubrium of a female (AMNH 117496) and a partial 4th and complete 5th sternebrae of a male (AMNH 117498) are also attributed to this species. Most of the sternal column of *S. tindalei* is present in AMNH 117493 (only the xiphisternum is missing) and a large 2nd sternebrae (AMNH 117499) of a male is also available. Fragments of much of the sternal column are represented in the *S. andersoni* skeleton. The elongate and slender proportions of the elements of the sternum of *S. andersoni* appear rather like those of *M. giganteus*; even the manubrium has a long shaft posterior to the anterior costal articulations. In decided contrast to these species, *S. stirlingi* and *S. tindalei* are similar in having short and robust sternebrae and a correspondingly short-shafted, shieldlike manubrium resembling that of man. The manubrium of *S. tindalei* is not laterally expanded across the anterior costal articulations as in the comparable sized *S. stirlingi* (e.g., AMNH 117496). The 5th sternebra in these sthenurines also differs from *M. giganteus* in the close approximation of the costal articulations for the 6th and 7th ribs and consequent lateral expansion of this bone across its posterior end. The xiphisternum of *S. stirlingi* is elongate and more like that of *Macropus* than the other sternebrae of this taxon. Its posterior end expands into a fanlike termination as in *Macropus.*

SCAPULA (table 11; fig. 25): Right and left scapulae of the holotype (SAM P22533), an almost complete left scapula (AMNH 117496), and a nearly complete right scapula (AMNH 117495) are available for *S. stirlingi.* Proximal right and left fragments (AMNH 117493) and a nearly complete left scapula (AMNH 117499) of *S. tindalei* were recovered. Only the proximal portion of the left scapula and acromion process is preserved in the *S. andersoni* specimen. *S. stirlingi* scapulae have sustained some damage to the vertebral borders; still, sufficient material is present to estimate the extent of the fossae. In *S. stirlingi* and *S. tindalei* the supraspinous fossa is small (ratio of supra/infraspinous area = 0.3) relative to that in *M. giganteus* (ratio = 0.4). The ratio of the total area of the scapula to the length of the humerus is similar in the holotype male *S. stirlingi* and *M. giganteus,* while a lower ratio for the female (AMNH 117496) is indicative of a relatively smaller scapula. The scapular notch is deep in all the sthenurine species. It reaches to the base of the acromion process as in *P. goliah.* The scapular spine extends from the acromion process in a gentle arc to merge with the blade approximately two thirds the distance to the vertebral border from the glenoid cavity. The acromion process is relatively more robust than in *M. giganteus.* The distal process of the acromion is flared laterally and rotated more medially than in *M. giganteus.* The coracoid process is much more robust than in *Macropus,* but not as robust as in *P. goliah*; it extends beyond the margin of the glenoid cavity, from which it is separated by a deep groove. The glenoid cavity is more narrow and shallow than in *M. giganteus,* tapering to a point behind the coracoid process. A rugose area on the caudal border opposite the base of the acromion marks the possible insertion of the long head of the triceps branchii. In *S. andersoni,* the coracoid process, glenoid cavity, and distal portion of the acromium are similar to those of the larger sthenurines. The subscapular fossa forms a large ovoid depressed area bisected by a low median rise and bounded by the caudal and cranial borders of the blade.

HUMERUS (table 11; fig. 26): The right and left humeri of the holotype (SAM P22533), a crushed left humerus (AMNH 117496), and distal end of a right humerus (AMNH 117498) of *S. stirlingi* are present. Both right and left humeri of *S. andersoni* and two left humeri (AMNH 117493 and 117499) of *S. tindalei* are available for comparison. The total length of the humerus in *S. tindalei* and *S. andersoni* bears the same relationship to length of tibia as in *M. giganteus*; in *S. stirlingi,* the humerus

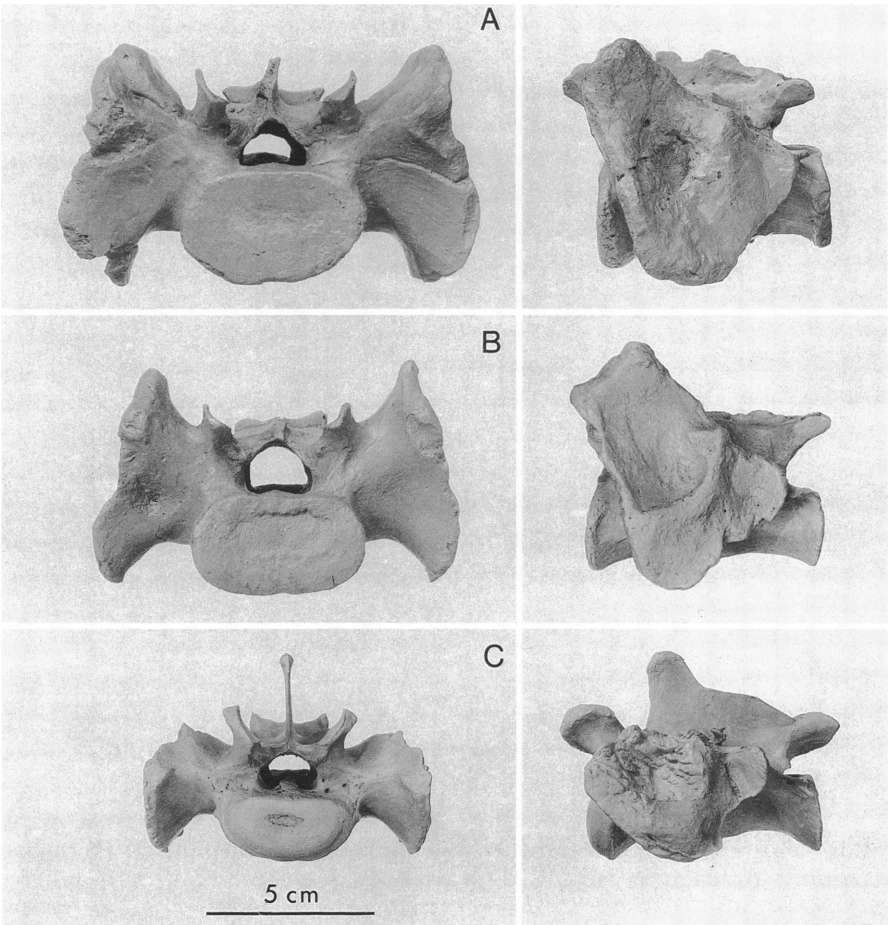

Fig. 21. Comparative anterior and lateral views of the sacrum of *Sthenurus stirlingi,* **A,** AMNH 117496; *S. tindalei,* **B,** AMNH 117493 (reversed); and *Macropus giganteus,* **C,** AMNH 2390.

is 12% longer than that in *M. giganteus.* The minimum cross-sectional area relative to shaft length is largest in *M. giganteus,* decreasing in the order *S. stirlingi, S. tindalei, S. andersoni.*

Viewed from the anteroposterior aspect, the proximal portion of the shaft is deflected more medially than in *M. giganteus.* In *S. tindalei* and *S. andersoni* the shaft is almost straight. Similarly, when viewed from the lateral aspect, the distal portion of the shaft in the sthenurines is deflected more anteriorly than in *M. giganteus.*

As in *P. goliah,* the lesser tuberosity in the sthenurine species is relatively smaller than in *M. giganteus,* and the radius of curvature of the head is slightly larger. The pectoral crest, although longer, is less well developed in *P. goliah* and the sthenurines compared here than it is in *M. giganteus.* Compared with *M. giganteus,* the deltoid crest is relatively larger in *S. stirlingi* and relatively smaller in *S. tindalei* and *S. andersoni.* In *S. stirlingi,* the elongate teres tuberosity is surrounded by a rugose area and is therefore a rather more prominent feature than in *M. giganteus*; it is weakly developed in *S. tindalei* and *S. andersoni.*

In these sthenurines the distal end of the humerus is more medially and laterally flared than in *M. giganteus.* The lateral supracondylar ridge is narrower in the sthenurines than

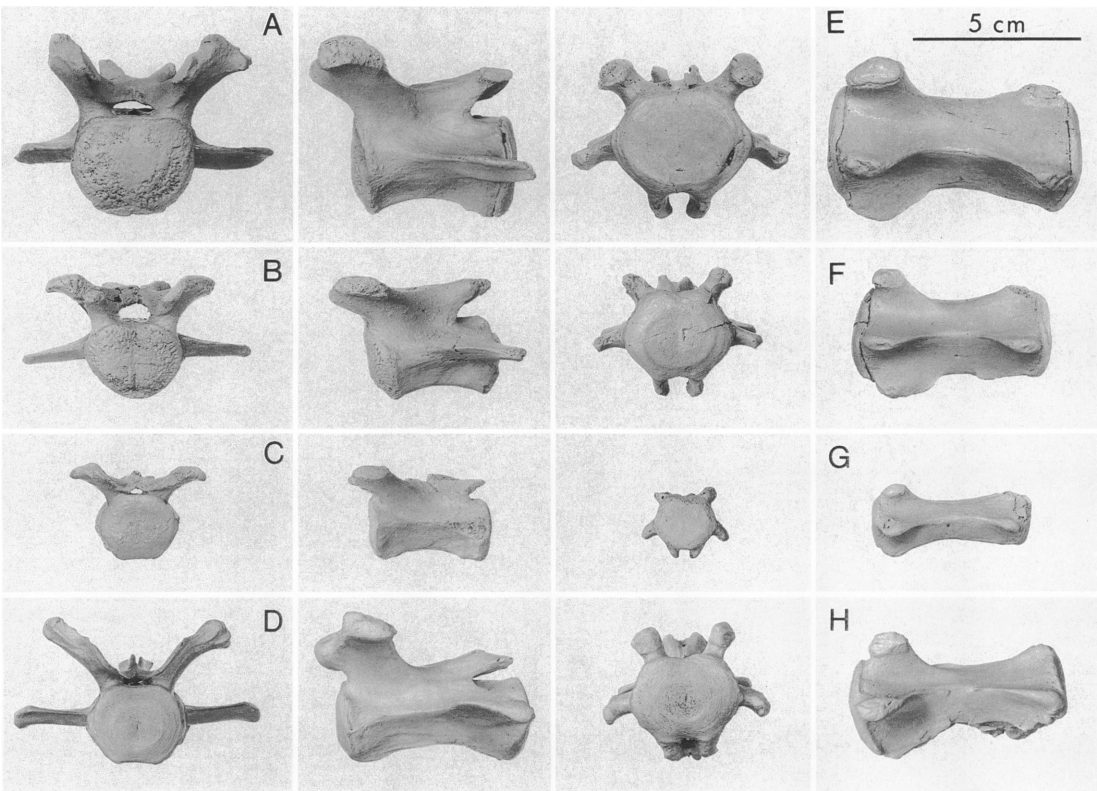

Fig. 22. Comparative anterior and lateral views of the 5th (**A–D**) and 9th (**E–H**) caudal vertebrae of *Sthenurus stirlingi,* **A,** holotype, SAM P22533 (reversed); *S. tindalei,* **B,** AMNH 117493 (reversed); *S. andersoni,* **C,** SAM P13673 (reversed); *Macropus giganteus,* **D,** AMNH 2390; *Sthenurus stirlingi,* **E,** holotype, SAM P22533 (reversed); *S. tindalei,* **F,** AMNH 117493 (reversed); *S. andersoni,* **G,** SAM P13673; and *Macropus giganteus,* **H,** AMNH 2390.

in *M. giganteus,* but the epicondyles are larger and more robust. The olecranon fossa is broader and shallower than in *M. giganteus.*

ULNA AND RADIUS (tables 11, 12; fig. 27, 28): Left and right ulnae of *S. stirlingi* (SAM P22533; AMNH 117496) are available. Left and right ulnae of AMNH 117493, left ulnae of *S. tindalei* (AMNH 117491 and 117499), and the left and right ulnae of *S. andersoni* are preserved. The ulna of *S. stirlingi,* although of similar length to that of *M. giganteus,* is more sharply curved and has a greater anteroposterior width along the full length of the shaft. The olecranon is similar in length to *Macropus,* but is not as wide. The semilunar notch, although narrower transversely, opens distally onto a much broader and more medially projecting coronoid facet than in *M. giganteus.* This articulation with the humerus and radius would appear to allow more pronation and supination of the forearm, yet restrict flexion and extension of the ulna about the humerus to approximately 65°; however, in *M. giganteus* the movement on the elbow joint is approximately 80°. The semilunar notch is more narrow and open in *S. tindalei* and *S. andersoni* than in *S. stirlingi* and is restricted to the lateral side of the shaft while its excursion about the humerus extends to approximately 90°. An elongate rugose area, which extends distally from the front of the coronoid process, marks the site of insertion of the m. brachialis and the gleno-ulnar division of the m. biceps brachii. The sharp interosseous ridge found on the lateral side of the shaft in *M. giganteus* is confined to the

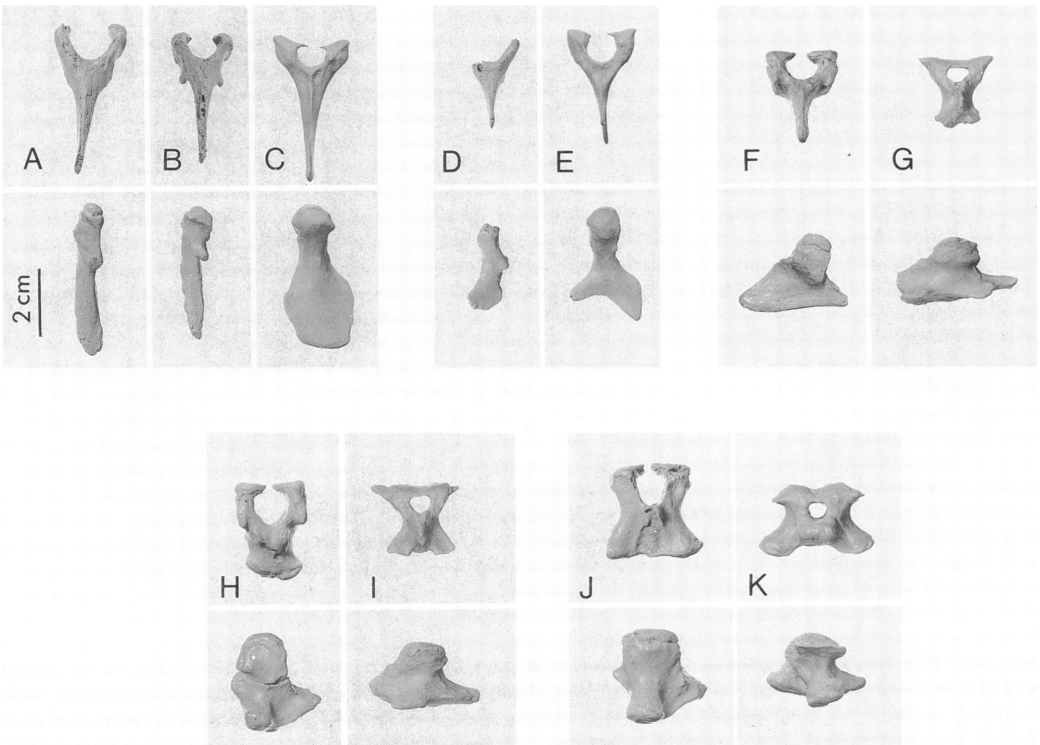

Fig. 23. Comparative anterior and lateral views of chevron bones 1/2 (**A–C**), 2/3 (**D, E**), 5/6 (**F, G**), 6/7 (**H, I**), and 7/8 (**J, K**). *Sthenurus stirlingi,* **A, F, H** (reversed), **J** (reversed), holotype, SAM P22533, and **B,** AMNH 117496; *S. tindalei,* **D,** AMNH 117493; and *Macropus giganteus,* **C, E, G, I, K,** AMNH 2390.

anterior edge of the shaft in *S. stirlingi* and *S. tindalei* and is weakly expressed in *S. andersoni.* The styloid process is a larger structure in the sthenurines and it extends more distally than in *M. giganteus.*

Both radii are available for the holotype of *S. stirlingi* (SAM P22533) as well as the female (AMNH 117496) of the same species. Only the somewhat distorted right ulna, which lacks epiphyses of AMNH 117493 representing *S. tindalei,* is available for comparison. *Sthenurus andersoni* is represented by a nearly complete, but crushed, left radius and the better preserved distal half of the right radius. The cross-sectional area of the midshaft is proportionally greater in the three sthenurine species than in *M. giganteus.* The shaft is oval to subquadrilateral for most of its length. The neck is relatively longer than in *M. giganteus* and is capped by a shallow discoid capitulum. Distally, the shaft is flattened at its articulation with the ulna. A shallow groove just proximal of midshaft is possibly the site of insertion of the M. pronator teres tendon. The styloid process of the distal epiphysis is not as strongly developed as in *M. giganteus.* The radii of *S. tindalei* and *S. andersoni* have a shorter neck but are otherwise similar in form to those of *S. stirlingi.*

MANUS (tables 13–17; fig. 29): Right and left forefeet of the holotype of *S. stirlingi* were recovered; the right forefoot lacks the scaphoid, trapezoid, trapezium, distal epiphysis of metatarsal II, proximal phalanx of digit II, medial phalanx of digit IV, and all of digit V; the left forefoot lacks the pisiform, cuneiform, scaphoid, trapezoid, trapezium, and medial and distal phalanges of digit V and the distal portion of the proximal phalanx of digit III. A more complete left manus of a female of *S. stirlingi* (AMNH 117496) lacks only the ungual of the hallux. Also available

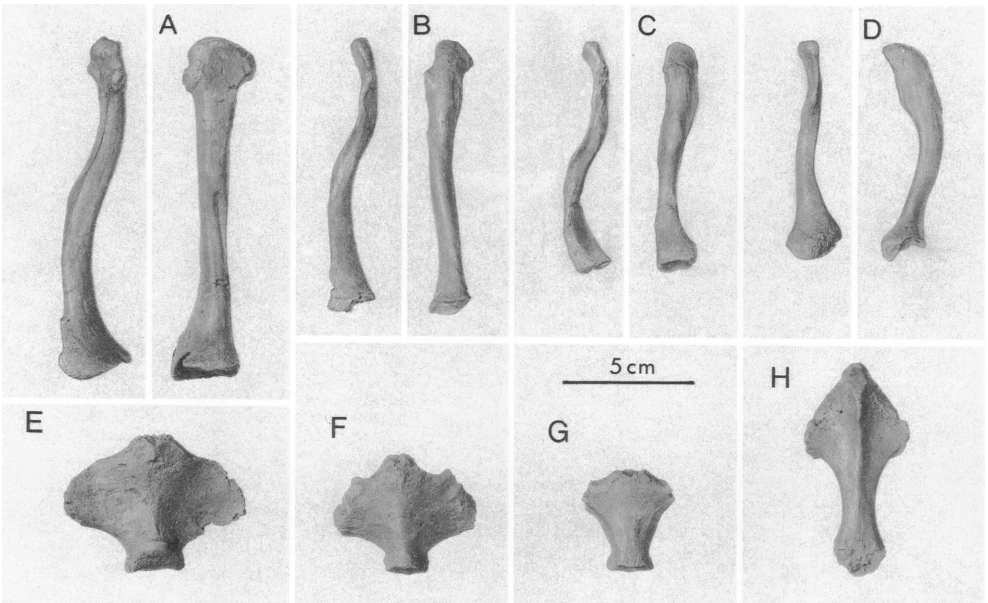

Fig. 24. Comparative views of the clavicles (**A–D,** dorsal [left] and anterior [right] views) and manubria (**E–H,** ventral view) of *Sthenurus stirlingi,* holotype, **A,** SAM P22533 (reversed), and **B,** AMNH 117496; *S. tindalei,* **C,** AMNH 117493; *Macropus giganteus,* **D,** AMNH 2390; *Sthenurus stirlingi,* **E,** holotype, SAM P22533, and **F,** AMNH 117496; *S. tindalei,* **G,** AMNH 117493; and *Macropus giganteus,* **H,** AMNH 2390.

are a partial left and right manus of *S. andersoni* and a partial left and right manus (AMNH 117493) and partial right manus (AMNH 117491) of *S. tindalei.*

The forefeet of *S. stirlingi, S. tindalei,* and *S. andersoni* differ markedly from those of *M. giganteus* in the pronounced elongation of digits II, III, and IV, particularly the metacarpals and unguals relative to the width of the carpal arch. The digital formula for both *S. stirlingi* and *S. tindalei* is III II IV V I and would appear to be similar to *S. andersoni.* It is identical with the bandicoots (*Isoodon obesulus, Macrotis lagotis*) and the rat kangaroos (*Bettongia lesuerui, B. gaimardi*). The articular surfaces of the carpus are more flattened in the sthenurine species than in *Macropus,* which restricts flexion of the wrist and increases its strength. This flattening may reflect the increased stresses placed on this joint by the elongation of the central digits.

The left carpus of *S. stirlingi* (AMNH 117496) is complete, and a comparison of the homologous elements in *S. tindalei* and *S. andersoni* indicates a similar morphology. The proximal row is composed of three elements: the scapholunar, the cuneiform, and sesamoid, the pisiform. The styloid process of the ulna rotates in a cavity formed exclusively by the cuneiform. The scapholunar articulates with five bones as in *Macropus,* viz. the radius, unciform, magnum, trapezoid, and trapezium. In *M. giganteus* the radial articular surface is evenly distributed in an arc across the anterior and posterior surface of the proximal aspect of the scapholunar. In these sthenurines the articular surface is more gently curved and confined to the proximal aspect of the scapholunar, thereby greatly limiting the extent of flexion with the radius. Distally, the scapholunar articulates with the trapezium, trapezoid, and magnum and the medial aspect of the unciform. The distal row of carpals comprises the trapezium, trapezoid, magnum, and unciform. Difficulty was experienced in determining the form of the trapezium. Small facets of the proximal aspect of metacarpal I and a groove in the distal

surface of the scapholunar give some indication of the form of the trapezium. A small cone-shaped bone bearing the required, albeit indistinct, facets has been identified as the trapezium in *S. stirlingi* (AMNH 117496). It is relatively much smaller than the trapezium in *M. giganteus,* reflecting the reduction in size of digit I. It wedges between the scapholunar and metacarpal I. The trapezoid is a small wedge-shaped bone similar in size to that in *M. giganteus.* It inserts in the articular groove in the proximal end of metacarpal II and articulates laterally with the magnum, medially with the trapezium, and proximally with the scapholunar. The magnum is more pyramidal in form than in *M. giganteus*; distally it articulates with metacarpal II and a portion of metacarpal III, medially with the trapezoid, proximomedially with the scapholunar, and proximomedially with the unciform. The unciform articulates distally with metacarpals IV and V and distomedially with a portion of metacarpal III and the magnum. It is thus functionally similar to the unciform of *M. giganteus,* although it differs markedly in form. The posterior aspect of the unciform in the sthenurine species is flat, not concave as in *Macropus.* The proximal aspect is also smooth and flat and lacks the medial eminence, which buttresses the cuneiform in *Macropus.* Likewise, the distal articular surface of the cuneiform is flat, not convex as in *Macropus.* The resulting carpal arch is thus considerably flatter than in *Macropus* species. The pisiform appears to have less articulation with the styloid process of the ulna than in *Macropus,* although it may make greater contact medially when extended.

Metacarpals I and V are much less robust and shorter than those of *Macropus* species, whereas metacarpals II, III, and IV are much longer. The proximal articulations with the carpus allow for considerable divergence of metacarpals I and V, while II, III, and IV are greatly constrained. Similarly, the proximal phalanges of digits I and V are considerably reduced, whereas those of II, III, and IV are of similar proportion to those of *M. giganteus.* The medial phalanx of digit V is short and proportionally smaller than in *M. giganteus,* whereas the medial phalanges of digits II, III, and IV are proportionally longer. The well-developed rugosities on the proximal posterior surface of the phalanges of digits II, III, and IV suggest the presence of paired sesamoids as in *Macropus,* although none have been identified.

The ungual processes of the distal segments of digits II, III, and IV are exceedingly long and spatulate, curving both posteriorly and slightly medially. Extension is restricted to the metacarpal–phalangeal joint, and flexion occurs largely at the medial and distal phalanges as in *Macropus.* These movements suggest that the rigid manus is incapable of the plantigrade stance exhibited by *Macropus,* yet is capable of slightly more flexion of the extremely elongated central digits. These features combined with a relatively immobile, yet strong, carpus would produce a hand that functions in a clasping manner.

PELVIS (table 18; fig. 30): Both left and right halves of the pelvis of *S. stirlingi* (SAM P22533) are present; the left half is fractured across the ischium and lacks the distal portion of the ilium; the right half, although complete, has sustained fractures to the ilium and pubic symphysis. Pelves of females of similar size of *S. stirlingi* (AMNH 117496) and *S. tindalei* (AMNH 117493) were recovered; both lack the distal portions of the ilium. The left half of the pelvis of a male *S. tindalei* (AMNH 117499) is also available, as is the disarticulated ilium and partial ischium of a juvenile *S. stirlingi* (SAM 117495). Proximal proportions of the ilia and ischia of *S. andersoni* were also recovered.

The pelvis of *S. stirlingi* differs from that of *M. giganteus* both in form and relative proportions. Although the width of the pelvis across the acetabula is equal to the length of the ischial portion of the pelvis in both species, the ilium of *S. stirlingi* is approximately 26 percent longer relative to pelvic width than in *M. giganteus.* The angle between the ilium and ischium about the acetabulum is more acute in *S. stirlingi* (145°) than in *M. giganteus* (170°). As in *Procoptodon,* the wing of the ilium is dorsoventrally flattened and much broader in both *S. stirlingi* and *S. tindalei* than in *M. giganteus.* This is reflected in the total area of origin of the gluteal musculature being 1.8 times greater per unit length of ilium than in *M. giganteus.* Similarly, the area of origin of the iliacus per unit length is 1.6 times that in *M. giganteus.* The ilial frag-

ments of *S. andersoni* are similar in form to the two larger sthenurines.

The iliopectineal tuberosity is a large rugose triangular area at the base of the iliac spine in *S. stirlingi*; it serves as the origin of the M. rectus femoris. The iliopectineal process, which is the origin of the M. pectineus, is a wedgelike structure extending from the anterior portion of the pubis. As in *S. tindalei,* the pubis of *S. stirlingi* is proportionally similar in length, although slightly wider than that of *M. giganteus.* The ischium parallels the pubic symphysis as in *M. giganteus,* but differs in a marked dorsal extension of the ischiatic tuberosity. This change in the form of the ischium affects the geometry of the pelvic limb musculature, particularly that of the M. biceps femoris and M. semitendinosus. It also increases (by approximately 38%) the area of origin relative to the ischial length of the M. quadratus femoris compared to that of *M. giganteus.* The acetabulum in *S. stirlingi, S. tindalei,* and *S. andersoni* is approximately 30 percent larger in diameter relative to the length of the ischium than in *M. giganteus*; it is deep and strongly buttressed anteriorly by the iliac spine. Unlike *M. giganteus,* the acetabular groove is shallow in the center of the fossa and deepens posteroventrally toward the border of the acetabulum, emerging again as a shallow groove in the ventral border of the ischium. The acetabular groove in *S. andersoni* is similar to that of *S. stirlingi,* although it is proportionally deeper. The pubic symphysis in both *S. stirlingi* and *S. tindalei* is much shorter relative to the length of the ischium than in *M. giganteus.* The pubic tubercle is preserved in *S. stirlingi* (SAM P22533, AMNH 117496) and *S. tindalei* (AMNH 117493). It is an ovate eminence far less prominent than the recurved spine in *M. giganteus.* The vertical

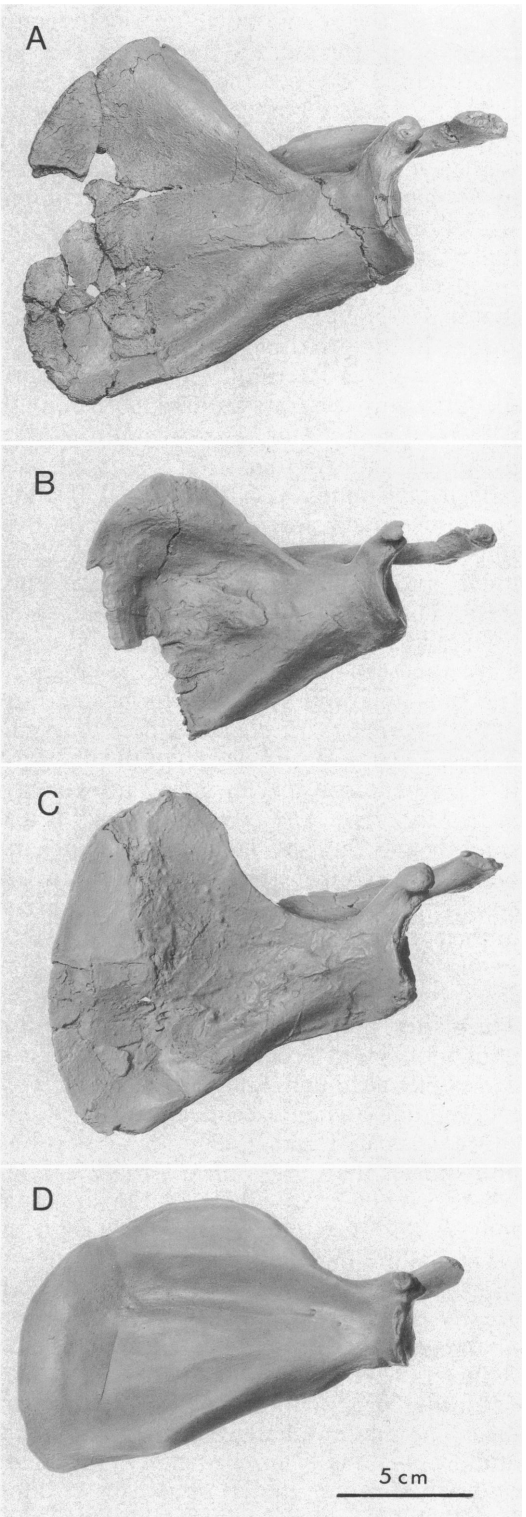

→

Fig. 25. Comparative medial (**A–D**), anterior (**E–H**), and lateral (**I–L**) views of the left scapula of *Sthenurus stirlingi,* **A, E, I,** holotype, SAM P22533 (reversed), and **B, F, J,** AMNH 117496; *S. tindalei,* **C, G, K,** AMNH 117499; and *Macropus giganteus,* **D, H, L,** AMNH 2390 (reversed).

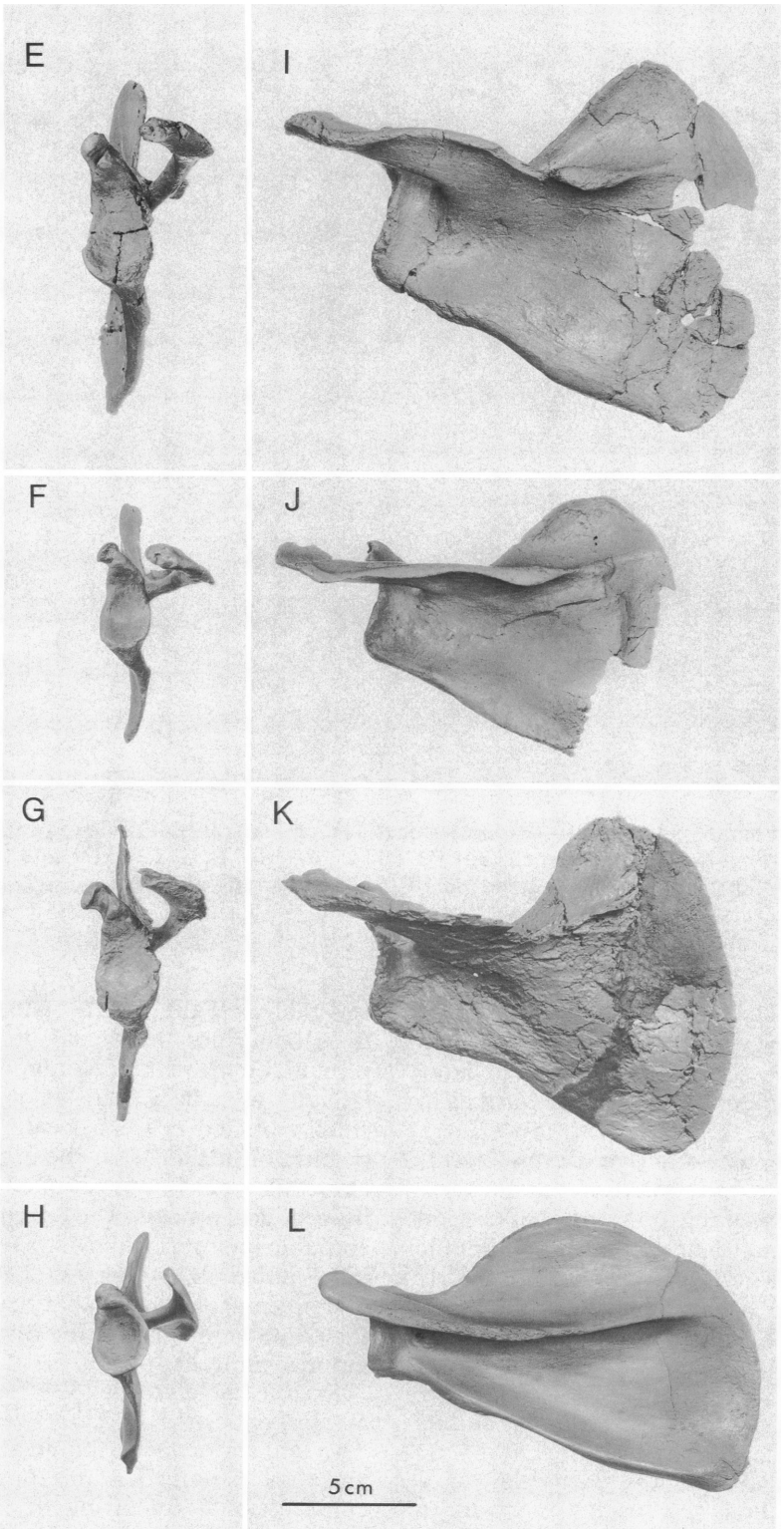

Fig. 25. Continued.

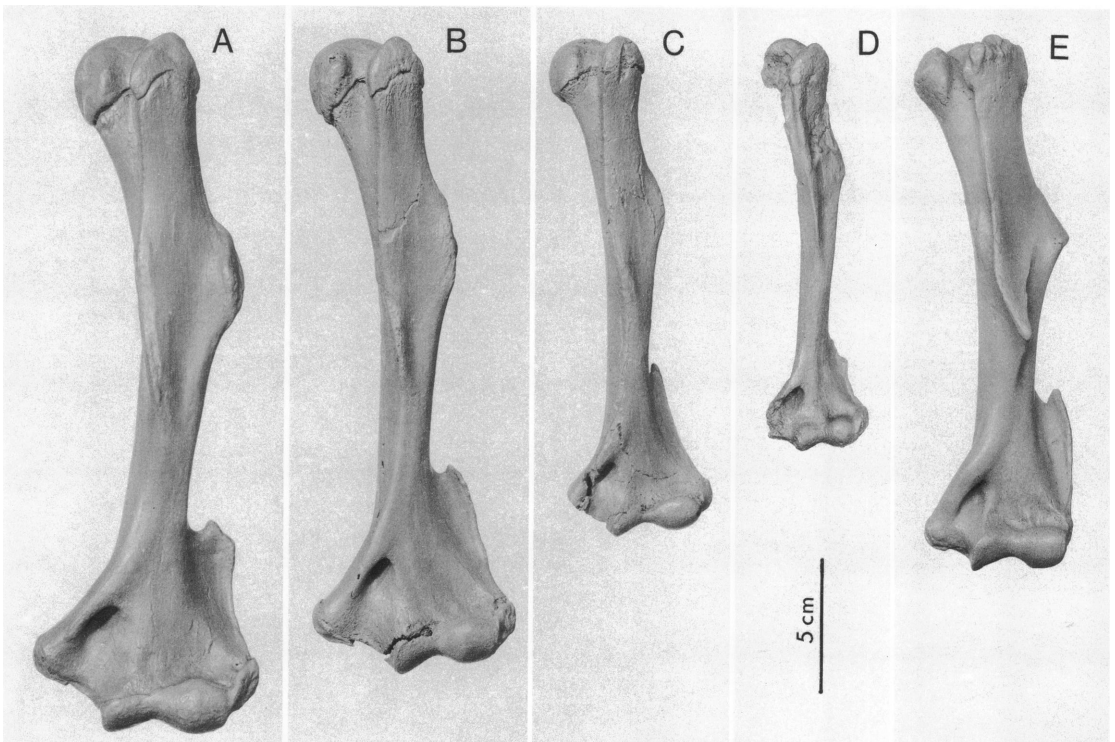

Fig. 26. Comparative anterior (**A–E**), posterior (**F–J**), and lateral (**K–O**) views of the left humerus of *Sthenurus stirlingi,* **A, F, K,** holotype, SAM P22533; *S. tindalei,* **B, G, L,** AMNH 117499, and **C, H, M,** AMNH 117493; *S. andersoni,* **D, I, N,** SAM P13673 (reversed); and *Macropus giganteus,* **E, J, O,** AMNH 2390 (reversed).

ramus of the ischium is narrow as in *P. goliah* and *S. tindalei,* with a relatively small area of origin for M. adductor magnus. The large obturator foramen is triangular in form as in *S. tindalei* and *P. goliah* (Tedford, 1967), rather than elongate and ovoid as in *Macropus.*

EPIPUBIC BONES (fig. 31): Most of the left and the proximal half of the right epipubic bones of the holotype of *S. stirlingi* are poorly preserved, but a complete left epipubic is available in a female (AMNH 117496) of this species and a complete right epipubic of a juvenile (AMNH 117495). These bones are compared with those of *M. giganteus* and an almost complete right epipubic (AMNH 117493) of *S. tindalei* and partial left of *S. andersoni.* In the larger species of *Sthenurus* the dorsoventrally flattened epipubic bones curve lateromedially and are longer than the ischium, whereas in *M. giganteus* they are less than half the length of the ischium. In the sthenurines the dorsal border near the proximal end of the epipubic bone extends laterally as a thin shelf. In these species a small rounded process occurs on the distal portion of this shelf; in the articulated skeleton this would be positioned opposite the iliopectineal process. The proximal end of the epipubic bones in both *S. stirlingi* and *S. tindalei,* unlike *M. giganteus,* is expanded into a subrectangular facet that articulates with the ovate eminences at the distal end of the pubic symphysis.

FEMUR (table 19; fig. 32): Both femora of *S. stirlingi* (SAM P22533) were recovered. The left femur lacks the greater trochanter and has sustained some postdepositional compressional fracturing of the head and lesser trochanter; the right femur is complete, although the distal portion of the shaft has been sheared and slightly compressed. Also

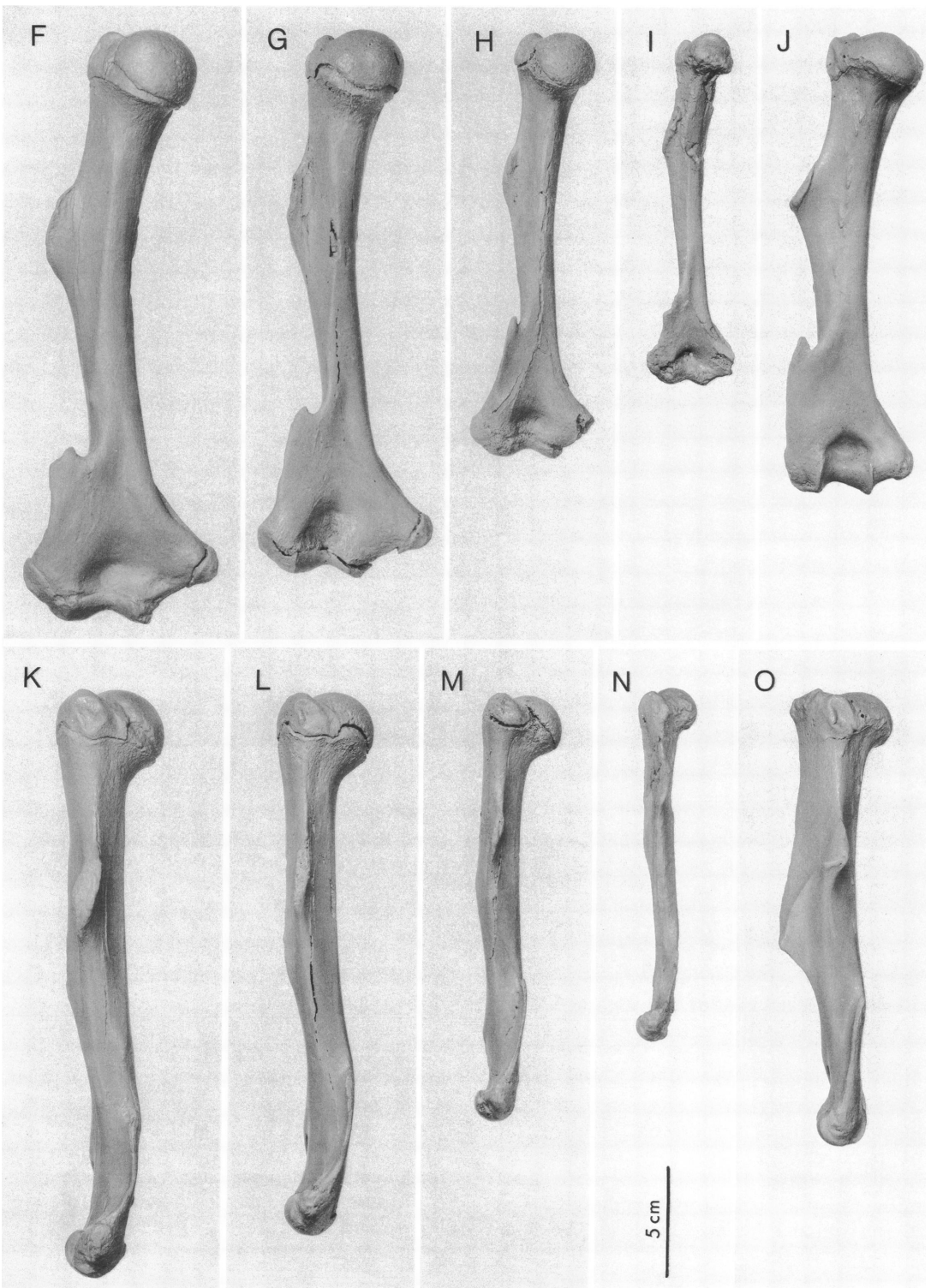

Fig. 26. Continued.

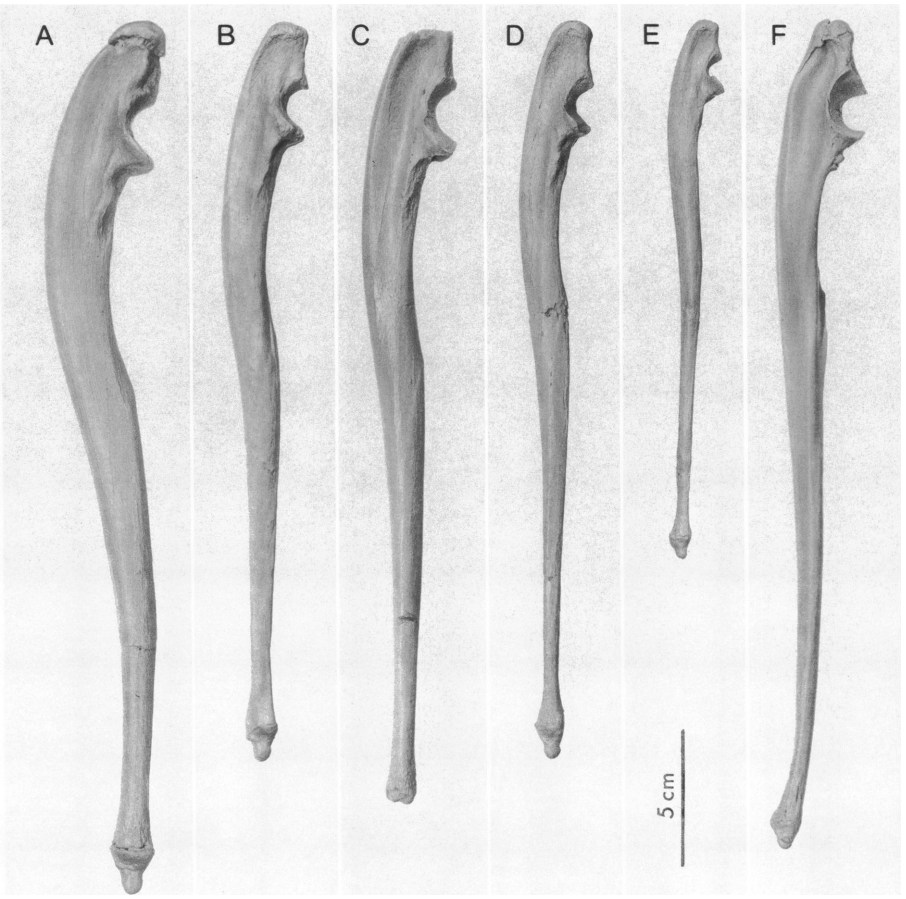

Fig. 27. Comparative medial (**A–F**), lateral (**G–L**), and anterior (**M–R**) views of the ulna of *Sthenurus stirlingi,* **A, G, M,** holotype, SAM P22533 (reversed), and **B, H, N,** AMNH 117496; *S. tindalei,* **C, I, O,** AMNH 117499, and **D, J, P,** AMNH 117491; *S. andersoni,* **E, K, Q,** SAM P13673 (reversed); and *Macropus giganteus,* **F, L, R,** AMNH 2390 (reversed).

representative of *S. stirlingi* are left and right femora (AMNH 117496), left femur (AMNH 117498), and right femur (SAM P13940). Partial left and right femora (AMNH 117493) and a complete left (AMNH 117499) femur of *S. tindalei* were also recovered. Both *S. andersoni* femora are present; the left, although crushed, is the most complete. Although the ratio of femur length to tibial length is similar in the three species of *Sthenurus,* as well as *P. goliah* (Tedford, 1967) and *M. giganteus,* the femora of the sthenurines are more massive than those of *M. giganteus.* The difference in the cross-sectional area at midshaft in the three sthenurine species is directly proportional to the square of the differences in shaft length, suggesting animals of similar build. Indeed the cross-sectional area is approximately twice that predicted for *Macropus* species of equivalent size. The greater trochanter is relatively more massive in both *S. stirlingi* and *S. tindalei* than in *S. andersoni* or *M. giganteus.* In *S. stirlingi* and *S. tindalei* the greater trochanter is relatively longer and more closely aligned with the axis of the femur shaft than in *M. giganteus.* The trochanteric fossa is likewise more medially placed. The lesser trochanter with its poorly

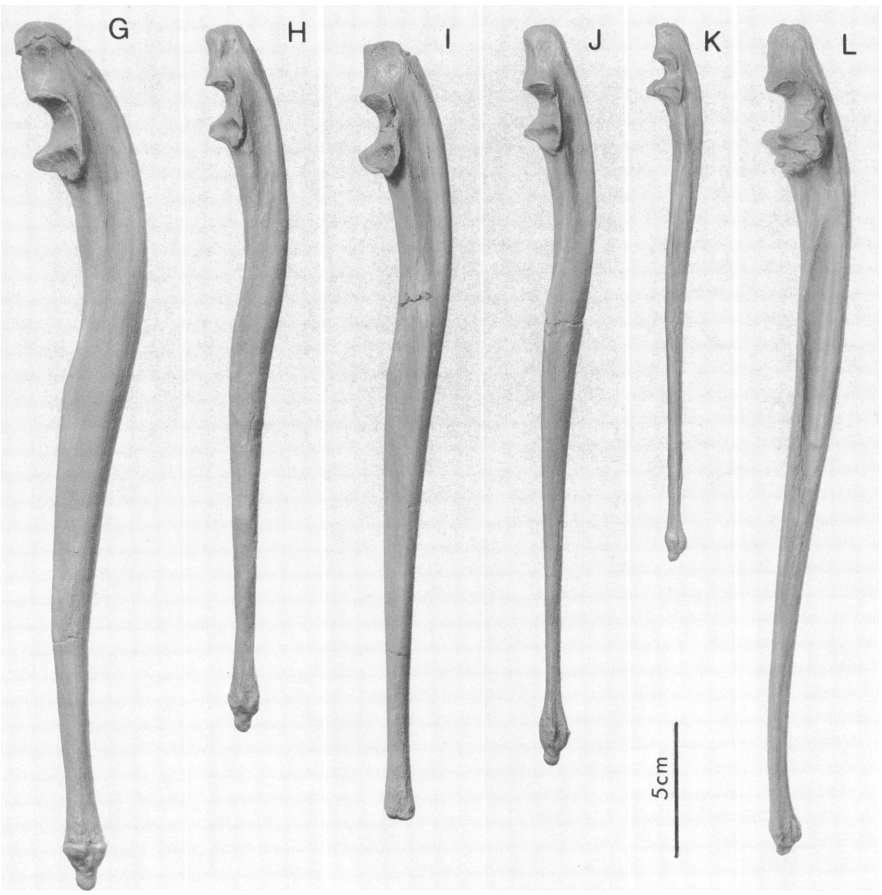

Fig. 27. Continued.

developed medial shelf is a weaker structure in *S. stirlingi* and *S. tindalei* than in *M. giganteus*.

The smooth distal condyles are similar in the sthenurines and differ from *M. giganteus* in which the lateral distal condyle is grooved for reception of the head of the fibula during extreme flexion of the knee joint. The femur bears a number of prominent scars at the sites of origin and insertion of the limb musculature. These are herein considered homologous with those described for *Macropus* species by Bauschultze (1972), Carlsson (1914, 1915), and Elftman (1929). On the distal posterior aspect of the greater trochanter, a large medial rugosity marks the probable insertion of the piriformis and the gluteus medius. This insertion is separated by a shallow groove from an elongate tuberosity for the insertion of the gluteus minimus, which lies more distally on the lateral side of the greater trochanter. A prominent flange on the lateral border of the shaft opposite the head serves as the origin of the vastus lateralis in both *S. stirlingi* and *S. tindalei*. An elongate scar extending along the lateral and distal border of the trochanteric fossa indicates the site of insertion of the oburator musculature. A prominent crest representing the insertion of the iliacus and psoas major extends along the medial side of the lesser trochanter and ends in an elongate pit containing a rugose eminence. Distal to this pit, on the medial side of the shaft, are two closely associated shallow, rugose pits for the pectineus. The insertion of the quadratus femoris is indicated by a large

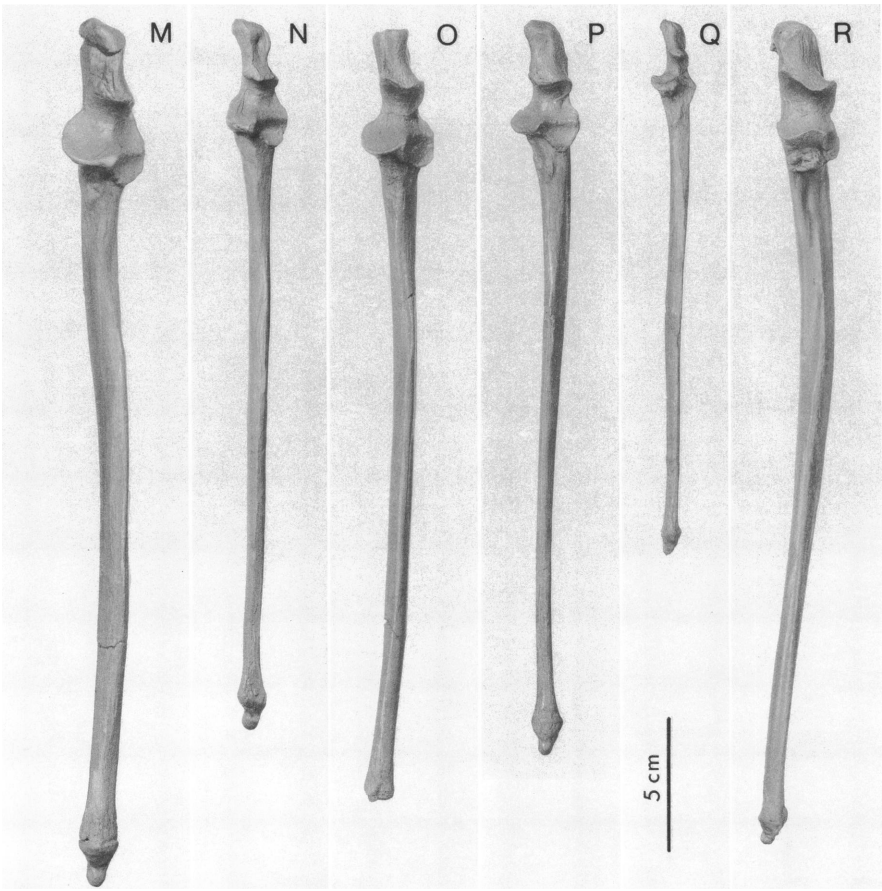

Fig. 27. Continued.

circular rugosity on the midposterior aspect of the shaft. A shallow groove arises just lateral to the insertion of the quadratus femoris and passes distally and medially to terminate in a small circular pit. It is similar to that described in *P. goliah* (Tedford, 1967) and, although less well developed, is also present in *S. tindalei* and *S. andersoni.* It may represent the insertion of the adductor magnus and brevis. A long arcuate scar, convex laterally, extends across the medial aspect of the shaft. This scar is not present in *Macropus,* but may represent the site of insertion of the medial and intermediate vastus muscles. A deep pit on the distal lateral aspect of the shaft just proximal to the condyle marks the usual site of attachment of the plantaris and gastrocnemius lateralis; it is a more prominent feature in *S. stirlingi* and *S. tindalei* than in *S. andersoni* or *M. giganteus.* A smaller scar on the distal medial aspect of the shaft correlates with the site of origin of the gastrocnemius medialis in *M. giganteus.* A prominent rugose pit on the lateral side of the epicondyle marks the origin of the popliteus muscle.

TIBIA AND FIBULA (table 19; figs. 33, 34): Left and right tibia and fibula, including proximal and distal epiphyses of the holotype of *S. stirlingi,* are present. The distal portion of the shaft of the left fibula is missing, while the left tibia exhibits some lateral compression of the proximal end and a number of postdepositional fractures of the shaft. Two

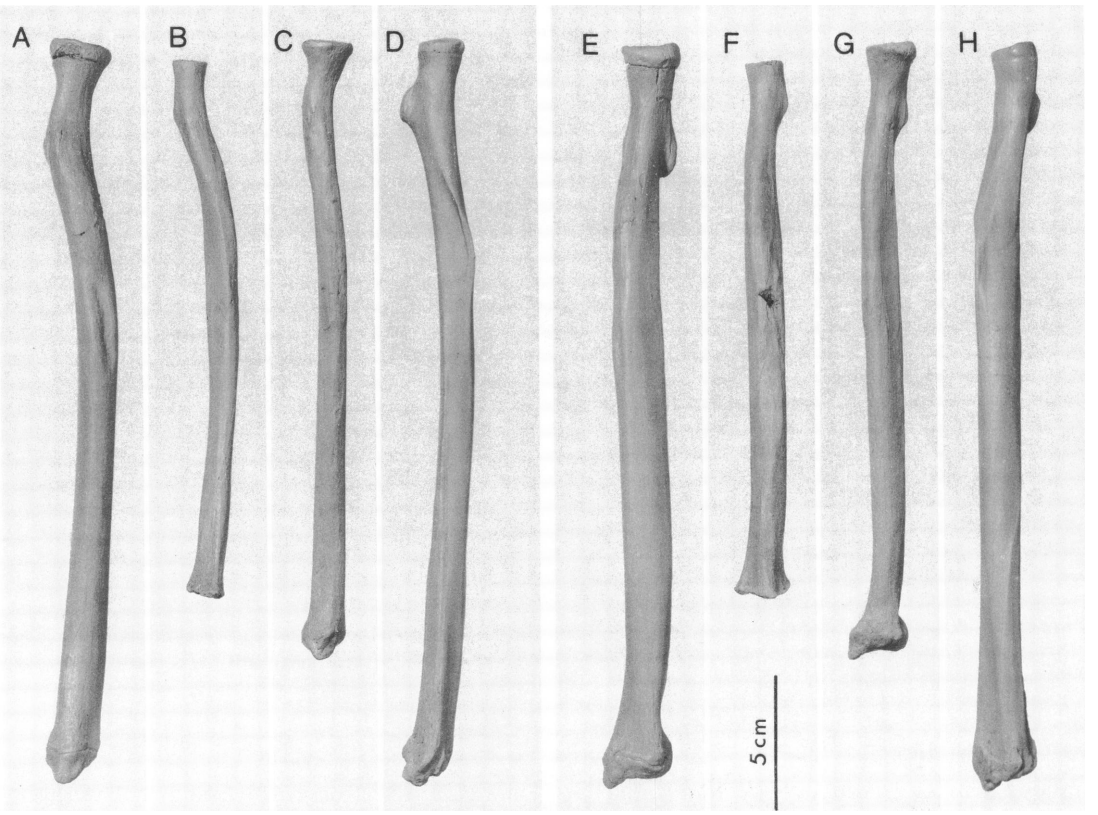

Fig. 28. Comparative anterior (**A–D**) and lateral (**E–H**) views radii of *Sthenurus stirlingi,* **A, E,** holotype SAM P22533 (reversed), and **B, F,** AMNH 117496 (reversed); *S. tindalei,* **C, G,** AMNH 117493; and *Macropus giganteus,* **D, H,** AMNH 2390.

right tibiae of *S. tindalei* (AMNH 117493 and 117499) and right and left tibiae of *S. andersoni* including proximal and distal epiphyses are also preserved. The tibia of *S. stirlingi* shows the same proportional relationship to the length of the femur as in *S. tindalei* and *M. giganteus*; however, as with the femur, both sthenurine species are more robust than *M. giganteus* of equivalent size. The intercondyloid eminences of *S. stirlingi* and *S. tindalei* are proportionally no larger than that of *M. giganteus.* The lateral and medial condylar surfaces are of approximately equal area; laterally, the groove for insertion of the fibula head is proportionally much longer in both *S. stirlingi* and *S. tindalei* than in *M. giganteus.* The lateral part of the proximal condyle bearing this groove is missing in the *S. andersoni* specimen. A narrow groove and associated nutrient foramen, similar to that found in *S. tindalei, S. andersoni, P. goliah,* and *M. giganteus,* occurs on the posterolateral border of the shaft approximately one third the length from the proximal end. A deep groove extends along the lateral surface of the shaft just anterior to the fibular surface. A similar groove is reported in *P. goliah* (Tedford, 1967), which is less well developed in *S. tindalei,* is barely discernible in *M. giganteus,* and appears to be absent in *S. andersoni.* It may represent the site of attachment of the interosseous binding the tibia and fibula and/or the site of partial origin of the peraneus brevis. The distal articular surface of the tibia is more massive and deeply grooved than in *M. giganteus.* The medial

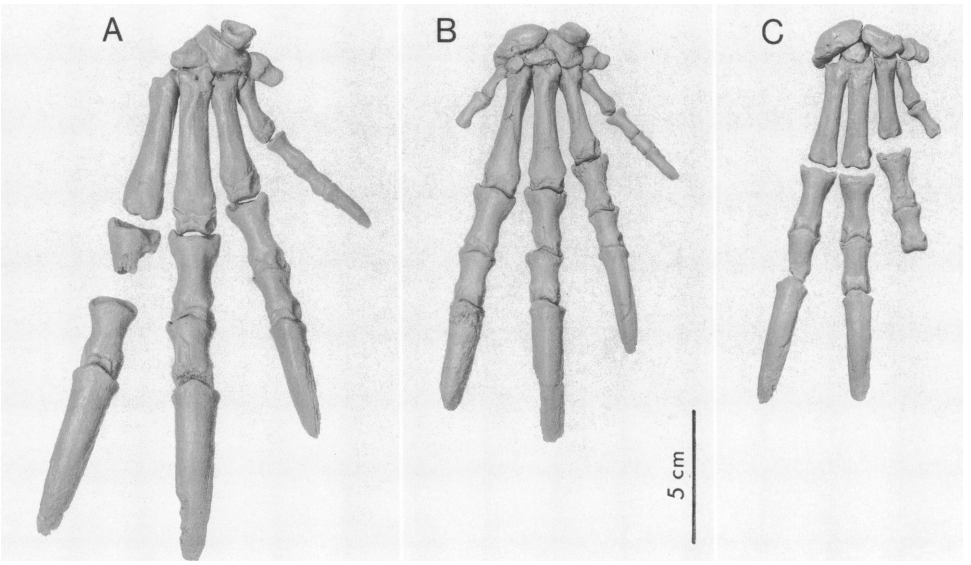

Fig. 29. Comparative dorsal views of the left manus of *Sthenurus stirlingi,* **A,** holotype, SAM P22533 (reversed), and **B,** AMNH 117496; *S. tindalei,* **C,** AMNH 117493 (reversed); and *Macropus giganteus,* **D,** AMNH 2390 (reversed).

malleolus in *S. stirlingi, S. tindalei,* and *S. andersoni* is longer and more robust than in *M. giganteus,* yet its area of contact with the facies malleolaris medialis of the astragalus is proportionally less than in *M. giganteus.* The median articular groove in both *S. stirlingi* and *S. tindalei* is an oblate cup rather than the shallow arcuate form of *M. giganteus.* The distal articular surface of the tibia is deeply grooved in these sthenurines and medially is in the form of an oblate cup rather than a shallow depression as in *M. giganteus.* This latter feature and the nature of the distal articular surfaces suggest an articulation with the astragalus in which movement is even more constrained to the sagittal plane than in *M. giganteus.*

The form of the fibula is essentially the same in *S. stirlingi* and *S. tindalei,* and although the distal ends of these bones resemble the corresponding part in *Macropus giganteus* rather closely, there are notable differences in the proximal epiphysis and adjacent shaft. Most striking is the deeply excavated groove on the anterolateral part of the proximal epiphysis and the contiguous shaft for insertion of the fibular collateral ligament that arises on the lateral epicondyle of the femur from an arcuate crest lying anterior to the pit for the tendon of the M. popliteus. The corresponding structure in the fibula head of *M. giganteus* consists of a pit for reception of the tendon in the epiphysis that is not continuous with the shallow grooving of the shaft below it. The sthenurines lack the proximal eminence that articulates with the groove in the femur epicondyle in extreme flexion that is present in *Macropus.* Instead, the facet for the femur on the proximal epiphysis is directly laterally from the tibial facet rather than parallel to it as in *M. giganteus.* A triangular facet on the anterior face of the proximal epiphysis represents part of the origin of the M. peroneus longus whose tendon extends down the lateral side of the fibula shaft to cross the malleolus in a shallow, narrow groove. In *Macropus* this muscle's origin is a distinct knob and the trace of the tendon is more impressed on the fibula shaft ventrally.

PES (tables 20–22; fig. 35): The right pes of the holotype of *S. stirlingi* (SAM P22533) is complete with the exception of the inferred

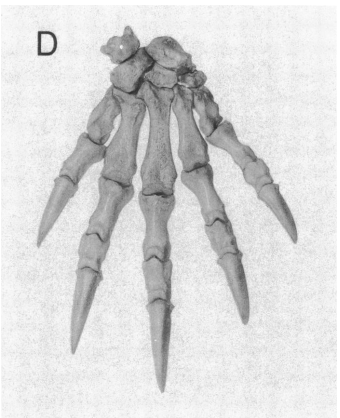

Fig. 29. Continued.

vestigial phalanges to metatarsal V and the distal part of the shaft and inferred vestigial phalanges of metatarsal III. The left pes lacks the distal portion of metatarsals III and V, their inferred phalanges, the navicular, and the sesamoids. The hind feet of a female of *S. stirlingi* (AMNH 117496) include the left and right pes, complete except for the left navicular, plantar sesamoid, and inferred distal phalanges of digits III and V. Additional partial hind feet of *S. stirlingi* include a large adult male (AMNH 117494) and the juvenile (AMNH 117495) in which the calcaneum lacks the epiphysis of the tuber calcis, and metatarsal IV has an unfused distal epiphysis. The left pes of *S. tindalei* (AMNH 117493) is complete except for possible distal phalanges of digits III and V. Additional partial hind feet of *S. tindalei* include the males AMNH 117491 and 117499. The pes of *S. andersoni* include all the tarsal bones, metatarsal IV, and associated phalanges. The proximal portions of metatarsals II, III, and V are present, as well as a fragmentary shaft and distal end of the left metatarsal V. The pes of the three sthenurines show remarkable reduction of metatarsals II, III, and V to produce a functionally monodactyl foot as previously noted in *P. goliah* and other species of *Sthenurus* (Tedford, 1966, 1967). The presence of a long slender shaft and small distal process on the right metatarsal V of *S. stirlingi* (SAM P22533) and left metatarsal V of *S. andersoni,* as well as the fragments of the midshaft of metatarsals III and V adhering to metatarsal IV in *S. tindalei* (AMNH 117493), suggests the presence of complete yet vestigial metatarsals III and V in all sthenurine species. The overall length of the pes relative to the length of the tibia is only slightly greater in these sthenurine species than in *M. giganteus.* Although individual elements of the IVth digit are more robust in *Sthenurus* species than in *Macropus* species, overall the pes is slightly broader in *M. giganteus* due to the greater development of the Vth digit. The transverse width of the pes across the cuboid and navicular is proportionally the same in these sthenurines; it is approximately 17% greater than that of *M. giganteus.* The distal portion of the calcaneum is also proportionally wider in both *S. stirlingi* and *S. tindalei* than in *M. giganteus.* The ratio of calcaneal length (distal end calcaneum to center line of astragalus) to tarsus length (center line astragalus to distal end of digit IV) in the three sthenurine species is identical to that of *M. giganteus.*

The astragali of *S. stirlingi, S. tindalei,* and *S. andersoni* are very similar in form and differ from those of *M. giganteus* in the development of a much higher median trochlear crest with a more rounded apex. The trochlear groove is slightly more excavated than in *M. giganteus,* and the lateral crest is lower with a more rounded lateral margin. The axis of articulation with the tibia is at right angles to the longitudinal axis of the pes, whereas in *M. giganteus* it is rotated medially as much as 9–10°.

The facet for the tibial malleolus on the astragalus is deflected more ventrally in these sthenurines than in *M. giganteus.* The median trochlear crest does not extend as far ventrally as in *M. giganteus*; it is inserted in a deep pocket in the proximal surface of the calcaneum. The posterior portion of the lateral trochlear ridge is sharply truncated posteromedially at the site of insertion of the lateral ligament as in *S. tindalei, S. andersoni,* and *P. goliah.* The facet so produced is incised by a narrow groove leading to a deep sulcus in the ventral surface of the astragalus. This sulcus, bordered by anterior and posterior facets, receives the strong cochlearis process of the calcaneum. A large concave

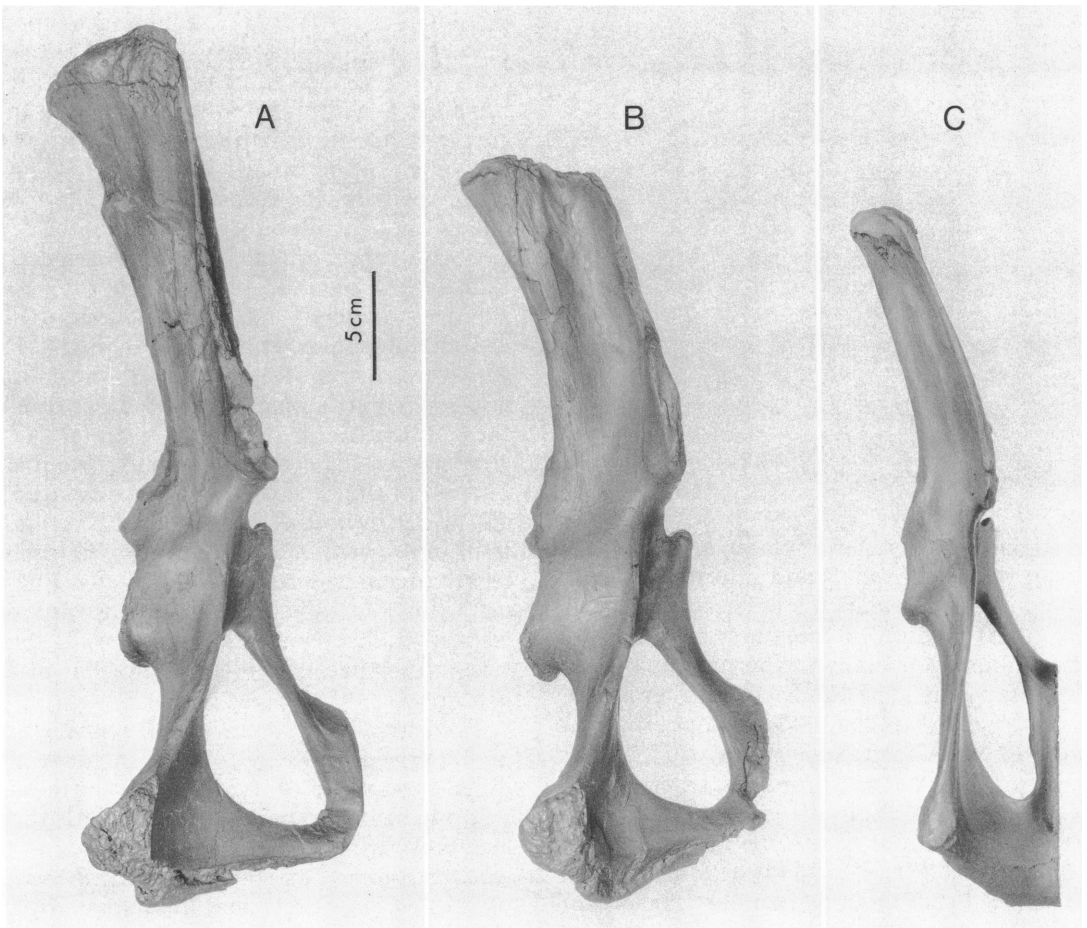

Fig. 30. Dorsal (**A–C**), ventral (**D–F**), and lateral (**G–I**) views of the pelvis of *Sthenurus stirlingi,* **A, D, G,** holotype, SAM P22533 (reversed); *S. tindalei,* **B, E, H,** AMNH 117499; and *Macropus giganteus,* **C, F, I,** AMNH 2390.

anterior lateral facet, a smaller internal contact along the lateral margin of the proximal end of the calcaneum, and a facet on the lateral surface of the head of the astragalus complete the astragalus–calcaneum contact. The navicular facet on the head of the astragalus is more laterally placed than in *M. giganteus*; more of the facet lies ventral to the median trochlea than in the gray kangaroos. In *S. stirlingi* (AMNH 117496) four sites of syndesmosis bind the astragalus to the calcaneum. These occur at the anterolateral, posterolateral, and medial corners of the astragalus in a similar manner to that described to *P. goliah* (Tedford, 1967). The form of the astragalus and its connection with the calcaneum in both *S. stirlingi* and *S. tindalei* is more robust than that of *M. giganteus* and reflects a tibia–tarsal articulation in which movement is confined more to the sagittal plane, and in which the major compressive stresses are directed more anteroventrally than in *M. giganteus.*

The calcaneum in *S. stirlingi, S. tindalei,* and *S. andersoni* is proportionally longer and much broader posteriorly than in *M. giganteus.* The plantar surface of the tuber calcis tapers anteriorly to the posterior border of the cuboid facet as in *P. goliah.* The sustentaculum in the sthenurine species is broader

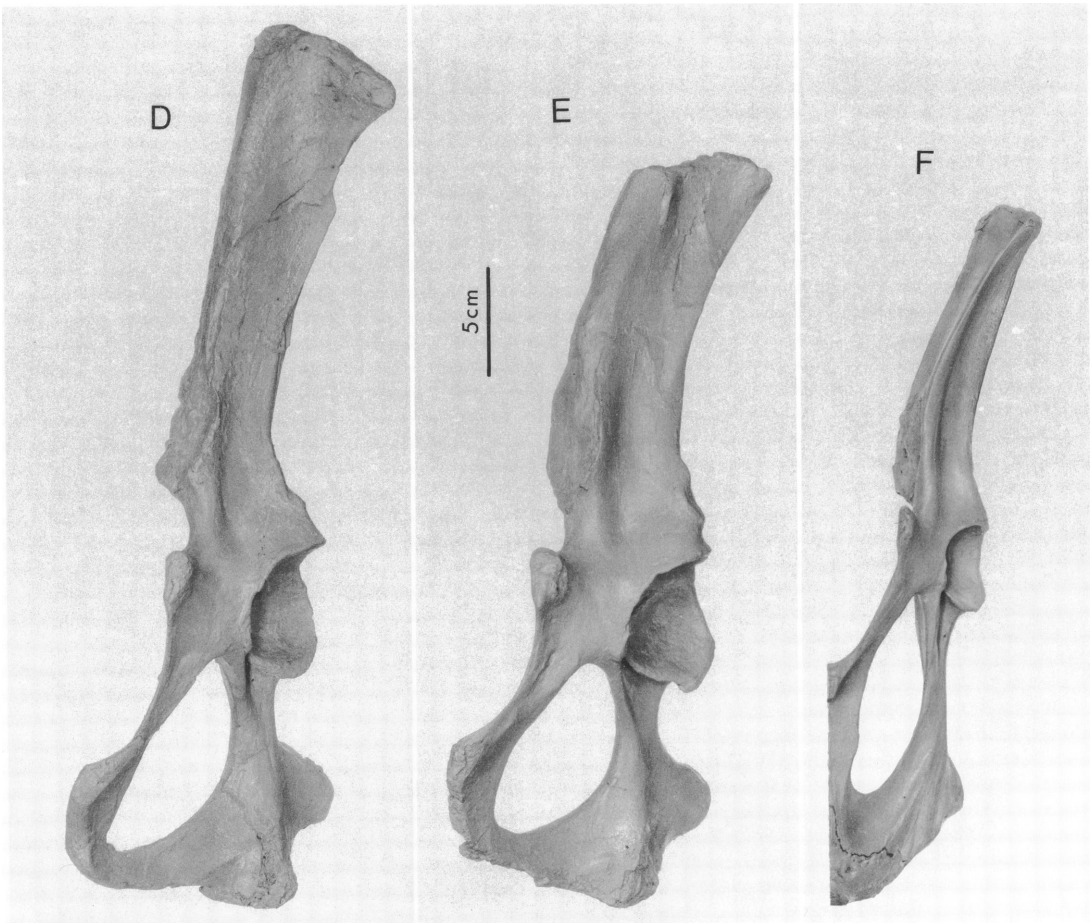

Fig. 30. Continued.

than in *M. giganteus* and is separated anteroventrally from the tuber calcis by a deep and narrow tarsal groove. The lateral condyle is not as produced as in *M. giganteus,* yet the concave channel beneath it is straighter and not blocked by the edge of the cuboid facet as in the latter species. This allows a more direct line of action for the tendon of the strong M. flexor digitorum longus. In *S. stirlingi* the dorsal border of the cuboid facets when viewed from the anterior aspect are inclined medially at approximately 25° to the base of the tuber calcis. The trochlea is similarly inclined. This is the same angle as in *S. tindalei* and *S. andersoni,* but less than in *M. giganteus* (30°). Unlike *M. giganteus,* the dorsal facets for the cuboid fuse with the ventral one to enclose a small intra-articular fossa.

The cuboid of *S. stirlingi,* as in *S. tindalei, S. andersoni,* and *P. goliah,* is proportionally much wider than that of *M. giganteus* and, unlike *S. tindalei,* is also proportionally slightly longer. The lateral plantar process is robust and extends across the base of the cuboid. It fuses with the incipient median plantar process rather than remaining separated from it by the deep groove, which in *M. giganteus* houses the tendon of the M. peroneus longus. In *S. tindalei* the median plantar process may remain discrete although weakly developed. The reduction of the median plantar process gives the cuboid a triangular outline rather than the rectangular form of *M. gi-*

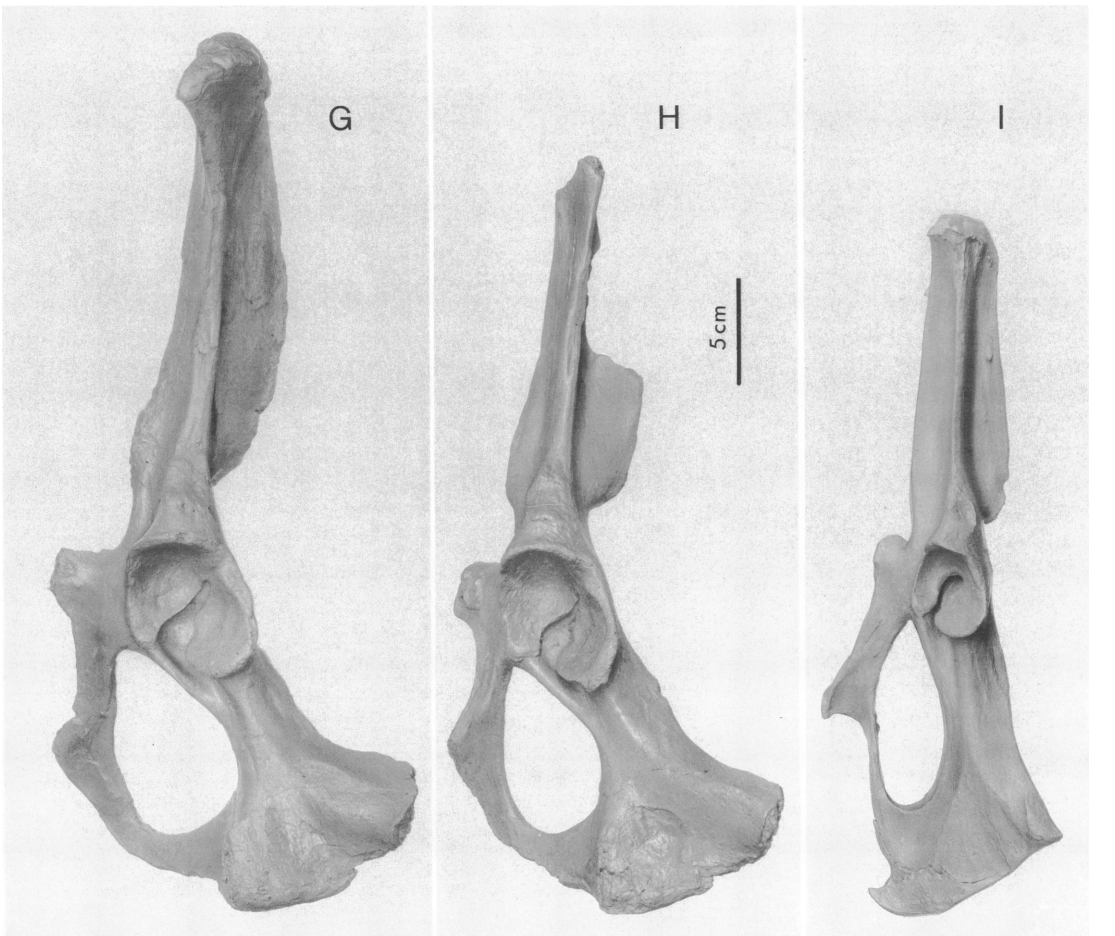

Fig. 30. Continued.

ganteus. As in *P. goliah,* the calcaneal facets are not as deeply stepped as in *Macropus.* The astragalar facet is larger than in *M. giganteus,* whereas the adjacent navicular facet is somewhat smaller. A small facet on the anterior medial surface and the large rugose area ventral to it mark the site of attachment of the cuneiforms. The anterior surface bears a large semicircular facet for the articulation with metatarsal IV and ventrally a posteriorly tilted smaller facet for metatarsal V.

The navicular of *S. stirlingi* and *S. tindalei* is essentially similar to that of *P. goliah* in which the ectocuneiform facet extends across the distal surface of the bone. A narrow groove on the medial aspect of the navicular represents the site of overlap of the proximal portion of the entocuneiform (Tedford, 1967). This is not apparent in *S. andersoni.*

In the holotype of *S. stirlingi* the three cuneiform bones form a composite including the proximal end of the vestigial 2nd metatarsal, which is fused proximally to the entocuneiform and anteriorly to the mesocuneiform, all of which are fused via the entocuneiform to the ectocuneiform. The anterior dorsal facet of the ectocuneiform forms the surface of articulation with the vestigial metatarsal III while the anterior ventral facet articulates with a facet on the medial side of the plantar process of metatarsal IV. The oblate plantar process of the ectocuneiform

curves medially in a smooth arc from beneath the fused entocuneiform. The fused cuneiforms contact the cuboid and metatarsal IV laterally via a rugose and presumably ligamentous attachment. A similar fusion of all cuneiforms was found in other adults (AMNH 117494 and 117496) of *S. stirlingi* and in *S. andersoni.* In adult *S. tindalei* (AMNH 117493 and 117499) and juvenile *S. stirlingi* (AMNH 117495), the entocuneiform remained discrete and bore a narrow rugose groove on its medial aspect, presumably the site of attachment of the meso- and entocuneiform bones. In *Procoptodon goliah* the cuneiform composite is formed by the ectocuneiform, mesocuneiform, and proximal end of metatarsal III (Tedford, 1967); the entocuneiform and metatarsal II were not fused to this entity. In moving kangaroos, most of the body weight is transferred directly to the metatarsals via the calcaneum and cuboid and to a lesser extent via the astragalus–navicular contact (Marshall, 1974). In the sthenurine kangaroos, metatarsal V is much reduced distally; however, its proximal plantar aspect is quite robust. Some indication of the relative weight distribution across the metatarsals can be gained from a comparison of the relative areas of the proximal facets. In both *S. stirlingi* and *S. tindalei,* approximately 83–85 percent of the total proximal contact area of the metatarsals is associated with IV, 10–11 percent with V, and approximately 6 percent with II and III. Approximately 70–73 percent of the contact with metatarsal IV is via the calcaneum, whereas 12–13 percent is via the ectocuneiform. This differs from *M. giganteus* where all the contact with metatarsal IV (approximately 55 percent of total) is via the cuboid while metatarsals II and III account for approximately 25 percent and metatarsal V approximately 20 percent.

The importance of metatarsal IV as a support for the weight of the animal is reflected by the cross-sectional area at midshaft. For *P. goliah, S. stirlingi, S. tindalei,* and *S. andersoni* it ranges from 1.2 to 1.5 times larger than that predicted for a similar size *M. giganteus.* Within the sthenurine kangaroos the most robust metatarsals IV (cross-sectional area/length) occur in *S. stirlingi* and *P. goliah. Sthenurus andersoni* metatarsal IV is the most gracile of this group. As the length of metatarsal IV to other hind limb elements is similar in all these sthenurine species and in *M. giganteus,* the differences in cross-sectional area provide insight into the relative bulk of each of the extinct species. The proximal articulating facet of metatarsal IV of these sthenurines forms a continuous arc from the plantar process to the midlateral aspect surrounding a narrow intra-articular depression similar to that of *P. goliah* (Tedford, 1967). A rugose crest arises posteromedially from the plantar process in the sthenurines compared here to form the posterior rim of a groove for the syndactylous digits. A small facet on this crest articulates with a matching facet on the ectocuneiform such that a small portion of the body weight is directed from the astragalus via the navicular and ectocuneiforms to metatarsal IV. The proximal portion of the shaft of metatarsal IV is lateromedially flattened while distal flattening occurs in a dorsoventral plane. When viewed laterally, the shaft is convex dorsally and concave ventrally; a median keel extends distally from the plantar process for approximately two thirds of the length of the shaft. A posterolateral depression of the proximal end of the plantar process houses metatarsal V; medially, another depression accommodates a large tarsal or plantar sesamoid that is deeply

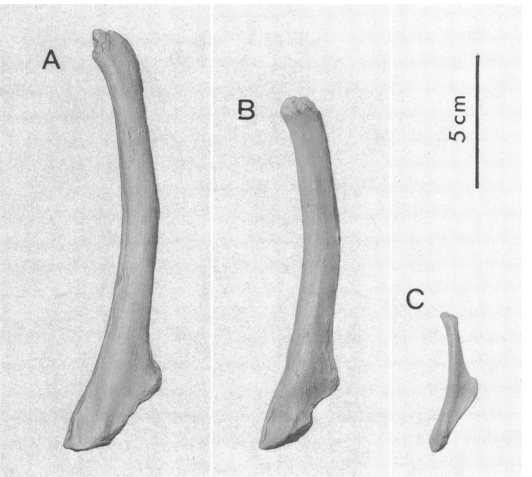

Fig. 31. Lateral views of the left epipubic bones of *Sthenurus stirlingi,* **A,** AMNH 117496 (reversed); *S. tindalei,* **B,** AMNH 117493; and *Macropus giganteus,* **C,** AMNH 2390.

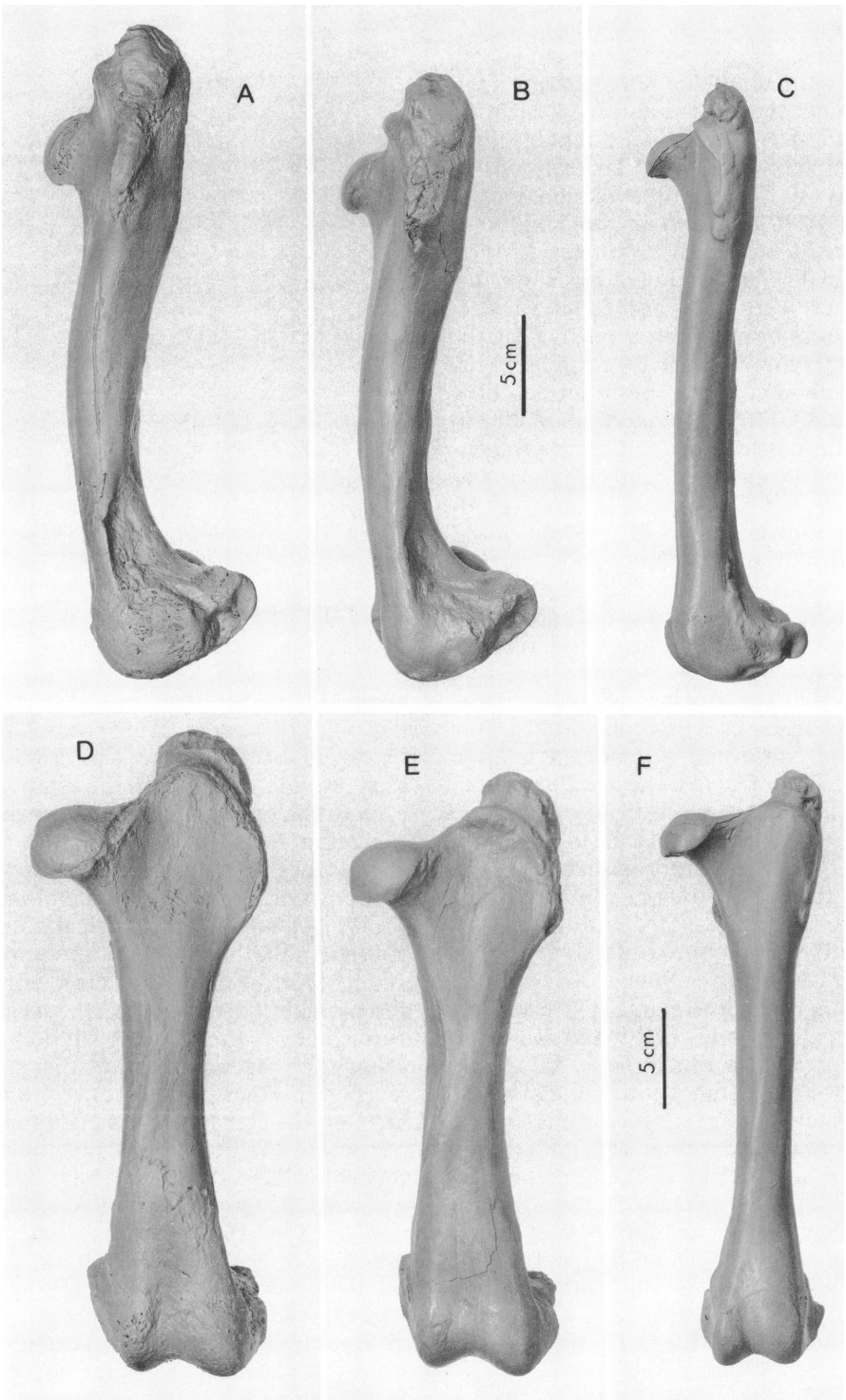

Fig. 32. Lateral (**A–C**), dorsal (**D–F**), and ventral (**G–I**) views of the femur of *Sthenurus stirlingi,* **A, D, G,** holotype, SAM P22533 (reversed); *S. tindalei,* **B, E, H,** AMNH 117499 (reversed); and *Macropus giganteus,* **C, F, I,** 2390.

grooved ventrally for the peroneal tendon. The transverse diameter of the distal articulating surface relative to the length of metatarsal IV is proportionally similar to *P. goliah* and is approximately 1.6 times that of *M. giganteus*. Two ovoid sesamoids fit over the distal posterior articulating surface on either side of a low median keel as in *Macropus* species. The presence of the keel in *S. andersoni* suggests a similar arrangement of sesamoids. Very shallow grooves on either side of the median keel mark the position of metatarsals V and III. These grooves converge distally.

The complete right and the proximal portion of left metatarsal V are preserved in the holotype of *S. stirlingi*. In *S. tindalei* a complete right metatarsal V is available (AMNH 117494), but in *S. andersoni* only the proximal left and the distal shaft and broken distal end adhering to metatarsal IV is preserved. Although distally the shaft is reduced to a thin splint, the proximal end of this metatarsal is quite robust and has a well-developed plantar process. The distal end of the shaft bears a small bulblike eminence with an oblong facet, suggesting the presence of a vestigial proximal phalanx.

Only the small triangular proximal portion of right metatarsal III is preserved in the holotype of *S. stirlingi*, whereas the left part, with a portion of its shaft still adhering to metatarsal IV, is present in *S. tindalei* (AMNH 117493). Poor preservation has obscured all details of this bone in *S. andersoni*. This bone is similar in both species. It articulates proximally with the anterior dorsal facet of the ectocuneiform and inserts laterally into a rugose channel on the medial aspect of metatarsal IV. Only the proximal half of the very thin straplike shaft is present in *S. tindalei*, but a shallow groove along metatarsal IV suggests that it extended the length of the median keel. The presence of a shaft is inferred in *S. stirlingi* from the nature of the distal end of the fragment preserved and

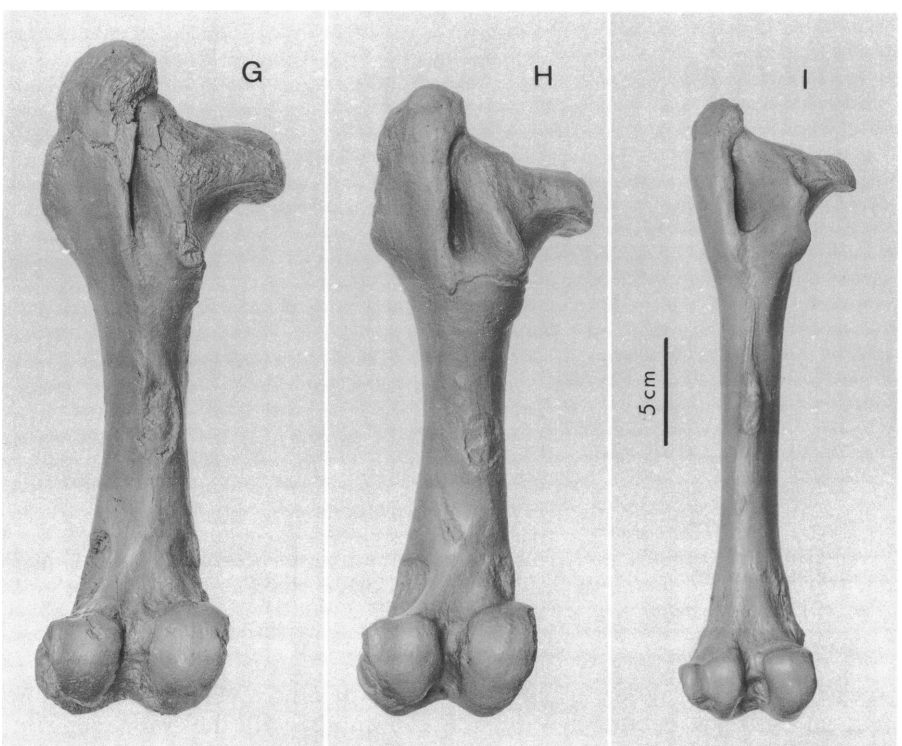

Fig. 32. Continued.

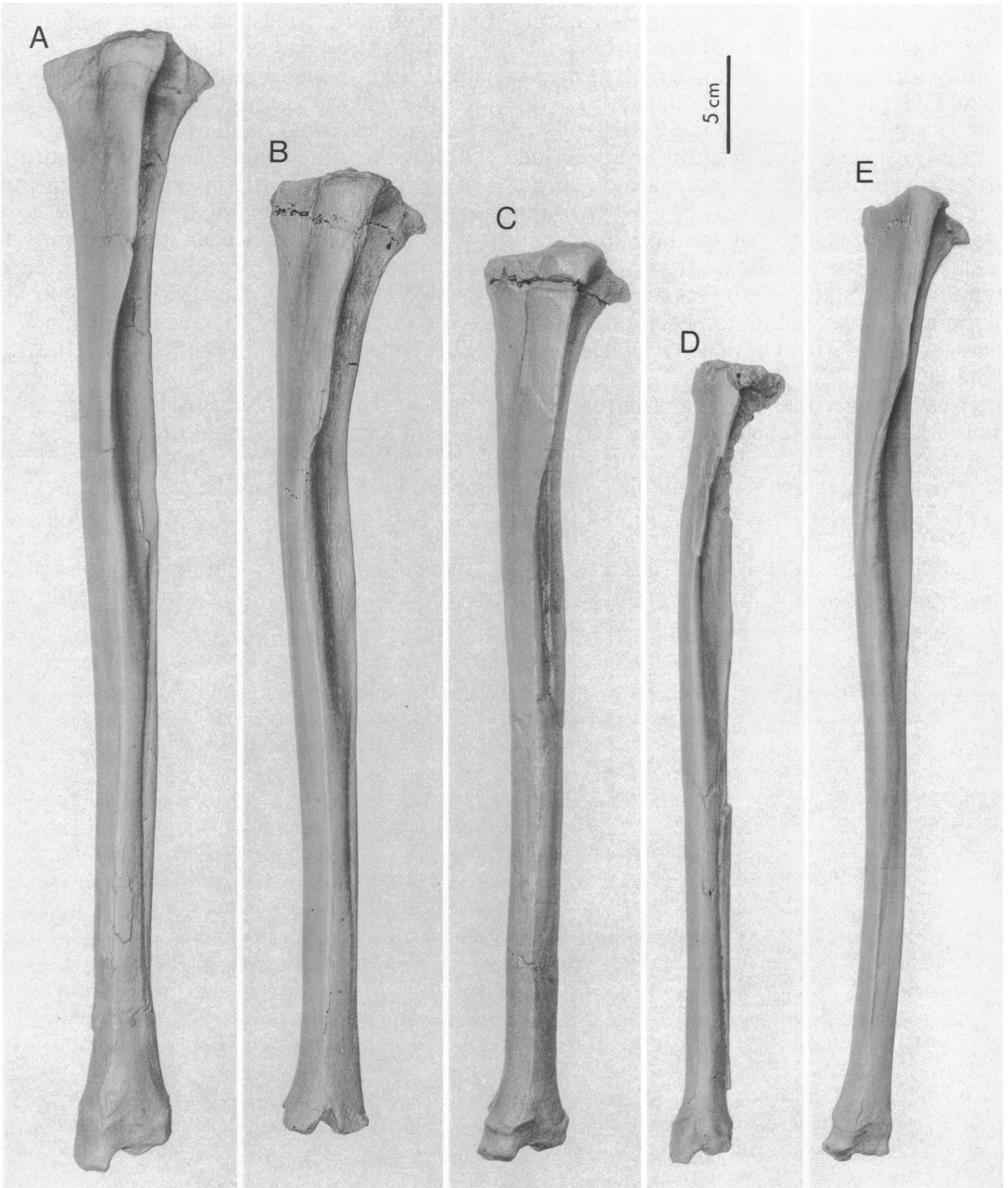

Fig. 33. Anterior (**A–E**) and lateral (**F–J**) views of the tibia of *Sthenurus stirlingi,* **A, F,** holotype, SAM P22533 (reversed); *S. tindalei,* **B, G,** 117499, and **C, H,** AMNH 117493; *S. andersoni,* **D, I,** SAM P13673 (reversed); and *Macropus giganteus,* **E, J,** AMNH 2390.

shallow groove extending at least halfway down metatarsal IV. Like metatarsal V, this bone may have borne a vestigial phalanx.

As previously described, metatarsal II persists as a tiny vestigial oblong bone fused proximally with the entocuneiform, laterally with the ectocuneiform, and anteriorly with the even small ovoid mesocuneiform. It has

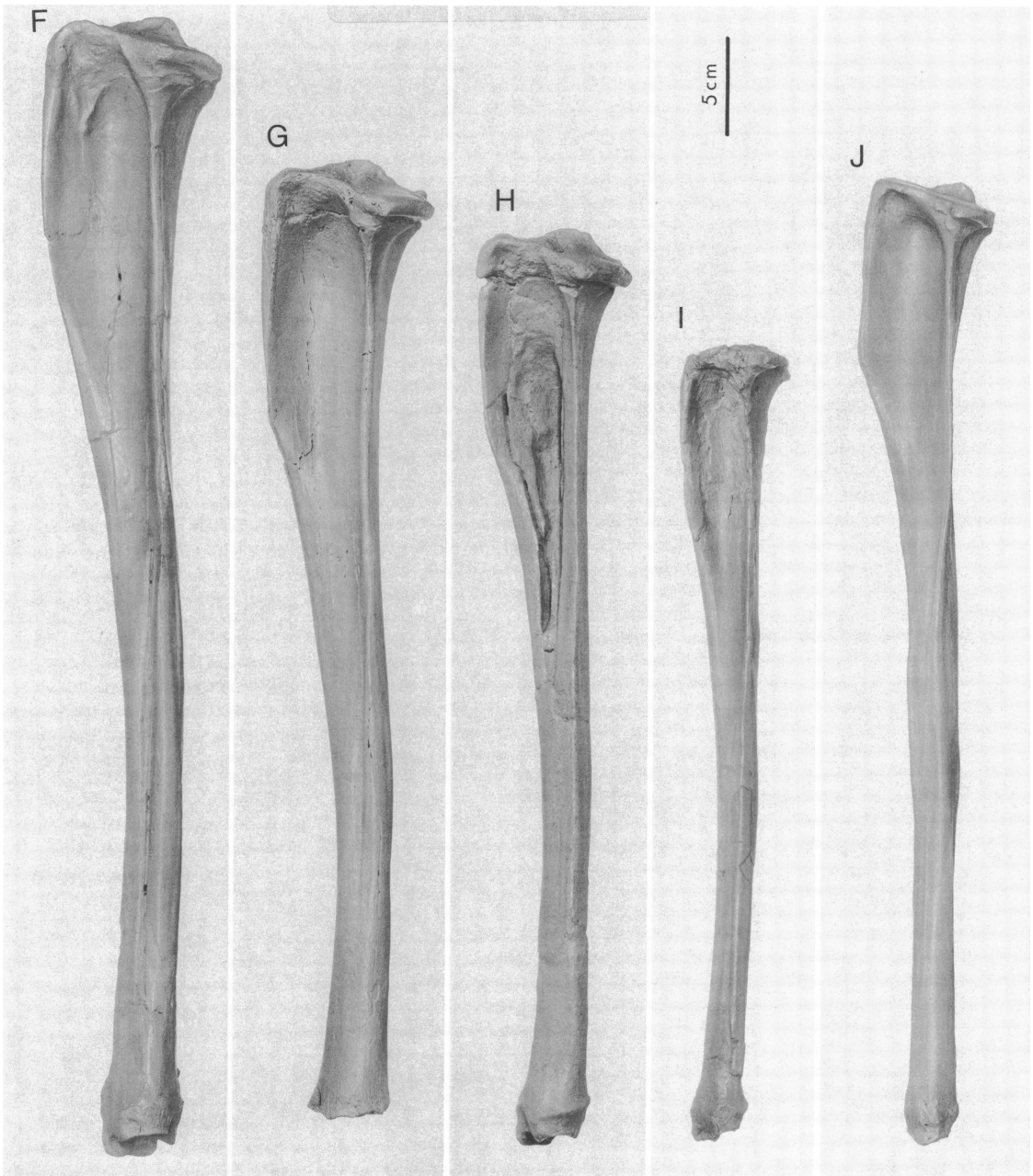

Fig. 33. Continued.

no shaft, with the distal termination being smoothly rounded in *S. stirlingi, S. tindalei,* and *S. andersoni.*

In the three sthenurine species the proximal phalanx of the 4th digit is similar in form to that described for *P. goliah* (Tedford, 1967). It is easily distinguished from that of *Macropus* by the more robust, flattened, subtriangular shaft, the greater lateral expansion of the proximal and distal ends, and the presence of paired ligament scars on the mid-posterior aspect of the shaft. Tedford (1967)

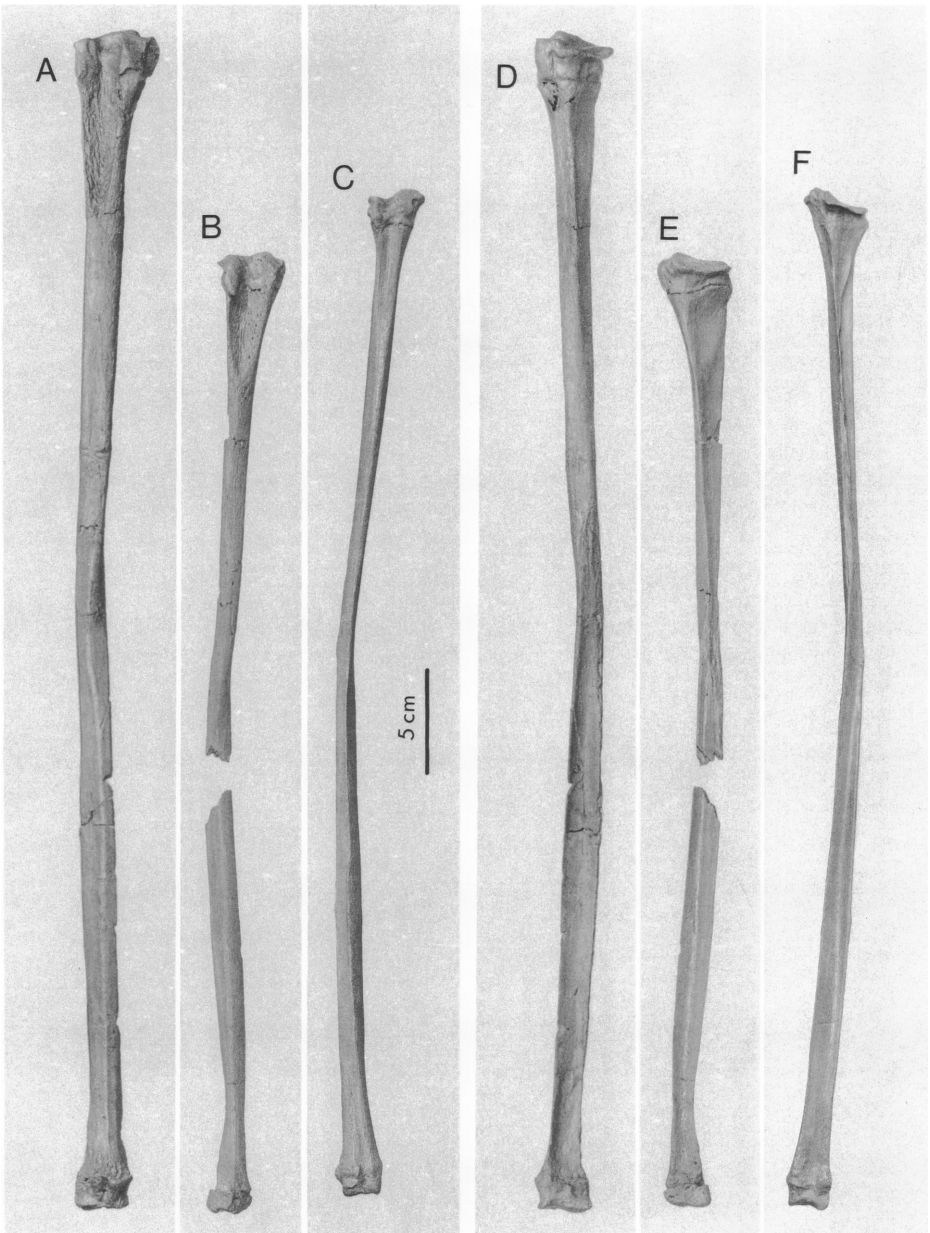

Fig. 34. Lateral (**A–C**) and medial (**D–F**) views, respectively, of the fibula of *Sthenurus stirlingi,* **A, D,** holotype, SAM P22533; *S. tindalei,* **B, E,** AMNH 117493; and *Macropus giganteus,* **C, F,** AMNH 2390, all views reversed.

suggested that these paired scars in *P. goliah* may be homologous with the sesamoid ligament scars in the Equidae. The scars of the short sesamoidean ligaments lie on either side of a median notch in the posterior border of the proximal articulation. A small pit distal to this notch marks the site of insertion of the crossed sesamoidean ligaments. The insertion of the collateral ligaments and the flexor tendon is marked by prominences on the lateral edges of the distal anterior surface of the phalanx. The site for insertion of the

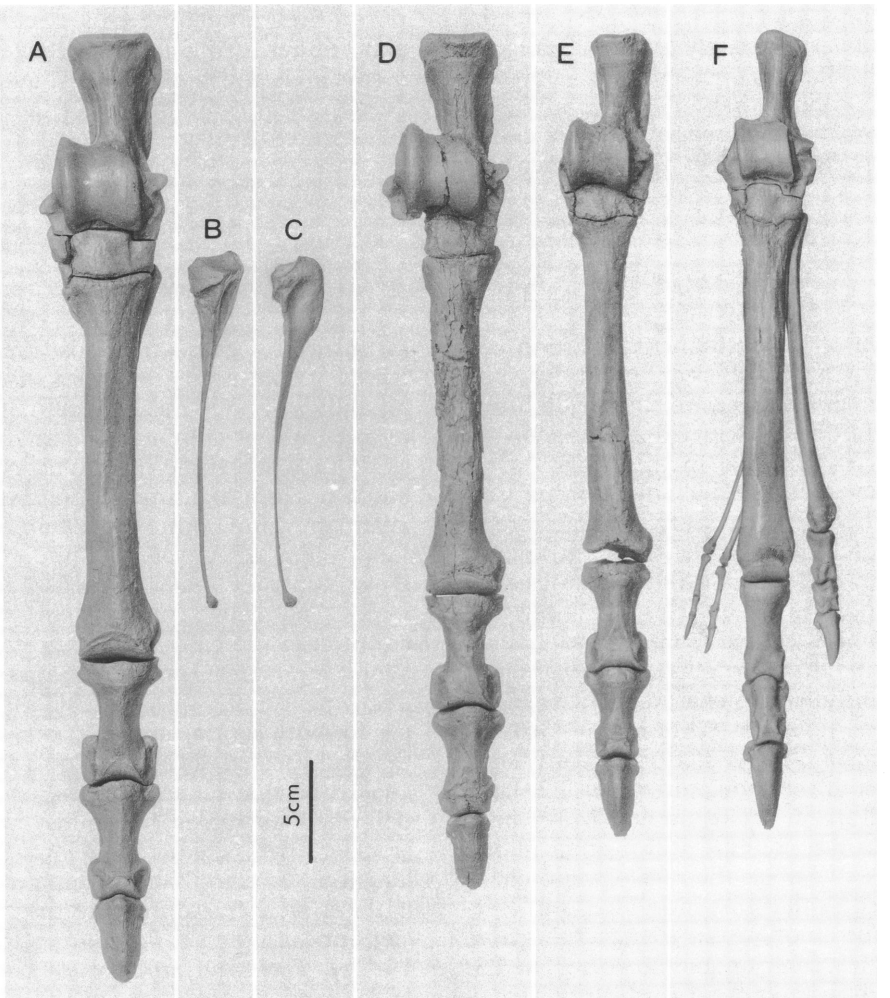

Fig. 35. Dorsal view of the pes of *Sthenurus stirlingi,* **A,** holotype, SAM P22533, **B,** anterior, and **C,** lateral views of 5th metatarsal of holotype; *S. tindalei,* **D,** AMNH 117493; *S. andersoni,* **E,** SAM P13673; and *Macropus giganteus,* **F,** AMNH 2390, all views reversed.

extensor tendon is marked by a well-developed ridge paralleling the dorsal proximal border.

The median phalanx of the 4th digit in *S. stirlingi, S. tindalei,* and *S. andersoni* is relatively long compared with that of *M. giganteus.* It is more tapered distally than the proximal phalanx. The strong shaft is triangular in cross section with a marked anterior median crest. In contrast to *M. giganteus,* the median phalanx in the three sthenurine species is almost equal in length to the proximal phalanx. The large rugose areas on the ventral surface of the proximal end mark the site of insertion of the plantaris tendon. Large processes on the lateral and medial aspects of the proximal articulation mark the site of attachment of the collateral ligaments. The distal articular surface is broadly sulcate as in *P. goliah.*

The distal phalanx of the 4th digit is proportionally shorter and more robust than in *M. giganteus.* It bears a relatively wide and deeper plantar process, which has a well-defined transverse groove marking the insertion of the flexor hallucus longus. Unlike *M. gi-*

ganteus, the ungual process in both *S. stirlingi* and *S. tindalei* is strongly arched distally and posteriorly. The tip of the process is broader and more rounded than in *M. giganteus.* The ungual process in *S. andersoni* more closely approaches *Macropus* in the presence of a dorsal keel, giving the cross section a triangular rather than a flattened shape. The process is arched as in the other sthenurines, but is more sharply terminated, thereby resembling *Macropus.*

ONTOGENY AND SEXUAL DIMORPHISM

Eruption of the permanent dentition provides one of the few reference points by which the ontogenetic changes in the skeleton may be gauged. The 12 individuals assigned to three species reported in this work do not provide an adequate base for comparison, particularly since the juvenile stages are so poorly represented (as befits an entrapment mechanism biased toward the largest, heaviest individuals). Nevertheless, it is possible to gain some idea of the eruption sequence (table 23) and to confirm that *S. stirlingi* shows the late eruption of P3 characteristic of sthenurines. The juvenile (AMNH 117495) has worn permanent upper incisors, an early stage in eruption of the molars in which P2, Dp3, and M1–2 are in occlusion and M3–4 have calcified crowns, but are still in their maxillary crypts. Wear on the incisors and cheek teeth indicates that this individual was free-ranging. The holotype is a young adult whose M4/m4 is in occlusion and unworn. The P3/p3 shows beginning wear, indicating that it must have erupted just prior to M4/m4, perhaps coordinated with beginning of wear on M3/m3. The conditions in *S. tindalei* (AMNH 117492 and 117493) closely resemble *S. stirlingi* and suggest that these two large *Sthenurus* species had an eruption sequence similar to *Procoptodon.* Comparative analysis of growth of living large kangaroos and Callabonna *Sthenurus* discussed below suggests that fully erupted permanent teeth accompany the attainment of near adult size.

Where associated portions of the postcranial skeleton were available, it was apparent that there were marked disparities in size of limb elements between some individuals within each taxon. Similar differences are to be found among extant kangaroos and are attributable to sexual dimorphism (Poole et al., 1982a, 1984). Poole et al. (1982a) studied the growth of gray kangaroos (*Macropus giganteus*) in captivity in order to ascertain the reliability of body measurements for age determination of animals in the field. In their study they compared the molar index (Kirkpatrick, 1965) of animals of known age with head, limb, and body lengths (table 24). They found that after vacating the pouch, the growth rate of males exceeded that of females. The growth curves of both sexes tended toward different asymptotes after 3 years. Wood et al. (1983) demonstrated that head and limb lengths were reliable indicators of age for both captive and wild gray kangaroos that had vacated the pouch. Poole et al. (1984) concluded that sexual dimorphism was best described as males becoming "larger and stockier, with greater development in the length of the arm than the females." Similar patterns were found in other macropod species, for example, *M. fuliginosus* (Poole et al., 1982b), *Petrogale xanthopus* (Poole et al., 1985), and in our own studies of museum specimens of *M. rufus.*

On the assumption that sexual dimorphism is a characteristic of the larger species of the Macropodidae, we sorted the Callabonna sthenurines into relative age classes based on molar eruption and wear (table 23) and then compared the proportions of skull and postcranial elements when available.

We assumed that growth curves for these sthenurines were similar to those published for *M. giganteus* (Poole et al., 1984); that is, after 3 years of age (MI = 2.37), growth curves tended toward the asymptote. For example, the youngest adult *S. stirlingi* (SAM P22533, table 23) has a tooth eruption and wear pattern that, if it were *M. giganteus,* would be close to the 3-year asymptote. We do not imply that this extinct species is the same chronological age (3 years), but rather the

same ontogenetic age (i.e., has reached the same point in the general growth curve, the asymptotic portion). Where the difference in size of similar age individuals of the same species is equal to or greater than the sex difference between extant species, the former were deemed sexual morphs. For example, if we compare humerus and femur lengths for *S. stirlingi* specimens P22533 and AMNH 117496, there is a 32 percent and 17 percent difference in size, respectively. Male and female *M. giganteus* of similar ages have an average difference in distal forearm and hind limb lengths of 17 percent and 11 percent, respectively (table 24). We therefore propose that the holotype of *S. stirlingi* is a male and that AMNH 117496 is a female. Similar comparisons were used to assign sex to other specimens.

FUNCTIONAL ANATOMY

In the section below we advance functional interpretations to account for the morphological differences observed between the Callabonna sthenurine skeletons and those of the larger extant species of macropodines.

THE CHEEK TEETH AND ZYGOMA: Sanson (1978, 1980) examined the relationships between aspects of molar morphology and dietary preferences within the Macropodinae. He recognizes two broad adaptive types, browsers and grazers. The former is typified by the living forms *Wallabia, Dorcopsis, Dorcopsulus, Dendrolagus, Thylogale, Setonix,* and *Lagostrophus*; the latter is represented by forms such as *Macropus, Megaleia, Peradorcus, Onychogalea,* and *Lagorchestes.* The character states associated with these broad dietary preferences are indicated in table 25 (taken from Sanson, 1980) along with the morphological features found in the Callabonna sthenurines.

Sanson viewed the characteristics of the browsing grade as primitive and those of the grazing grade as derived. The derived characters of the grazing molar include the presence of mid- and forelinks and broad anterior cingula. Both adaptations increase the surface area for shearing and grinding and are coupled with high crowns and molar progression as adaptations to compensate for wear produced by the tough and high abrasive grasses. In contrast, the browsing molar tends to be a simple, low-crowned tooth with weak or incipient links that maintains a fixed position within the jar or palate.

We interpret the molars of the Callabonna sthenurines as an advanced browsing grade. They tend to be proportionally high-crowned; they have weakly developed midlinks and broad anterior cingula; and, although the large premolars preclude molar progression, the plane of occlusion of both upper and lower cheek teeth is curved such that throughout the life of the animal wear on the anterior teeth brings the posterior teeth further into occlusion. The increased wear on the lingual side and the pattern of striae on the enamel/dentine surfaces indicate a sequence of jaw movements similar to those proposed for the browsing *Wallabia bicolor* by Sanson (1980). The closure of the median valley on the labial side of the upper molars may prevent loss of food to the cheek region in the first phase of the chewing cycle (Phase 1 of Sanson, 1980).

In Phase 2 of the chewing cycle in browsers (Sanson, 1980) the jaw is moved anteriorly, thereby forcing the anterior face of the lophids down the posterior face of the lophs and moving the jaws apart. Sanson suggested that this phase serves to rupture soft palasade or mesenchymatous cells of the browse. The pattern of wear facets on the posterior faces of the lophs and anterior faces of the lophids (wear facets 3 and 4 of Sanson, 1980) of the large Callabonna sthenurines is indicative of a similar jaw movement. The midlink descending to the protocone and the weaker posterior cingulum descending to the metaconule serve to direct the jaw labially. The deepening of the medial valley lingual of the midlink would result in at least part of the diced plant material being shed from the tooth at the close of Phase 1 to be picked up by the tongue and returned for further treatment or swallowed. The remaining part trapped between the lophs as the jaw opens (Phase 2)

would be ground and spread across the posterior face of the lophs, ready for the next shearing phase. In this manner the diced plant material would be moved anteriorly along the tooth row, encountering progressively more worn teeth. With increasing wear, the anterior molars would function more and more as pestles and mortars, grinding and pulping the finely comminuted food. The lingual crests of the broad subtriangular upper premolars would provide a similar function. Indeed, the marked anterior curvature of the upper cheek tooth row medially, lingually, and dorsally of a point opposite the masseteric process produces the shift in cheek tooth function from simple shearing on the posterior molars (almost exclusively Phase 1), then shearing and grinding (Phases 1 and 2) in midtooth row, to almost exclusive grinding on anterior cheek teeth.

The decrease in molar widths anteriorly and posteriorly of the masseteric process may allow for a more equable distribution of bite forces per unit area of tooth contact along the cheek tooth row (i.e., this represents a balance between the frictional forces involved in tooth-to-tooth contact and the area of movement about the fulcrum). Further refinement of tooth function is to be found in the concave form of the lophs and lophids producing point shearing in the first phase of occlusion. The slight lingual convergence of the lophs would also serve to exert increased pressure on the shearing and grinding faces at the end of each phase of the chewing cycle.

The masseteric process of the zygoma, a mere nubbin in *S. andersoni* and *S. tindalei,* develops a descending process in *S. stirlingi.* In the tree sloths this process allows for the development of a strong horizontal portion of the masseter muscle (Sicher, 1944) that is responsible for the grinding movement in the last phase of protraction of the mandible. By analogy with the sloth, this process may have played a similar role in Phase 2 of the masticatory cycle of *S. stirlingi.* Note that lines drawn along the axis of each loph converge in approximately the position of the masseteric process on the nonoccluding side, suggesting that the balancing side musculature may play an important role in the masticatory cycle. The geometry suggests that the anteriorly directed fibers of the masseter on the balancing side may act as antagonists to those of the occluding side, thereby serving to control the medial rotation of the jaw about a vertical axis centered on the masseteric process of the nonoccluding side.

ANTERIOR PALATE, MANDIBLE, AND INCISOR ARRAY: The most obvious characters separating the genera *Sthenurus* and *Procoptodon* relate to the proportions of the anterior part of the skull. The more elongate nasal region, the longer diastemata, the procumbent lower incisors, and the weak symphyseal union endow the genus *Sthenurus* with macropodine-like features. These skull proportions are in marked contrast to the almost edentate-like skulls of species of *Procoptodon* (Tedford, 1966, 1967). Macropodine-like structures are thought to correlate with the adoption of a grazing habit (Anderson, 1927; Ardran et al., 1958; Ride, 1959; Tedford, 1966), the increase in diastemal length with an increase in tongue length necessary for the procurement and manipulation of food, the procumbent lower incisors with gathering of food, and the weak symphyseal union with mandibular movements allowing the maximum surface of the lower incisors to be opposed to the upper incisors during biting (Ride, 1959). Although all three Callabonna species exhibit some grazing macropodine characters, only *S. tindalei* has the combination that includes procumbent lower incisors, relatively long diastemata, and a weak symphyseal union. Furthermore, the ascending ramus is raked posteriorly as in *Macropus* species, although the masseteric foramen invades the body of the mandible only as far forward as M4. Abbie (1939) suggested that the more medial migration of the deep portion of the masseter in the Macropodidae reinforces the poorly developed lateral pterygoid musculature of the opposite side to provide the lateral movements of the jaw that occur during the second phase of the masticatory cycle (Sanson, 1980). The more anterior insertion also compensates for the loss of leverage resulting from an increase in diastema length and the procumbency of the lower incisors (Abbie, 1939).

Both *S. stirlingi* and *S. andersoni* have less procumbent lower incisors and proportionally shorter diastemata than *S. tindalei.* They do not exhibit the anterior development of

the masseteric foramen, suggesting a jaw musculature in which the major emphasis is placed on the first or occlusal phase of the masticatory cycle, and in which less emphasis is placed on the lateral or grinding movements of the jaw in the second phase of mastication. In all three species, enamel covers both the labial and lingual faces of the upper incisors, but only the labial surface and midline contact of the lower incisors. The dentine on the lingual side of i1 wears to leave an enamel ridge along the labial aspect of the tooth. Striae patterns shown on the enamel and dentine of the upper incisors can only be produced by an anteromedial movement of the lower incisor. Forward excursion of the jaw appears to be halted by I1, which acts as a stop at the apex of the V formed by the upper incisors. The gathering of plant material is presumably affected by the oblique movement of the enamel ridge of the lower incisor across the enamel ridges of I2.3 in a shearing action similar to that described by Anderson (1927). Ride (1959) observed incisor biting in *M. rufogriseus* and noted that grass stems were seized between the lower and upper incisors and severed by a jerk of the head rather than by incisor movements. However, these animals were eating "long grass," and incisor shearing may be more important when animals are cropping small blades close to the ground. Certainly the resulting wear on the more procumbent lower incisors of *S. tindalei* produces a relatively longer occlusal surface for biting than in *S. stirlingi* or *S. andersoni.* In contrast, *Procoptodon goliah* has a very small area of incisor contact. The narrow, more steeply inclined lower incisors are opposed by a small peglike array of upper incisors similar to that of the leaf-eating koala and brush-tailed possum, a configuration that in combination with a short diastema allows the exertion of considerable bite pressure when severing leaf petioles or small stems. By analogy, the food of *S. stirlingi* and *S. andersoni* ought to require more pressure but less bite contact to harvest than that of *S. tindalei,* notwithstanding the increase in leverage obtained by the more anterior insertion of the deep masseter in the latter species. The relatively shorter diastema in *S. stirlingi* and *S. andersoni* suggests a diet requiring a less manipulative tongue than in *S. tindalei,* whereas the relatively higher-crowned cheek teeth and jaw mechanics are indicative of a diet that requires more shearing than grinding than that of *S. tindalei. Sthenurus tindalei* is thus considered to be a grazer/browser with a diet that was finer-textured than that of *S. stirlingi.* The latter probably had a diet that included leaf petioles and the occasional leafy stems where larger plant cells interspersed with lignified ribs and veins required a dicing treatment with slightly less emphasis on grinding. *Sthenurus andersoni,* although a much smaller animal, is a closer functional analogue to *S. stirlingi* than *S. tindalei.*

NASAL SINUS: The inflated supraorbital region is an outstanding feature of *S. stirlingi* and is characteristic of at least two other sthenurine species (viz. *Simosthenurus brownei* and *S. maddocki*; Wells and Murray, 1979). Sagittal sections of the latter species reveal two large sinuses above the ethmoturbinals, connected to the nasal passageway via small ostia. Similar structures occur in both the red kangaroo *M. rufus* and the gray kangaroo *M. giganteus,* but not in the tree kangaroo (Negus, 1958). Their function is unknown, although their position relative to the nasal sinus is suggestive of an olfactory rather than a thermoregulatory role.

POSTCRANIAL SKELETON: The most striking difference between the skeletons of the sthenurine kangaroos and the large macropodines is the more robust nature of the individual bones; indeed, by comparison the macropodines appear quite gracile. For example, the ratio of midshaft cross-sectional area to femur length in sthenurines is almost double that of macropodines. If we assume that size-adjusted cross-sectional area is a function of body mass, then *S. tindalei* and *S. stirlingi* are considerably more robust than the gracile macropodines.

Windsor and Dagg (1971) used cinematographic techniques to study the gaits of 19 species of macropodines. They suggested that the fastest gait, the bipedal hop, evolved from the quadrupedal bound and that the nature of the former correlates well with the habitat of the species. They found no correlation between the lengths of the femur and tibia and the bipedal hop pattern; however, they did

report a greater increase in the length of the tibia over that of the femur in larger species.

The tree kangaroos, *Dendrolagus* species, retain the primitive gaits, the walk, and the quadrupedal bound, and even when hopping bipedally, their mean stride length is shorter than their body size would suggest (Windsor and Dagg, 1971). Among the remaining larger species, stride length is correlated with size. However, the percentage of time that the hind feet were in contact with the ground per stride did not correlate with size, and seemed more to reflect the habitat of the species; that is, those that live in dense scrublands have increased the time their feet remain in suspension during a stride. The red kangaroo, *M. rufus,* had the longest ground contact during a stride, which in turn is a function of the hind limb trajectories and subsequent posture when hopping.

The proportions of the tree kangaroo, *Dendrolagus lumholtzii,* reflect its adaptations to an arboreal life (i.e., it has a relatively short body and long balancing tail). The forelimb to hind limb ratio is high, while the proximal portions of both forelimbs and hind limbs are relatively long, reflecting the necessity to provide power for climbing. In contrast, the terrestrial macropodines have relatively long hind limbs with longer distal elements, adaptations that increased stride length.

The skeletal remains of two Callabonna species, *S. stirlingi* and *S. tindalei,* are sufficiently complete to allow comparisons of limb and vertebral column proportions with the extant species for which the gait is known (tables 26, 27).

In the Callabonna sthenurines the proportions of the vertebral column, with the exception of the tail, most closely resemble those of the large extant macropodines. Their skeletons differ in the following proportions from those of *Macropus* species: (1) the sthenurines have slightly shorter tails; (2) their forelimbs are similar to *Macropus* in overall length, yet have a relatively longer manus and shorter radius/ulna; (3) their hind limbs are proportionally similar to those of the large extant macropodines, but are much longer relative to the vertebral column (fig. 36).

These characters suggest greater biomechanical affinity with the bipedal terrestrial forms rather than the tree kangaroos, although one can only speculate on the selective advantage of lengthening the hind limbs. This could be related to increasing stride length or height when standing erect or both.

Little can be deduced about the locomotor abilities of *Sthenurus.* A comparison of the pelvic structures with those of macropodines reveals some differences in muscle mechanics. The increase in length and width of the ilium and the more acute ilial angle provides both greater area and leverage to the gluteus medius, the flexor of the thigh, and the erector spinae. The origin and insertions of the femoral flexors are well developed on the ilium, and the lever arms for the femoral extensors, as well as the adductor muscles, are relatively much shorter than in *Macropus.* This arrangement would decrease the power the adductor muscles could deliver in the latter part of the propulsive phase; however, such arrangement does increase such muscles' value in preventing the legs from spreading under the weight of the body when standing, particularly given the broad pelvis and divergent resting position of the femur. Further mechanical advantage is gained by the greater depth of the ischiopubic region of the pelvis, which effectively increases the horizontal component of the adductor action. There is little difference in the lever arms of the remaining femoral and tibial flexors, the biceps femoris, and the semi-membranosis. It appears that these pelvic differences are related to supporting the great mass of the animal when standing on the hind legs and raising the body either when feeding or during the first phase of propulsion.

The relationship between the fibula and tibia has been studied in macropodines. Parsons (1896) suggested that "during internal rotation of the leg on the thigh the head of the fibula is pressed back by the external condyle of the femur and forms a spring like buffer to check that movement." Craven (1971) noted that the shallow groove down the lateral proximal aspect of the fibula is the site of insertion of the m. peroneus longus, which sends a tendon across to the medial side of the foot in the channel between metatarsal IV and the cuboid. Its action involves both dorsi-flexion and weak eversion of the foot. In these sthenurine kangaroos the groove for the origin of the m. peroneus longus is a prominent feature, although the groove on the lateral malleolus and across the calca-

neum and astragalus appears rather narrow compared with *Macropus* species. Nonetheless, it suggests the presence of a powerful muscle for everting and dorsal flexing of the foot. The cuplike structure of the lateral distal articulating facet of the tibia would be ideally suited to rotation and eversion of the foot about the tibia.

Two points are noteworthy when examining the head of the sthenurine fibula. First, this head lacks the distinctive posterior process of *Macropus* species. This process inserts in the groove in the lateral condyle of the femur in *Macropus*; the subdued process allows greater flexion of the knee in *Sthenurus*. Second, the groove in the proximal tibial epiphysis for insertion of the fibula head is relatively longer in sthenurines, whereas the fibula head is about the same relative length as that of macropodines. This suggests a capacity for greater internal rotation of the lower limb about the femur.

All of these limb movements can be observed in the Muybridge (1887) photographs of hopping kangaroos. The differences suggested for the sthenurines relate only to the degree of movement. For example, the articular facets on the distal condyle of the femur suggest a greater arc of movement of the tibia in *Sthenurus* than in *Macropus,* while reduction of the posterior proximal process of the fibula would allow greater internal rotation of the lower limb.

A possible explanation for these differences is to be found in the structure of the pelvis, which in sthenurines is very wide across the acetabula. However, the relative lengths of the hind limb elements are not significantly different from *Macropus* species. When hopping, the lower limbs would need to be rotated even more medially to position the toes centrally prior to landing. The evidence for this rotation is found in the longer groove for articulation of the fibula with the tibial head. The collateral ligaments binding the fibula head to the distal end of the femur would presumably cause the proximal end of the fibula to slide posteriorly relative to the tibia as the latter was rotated internally. There may be a large enough process on the head of the fibula for it to be pressed back by the lateral condyle of the femur to form a "springlike buffer" (Parsons, 1896). Thus, on leaving the ground, the lower limb would spring back into the sagittal plane just as the phalanges and calcaneum snap back on the release of the load on the foot ligaments. This spring system would require strong binding of the fibula to the tibia by interosseous ligaments and may account for the groove on the tibial shaft of *S. stirlingi.* The well-developed sesamoidean ligament scars on the underside of the pes suggest that elastic tendons and ligaments may have greatly assisted locomotion in these species and in *Procoptodon,* as suggested by Tedford (1967: 144).

The almost vestigial nature of metatarsal V in the sthenurines results in a monodactyl pes (digit IV). Among extinct macropodines only the open plains red kangaroo *M. rufus* approaches this condition, whereas the reverse is to be found among the small thicket-dwelling rat kangaroos. In the absence of correlates with the locomotory modes of living species, speculation is hazardous; however, this state suggests a gait involving less lateral maneuverability than forms with divergent toes.

Support for this hypothesis is found in the structure of the vertebral column. Alternate limb loadings in mammals, be they quadrupedal or bipedal, place rotational stresses on the backbone. These rotational stresses are resisted by both the zygapophyseal joints and the muscles and ligaments attached to the vertebral process. In the Callabonna sthenurines the vestigial nature of the diapophyses and anapophyses suggests a reduction in importance of those axial muscles involved in flexing the back. Similarly, these animals lack zygapophyseal modifications to the anticlinal vertebra of the type found in *Macropus* species which resist dorsiflexion. The extended metapophyses in the lumbar region in sthenurines would give greater leverage to muscles supporting the fore end of the body, while their almost vertical orientation would also resist both lateral and rotational deflection of the backbone. Similarly, the vestigial anapophyses of the caudal vertebrae suggest an insignificant role for those muscles (M. extensor caudae lateralis) involved in the lateral extension of the tail, while the deep, broad chevrons would provide increased leverage to the caudal flexors.

The close juxtaposition of the neural spines across the lumbar–sacral joint in *S. stirlingi* is indicative of a strong ligamentous connec-

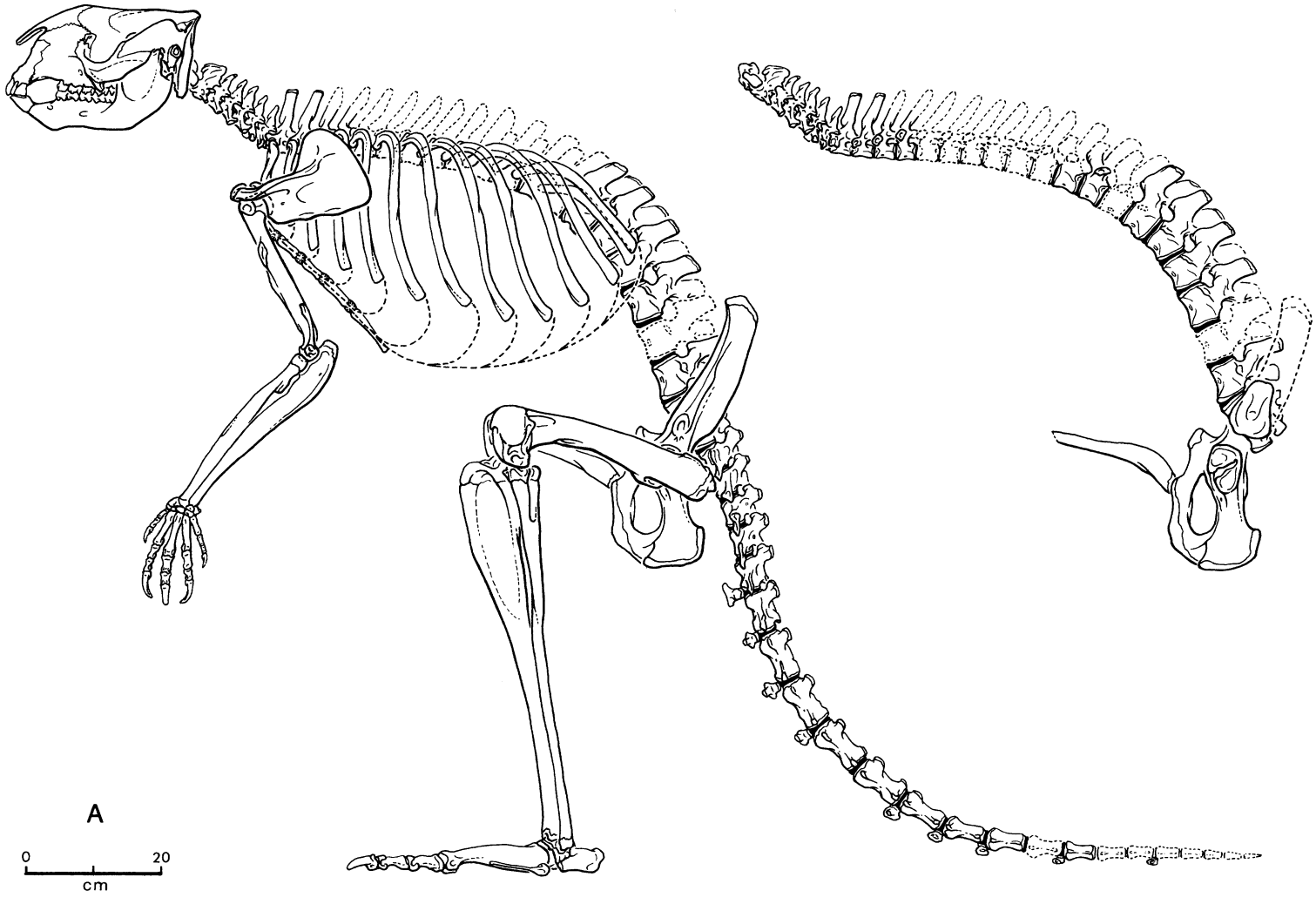

Fig. 36. Comparative lateral views of the articulated skeletons, trunk vertebrae, and pelvis of **A,** *S. stirlingi,* based on the holotype SAM P22533, a male; **B,** *S. tindalei* based mostly on AMNH 117493, a female; and **C,** *Macropus giganteus,* SAM M667, a male; all to the same scale.

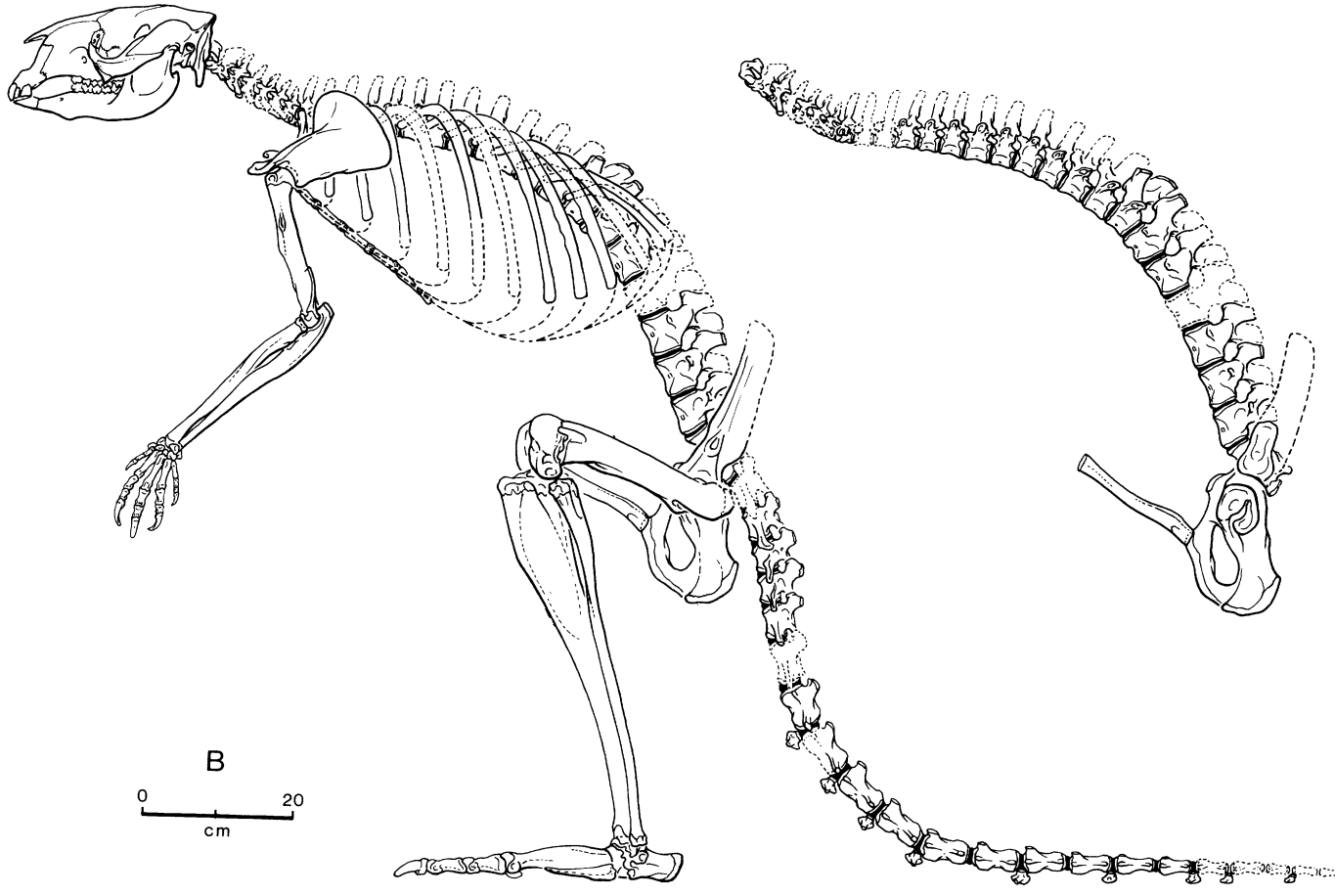

Fig. 36. Continued.

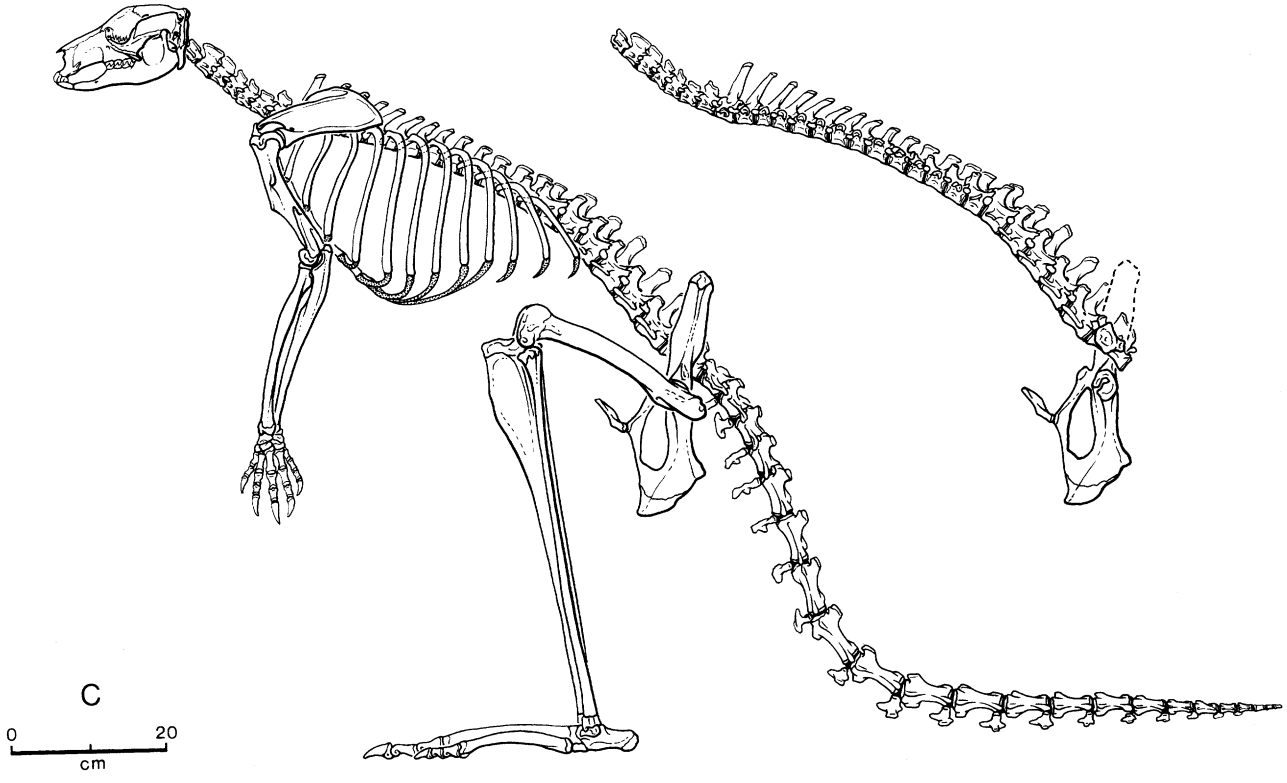

Fig. 36. Continued.

tion, which is less well developed in *S. tindalei*. Even the cervical vertebrae in these species with their short, almost platycoelous, centra would almost totally eliminate neck flexibility.

In summary, it appears that in these sthenurines selection has favored the development of a rigid backbone capable of limited flexion in the dorsoventral plane, with a trunk and hind limb musculature having maximum mechanical advantage either in the early phase of propulsion or in rotation of the body about the hip joint when standing. The relatively short tail with restricted lateral movement, in combination with a monodactyl pes and rigid backbone, creates the impression of a locomotory mode of limited maneuverability. All these features are not inconsistent with the broad pelvis and long epipubic bones that possibly function to support the large bulk of the alimentary canal expected in a browsing mammal.

The forelimb of the sthenurine kangaroos, although relatively no longer than that of the larger macropodines, is proportionally different. Selection has favored an increase in the length of the manus and a concomitant reduction in that of the radius and ulna. The greatly elongated central digits are capable of considerable flexion, greatly increasing their prehensile ability. Paradoxically, the wrist, although pivoting about the prominent styloid process of the ulna, lacks the ellipsoid form to the carpus, thereby restricting movement largely to extension and flexion. However, the subequally developed radius and ulna allow for considerable pronation and supination. The olecranon process, out-lever of the triceps, is relatively short in comparison with the in-lever of the biceps. This lessens the ability of the triceps and anconeus to resists flexion of the elbow under pressure of the body weight or provide propulsion during quadrupedal locomotion, and probably relates to the emancipation of the forelimb from a locomotory role. The long and strong acromion process of the scapula, large infraspinous fossa, large and strong clavicles, and broad sternum are all features suggesting adaptations for reaching and pulling with the forearms. Indeed, the acromion process is long enough to allow the clavicle to pass over the coracoid process when the forearm is raised, a feature not found in macropodine kangaroos. This latter characteristic suggests that the forearms may well have been particularly adapted as tools used in the procurement of browse.

CONCLUSIONS

This study of sthenurine kangaroo remains from Lake Callabonna, South Australia, has treated their comparative morphology and functional anatomy, as well as the systematics of species within the genus *Sthenurus*. We have also considered the history of the stratigraphic succession exposed at Lake Callabonna and the mode of accumulation of the remains. The deposits at Lake Callabonna are of special significance in the study of large Pleistocene marsupials in that well-preserved remains of individual animals can be recovered in reasonable articulation and quantity. In the case of the *Sthenurus* material described above, this provides an unprecedented view of the osteology of new taxa and of forms known from much more incomplete material. The presence of such complete material allows much fuller ancillary studies in functional anatomy and variation.

Our stratigraphic and geochronologic results show that the fossil vertebrate remains at Lake Callabonna accumulated in a shallow, saline lacustrine basin, considerably larger in dimensions than the present-day salina. The fossil fauna lived in medial Pleistocene time sometime within the span 0.2–0.7 Ma. At the time of accumulation, the vicinity of the lake supported a more arborescent flora than that of today, but one containing most of the same taxa that presently exist in better watered parts of the surrounding region. The stratigraphic record indicates dry climatic cycles of yearly or greater periodicity. The mode of entrapment of the animals was by bogging, and hence the fossil fauna is biased toward large, heavy mammals and ratite birds. This type of entrapment provides articulated remains as well as some unusual modes of preservation such as impres-

sions of tissues (skin) due to the evaporitic geochemical environment within the enclosing sediments.

Remains of sthenurine kangaroos were relatively common at site 4, and we have identified three closely related species within the genus *Sthenurus* Owen, 1873. Apart from their primitive living representative *Lagostrophus,* the Sthenurinae are a unique subfamily of Macropodidae known principally from Pliocene and Pleistocene deposits in Australia (they are so far unknown in New Guinea). The fossil forms are characterized by virtual monodactyly of the pes, great modification of the manus and forelimb, and many other aspects of the skeleton that make their remains readily identifiable with respect to other kangaroos. Their deep skulls and robust mandibles and strongly bilophodont teeth lacking prominent longitudinal crests ("links") have long been the most easily distinguished remains. The postcranial materials reported here for the first time now enable recognition of most of the bones of the sthenurine skeleton.

Prior to this work, the most completely known fossil sthenurine was *Procoptodon goliah* based on a referred specimen from the late Pleistocene deposits at Lake Menindee, New South Wales (Tedford, 1967). In this specimen, fragments of much of the appendicular skeleton were represented, and these now provide a basis for comparison with the *Sthenurus* skeletons from Lake Callabonna. The very close resemblance of the postcranial skeleton of the largest *Sthenurus, S. stirlingi,* and *Procoptodon goliah* shows that there is a unique suite of features that unite these taxa despite the differences in their skulls and dentitions.

The three Callabonna *Sthenurus* species differ in size: *S. andersoni* Marcus, 1962 is the smallest, about the size of the living euros (*Osphranter*); *S. tindalei* Tedford, 1966 and *S. stirlingi* (described in this paper) are closer in size, the latter being the largest. Strong sexual dimorphism appears to characterize the genus, resulting in size overlap between individuals of the larger taxa. The large species equal the largest living kangaroos in lengths of appendicular bones, but comparable sthenurine elements are heavier and the axial skeleton has different proportions.

The strong morphological differences between the skeleton of sthenurines and living kangaroos inhibit functional anatomical analysis for lack of a closely comparable living model. Despite the completeness of skeletal material, our results are somewhat equivocal. Dentally, most sthenurines seem to fit the browsing grade in Sanson's (1978) model. The exception is *Procoptodon,* whose strongly linked cheek teeth correspond to the grazing-grade despite the lack of a cropping incisive battery. There are no comparable large browsing kangaroos in the present-day fauna, yet the sthenurines constituted a diverse group of species in the Pleistocene (Bartholomai, 1963; Tedford, 1966). Further evidence indicative of a browsing adaptation is found in the osteology of the forelimb with its greatly elongated manus with strongly reduced lateral digits. The slender forearm and humerus and curiously humanlike scapula are all features suggesting mobility of the forelimb and ability to raise the limb above the head to procure browse. The forelimb seems to have become emancipated from its primitive locomotor role to a degree not seen in living kangaroos. These differences suggest that *Sthenurus* was mostly a stand-up browser and the axial and hind limb structures reinforce this notion. The spinal column is constructed to eliminate flexibility with its short cervical column, thoracics, and lumbars with reduced sites for insertion of the axial muscles flexing the back and short tail with similarly reduced flexors. The lumbar vertebrae on the other hand have greatly enlarged metapophyses that would give greater leverage in extension of the fore end of the body. The axial column seems organized as a rigid structure capable of limited flexion, but of considerable extension of the anterior part of the body that would be important in stretching upward for high browsing.

The striking differences in form of the sthenurine pelvis when compared to macropodines seems related to flexion and adduction of the thigh required to support the large-bodied animal when standing, raising the body when feeding, or in the initial phase of bipedal locomotion. Hind limb element proportions in *Sthenurus* do not differ significantly from *Macropus,* but the limbs are longer relative to the axial column and have more massive cross sections. The hind limb and foot of sthenurines use the elastic properties

of tendons and ligaments to augment muscular action across joints, especially at the knee and plantar parts of the pes. A complex spring mechanism involving the mortised tibia–fibula articulation, fibula–femur articulation, and collateral ligaments binding the later joint indicate a mechanism for realigning the lower limb during the suspended phase of propulsion so that the feet are positioned centrally prior to landing. Sthenurines show great elaboration of the sesamoidean and collateral ligaments of the pes that would provide increased spring-flexion of the foot during the propulsive phase of locomotion and would also provide tension of the phalangeal array during extension of the foot while standing on the distal phalanges during high browsing.

The overall impression our functional speculations have produced is that *Sthenurus* was a bulky, browsing kangaroo that sacrificed quadrupedal or pentapedal movement for greater dependence on bipedal saltation and extension of the body and forelimbs for higher browsing. Just how the three species coexisting at Lake Callabonna partitioned this broad feeding niche beyond utilizing plants of different height is difficult to understand. Our functional analysis of the dentition and jaws suggests different masticatory mechanisms that may be related to differences in browse among these species. Other sthenurine faunas (Tedford, 1966: fig. 20) are similarly diverse and may have several taxa of closely comparable size that challenge our understanding of a group with only a single, very primitive living representative (*Lagostrophus*; Flannery, 1983).

REFERENCES

Abbie, A. A.
1939. A masticatory adaptation peculiar to some diprotodont marsupials. Proc. Zool. Soc. London 109: 261–279.

Anderson, C.
1927. The incisor teeth of the Macropodinae. Australian Zool. 5: 105–112.

Archer, M.
1978. The nature of the molar–premolar boundary in marsupials and a reinterpretation of the homology of marsupial cheek teeth. Mem. Queensland Mus. 19(2): 157–164.
1984. The Australian marsupial radiation. *In* M. Archer and G. Clayton (eds.), Vertebrate zoogeography and evolution in Australasia, pp. 633–808. W. Australia: Hesperian Press.

Ardran, G. M., F. M. Kemp, and W. D. L. Ride
1958. A radiographic analysis of mastication and swallowing in the domestic rabbit: *Oryctolagus cuniculus* (L.). Proc. Zool. Soc. London 130: 257–274.

Bartholomai, A.
1963. Revision of the extinct macropodid genus *Sthenurus* Owen in Queensland. Mem. Queensland Mus. 14(3): 53–76.
1978. The Macropodidae (Marsupialia) from the Allingham Formation, northern Queensland. Results of the Ray E. Lemley Expeditions, Part 2. Mem. Queensland Mus. 18(2): 127–143.

Bauschulte, C.
1972. Morphologische und biochemische Grundlagen einer functionelle Analyse der Muskeln der Hinterextremität (Untersuchung on quadrupeden Affen und Känguruhs). Z. Anat. Entwicklungs gesch. 138: 167–214.

Bowler, J. M.
1976. Aridity in Australia: age, origins and expression in aeolian land forms and sediments. Earth-Sci. Rev. 12: 279–310.

Bowler, J. M., and J. T. Teller
1986. Quaternary evaporites and hydrological changes, Lake Tyrell, northwest Victoria. Australian J. Earth Sci. 33: 43–63.

Brown, H. Y. L.
1894. Annual report of the Government Geologist for the year ended June 30th 1894. Adelaide: Govt. Printer. 26 pp., 3 pls.

Buckley, J.
1973. Isotopes' radiocarbon measurements X. Radiocarbon 15(2): 280–298.

Callen, R. A.
1977. Late Cainozoic environments of part of northeastern South Australia. J. Geol. Soc. Australia 24(3): 151–169.
1984. Quaternary climatic cycles, Lake Millyera region, southern Strzelecki Desert. Trans. Roy. Soc. S. Australia 108(3): 163–173.

Callen, R. A., and R. H. Tedford
1976. New late Cainozoic rock units and depositional environments, Lake Frome area, South Australia. Trans. Roy. Soc. S. Australia 100(3): 125–168.

Callen, R. A., R. J. Wasson, and R. Gillespie
1983. Reliability of radiocarbon dating of

pedogenic carbonate in the Australian arid zone. Sediment. Geol. 35(1): 1–14.

Carlsson, A.
1914. Uber *Dendrolagus dorianus*. Zool. Jahr. Systematik 26: 547–617.
1915. Zur Morphologie des *Hypsiprymnodon moschatus*. K. Svenska Vetenskaps akad. Handl. 52: 1–48.

Craven, H.
1971. Functional aspects of the anatomy of the lower limb in *Megaleia rufa* with references to the richochetal mode of locomotion. Honor's thesis, Dept. Zoology, Monash University, Victoria, Australia.

Elftman, H. O.
1929. Functional adaptations of the pelvis in marsupials. Bull. Am. Mus. Nat. Hist. 58: 189–232.

Evans, H. E., and G. C. Christensen
1979. Miller's anatomy of the dog. Philadelphia: W. B. Sanders, i–xv, 1–1181 pp.

Firman, J.
1974. Structural lineaments in South Australia. Trans. Roy. Soc. S. Australia 98(3): 153–171.

Flannery, T. F.
1983. Revision in the macropodid subfamily Sthenurinae (Marsupialia: Macropodidae) and the relationships of the species of *Troposodon* and *Lagostrophus*. Australian Mammal. 6: 15–28.

Flannery, T. F., and M. Archer
1984. The macropodoids (Marsupialia) of the early Pliocene Bow Local Fauna, central eastern New South Wales. Australian Zool. 21(4): 357–383.

Flannery, T. F., M. Archer, and M. D. Plane
1983. Middle Miocene kangaroos (Macropodoidea: Marsupialia) from three localities in northern Australia, with a description of two new subfamilies. Bur. Miner. Resour. Geol. Geophys. Rep. (Canberra) 7: 287–302.

Fletcher, H. O.
1948. Fossil hunting "West of the Darling" and a visit to Lake Callabonna. Australian Mus. Mag. 9(9): 315–321.

Glauert, L.
1926. A list of Western Australian fossils. Geol. Surv. W. Australia Bull. 88: 36–71.

Hatt, R. J.
1932. Vetebral columns of richochetal rodents. Bull. Am. Mus. Nat. Hist. 63: 219 pp.

Hardy, M. H.
1947. The group arrangement of hair follicles in the mammalian skin. Part I. Notes on follicle group arrangement in thirteen Australian marsupials. Proc. Roy. Soc. Queensland 58: 125–148.

Kirkpatrick, T. H.
1964. Molar progression and macropod age. Queensland J. Agric. Sci. 21: 163–165.
1965. Studies of the Macropodidae in Queensland. 2. Age estimation in the grey kangaroo, the red kangaroo, the eastern wallaroo and the red-necked wallaby, with notes on dental abnormalities. Queensland J. Agric. Anim. Sci. 22: 301–307.

Löffler, E., and M. E. Sullivan
1979. Lake Dieri resurrected: an interpretation using satellite imagery. Z. Geomorph. N. F. 23(3): 233–242.

Marcus, L. F.
1962. A new species of *Sthenurus* (Marsupialia, Macropodidae) from the Pleistocene of New South Wales. Rec. Australian Mus. 25(14): 299–304.

Marshall, L. G.
1974. Why kangaroos hop. Nature 248: 174–176.

Muybridge, E.
1887. Animals in motion. Ed. Lewis S. Brown. New York: Dover (1957), 264 pp.

Nanson, G. C., D. M. Price, and S. A. Short
1992. Wetting and drying of Australia over the past 300 ka. Geology 20: 791–794.

Negus, V. W.
1958. The comparative anatomy and physiology of the nose and paranasal sinuses. Edinburgh and London: E. & S. Livingstone Ltd.

Parsons, F. G.
1896. On the anatomy of *Petrogale xanthopus* compared with that of other kangaroos. Proc. Zool. Soc. London, 1896: 683–714.

Poole, W. E., S. M. Carpenter, and J. T. Wood
1982a. Growth of grey kangaroos and the reliability of age determination from body measurements. I. The eastern grey kangaroo, *Macropus giganteus*. Australian Wildl. Res. 9: 9–20.
1982b. Growth of grey kangaroos and the reliability of age determination from body measurements. II. The western grey kangaroos, *Macropus fuliginosus fuliginosus, M. f. melanops* and *M. f. ocydromus*. Australian Wildl. Res. 9: 203–212.
1984. Growth of grey kangaroos and the reliability of age determination from body measurements. III. Interspecific comparisons between eastern and western grey kangaroos, *Macropus giganteus* and

M. fuliginosus. Australian Wildl. Res. 11: 11–19.

Poole, W. E., J. C. Merchant, S. M. Carpenter, and J. H. Calaby
1985. Reproduction, growth and age determination in the yellow-footed rock wallaby *Petrogale xanthopus* Gray, in captivity. Australian Wildl. Res 12: 127–136.

Rich, T. H.
1984. News from foreign members: Australia. Soc. Vertebr. Paleontol. News Bull. 130: 28.

Ride, W. D. L.
1959. Mastication and taxonomy in the macropodine skull. Syst. Assoc. Publ. 3: 33–59.

Rose, R. W.
1978. Reproduction and evolution in female Macropodidae. Australian Mammal. 2: 65–72.

Sanson, G. D.
1978. The evolution and significance of mastication in the Macropodidae. Australian Mammal. 2: 23–28.
1980. The morphology and occlusion of the molariform cheek teeth in some Macropodinae (Marsupialia: Macrpodidae). Australian J. Zool. 28: 341–365.

Semichon, L.
1926. Caractéres particuliers de la peau de la queue du kangaroo, *Macropus rufus* Desmarest. Arch. de Zool. Exp. Gén., Notes et Rev. 65: 96–102.

Sicher, H.
1944. Masticatory apparatus of the sloths. Field Mus. Nat. Hist. Zool. Ser. 29: 161–167.

Stirling, E. C.
1894. The recent discovery of fossil remains at Lake Callabonna, South Australia (Parts I and II). Nature 50(1286): 184–188; (1287): 206–211.
1900. Fossil remains of Lake Callabonna. Part II. 2. The physical features of Lake Callabonna. Mem. Roy. Soc. S. Australia I(pt. II): i–xv.
1913a. Fossil remains of Lake Callabonna. Part IV. Description of some further remains of *Genyornis newtoni* Stirling and Zietz. Ibid. 1(4): 111–126.
1913b. Fossil remains of Lake Callabonna. Part IV. 2. On the identity of *Phascalomys* (*Phascolonus*) *gigas* owen and *Sceparnodon ramsayi* Owen with a description of some of its remains. 1(4): 127–178.

Stirling, E. C., and A. H. C. Zietz
1899. Fossil remains of Lake Callabonna. Part I. Description of the manus and pes of *Diprotodon australis* Owen. Mem. Roy. Soc. S. Australia 1(4): 1–40.
1900. Fossil remains of Lake Callabonna. Part II. 1. *Genyornis newtoni* a new genus and species of fossil struthious bird. Ibid. 1(2): 41–80.
1905. Fossil remains of Lake Callabonna. Part III. Description of the vertebrae of *Genyornis newtoni*. Ibid. 1(3): 81–110.

Stirton, R. A.
1954. Digging down under. Pac. Discovery 7(2): 2–13.
1963. A review of the macropodid genus *Protemnodon*. Univ. California Publ. Geol. Sci. 44(2): 97–162.

Tedford, R. H.
1966. A review of the macropodid genus *Sthenurus*. Univ. California Publ. Geol. Sci. 57: 71 pp.
1967. The fossil Macropodidae from Lake Menindee, New South Wales. Univ. California Publ. Geol. Sci. 64: 156 pp.
1973. The diprotodons of Lake Callabonna. Australian Nat. Hist. 17(11): 349–354.
1980. Stratigraphic studies at Lake Callabonna, South Australia. Australian Quat. Newsletter 14: 20–21.

Thomas, O.
1888. Catalogue of the Marsupialia and Monotremata in the collection of the British Museum (Natural History), London: i–xiii, 1–401 pp.

Wells, R. T., and P. Murray
1979. A new sthenurine kangaroo (Marsupialia, Macropodidae) from southeastern South Australia. Trans. R. Soc. S. Australia 103(8): 213–219.

Williams, D. L. G.
1980. Catalogue of Pleistocene vertebrate fossils and sites in South Australia. Trans. R. Soc. S. Australia 104(5): 101–115.

Windsor, D. E., and A. I. Dagg
1971. The gaits of the Macropodinae (Marsupialia). J. Zool. London 163: 165–175.

Wood, J. T., W. E. Poole, and S. M. Carpenter
1983. Validation of aging keys for eastern grey kangaroos, *Macropus giganteus*. Australian Wildl. Res 10: 213–217.

Woodburne, M. O., H. R. Tedford, M. Archer, W. D. Turnbull, M. D. Plane, and E. L. Lundelius
1985. Biochronology of the continental mammal record of Australia and New Guinea. Spec. Publ. S. Australian Dept. Mines and Energy 5: 347–363.

Wopfner, H., R. Callen, and W. K. Harris
1974. The lower Tertiary Eyre Formation of the Southwestern Great Artesian Basin. J. Geol. Soc. Australia 21: 17–52.

TABLE 1
Measurements of Skulls of *Sthenurus*

Measurements	*S. stirlingi* SAM P22533	*S. stirlingi* SAM P12882	*S. tindalei* AMNH 117493	*S. tindalei* AMNH 117491
Condylobasal length, ant. edge I^1 to post. edge occipital condyle	—	312.3	—	—
Bizygomatic width	151.0	—	129.5	—
Width across paroccipital process	115.0	—	82.1	—
Palatal length, post. edge post. palatine bar to post. edge I^1 alveolus	154.1	180.0	136.0	152
Diastema length, post. edge I^3 alveolus to ant. edge P^3 alveolus	46.8	60.0	52.0	53.4
Palatal width at ant. root M^1	43.5	41.1	40.8	—
Palatal width at ant. root M^4	44.4	54.2	41.3	—
Palatal width at I^3	33.5	22.1	21.0	25.5
Palatal width at P^3	44.3	45.3	40.8	46
Max. width across premaxillary at narial opening	66.5	—	66.0	48
Max. length of nasals	134.0	—	—	93.9
Max. width across nasals at nasofrontal suture	68.0	—	—	—
Length of malar process	13.7	—	8.9	—
Elevation of ventral surface of foramen magnum above occlusal plane at M^4	55.9	—	—	—

TABLE 2
Measurements of Upper Incisors of *Sthenurus*

	I^1				I^2			I^3			
	L	AW	PW	Height of crown	L	Width	Height of crown	L	AW	PW	Height of crown
S. stirlingi											
SAM P22533	10.0	2.9	6.7	25.0	5.0	6.7	16.1	21.0	7.8	5.0	17.0
SAM P12882	9.2	—	7.8	14.9	3.8	7.5	12.7	—	—	9.6	24.9
AM 117496	8.0	8.2	8.2	—	4.8	9.4	—	18.3	12.4	8.2	—
AM 117495	—	—	—	—	7.0	7.7	21.2	20.2	7.4	2.4	23.5
S. tindalei											
AM 117493	9.0	3.4	5.7	18.8	4.4	5.6	11.5	27.2	5.4	1.5	13.4
AM 117491	8.7	2.8	6.1	9.8	4.7	6.0	9.5	14.5	8.6	3.5	14.1

L: length; AW: width anteriorly; PW: width posteriorly.

TABLE 3
Measurements of Upper Cheek Teeth of *Sthenurus*

	P^2			dP^3			P^3			M^1			M^2			M^3			M^4		
	L	AW	PW	L	AW	PW	L	AW	PW	L	AW	PW	L	AW	PW	L	AW	PW	L	AW	PW
S. stirlingi																					
SAM P22533	—	—	—	—	—	—	20.6	11.4	15.4	17.6	20.5	20.2	19.2	22.4	20.4	20.0	22.4	19.9	19.0	20.4	15.7
SAM P12882	—	—	—	—	—	—	19.6	11.4	14.7	14.7	18.6	19.5	18.8	20.9	20.2	20.3	20.1	18.6	19.0	18.2	15.9
AM 117496	—	—	—	—	—	—	—	—	—	—	—	—	19.5	—	—	20.3	—	—	18.1	—	—
AM 117495	12.6	8.9	12.4	15.8	15.5	17.2	20.8	11.0	15.2	19.6	19.2	19.3	21.8	19.6	18.3	22.2	20.0	—	21.0	17.5	15.7
S. tindalei																					
AM 117493	—	—	—	—	—	—	18.4	9.4	12.7	13.4	16.7	16.8	16.2	16.9	16.6	17.3	15.3	15.1	16.9	14.7	13.0
AM 117498	—	—	—	—	—	—	19.1	10.0	12.0	14.1	15.4	15.8	17.8	16.6	15.5	18.5	16.9	14.7	16.6	15.0	11.2
AM 117491	—	—	—	—	—	—	20.1	11.0	13.8	—	—	—	—	—	16.6	16.9	16.8	15.8	16.6	14.0	12.6

L: length; AW: width anteriorly; PW: width posteriorly.

TABLE 4
Measurements of Lower Cheek Teeth of *Sthenurus*

	P_3			M_1			M_2			M_3			M_4		
	L	AW	PW	L	AW	PW	L	AW	PW	L	AW	PW	L	AW	PW
S. stirlingi															
SAM P22533	18.2	8.0	10.9	15.5	15.5	15.5	18.3	17.5	17.5	18.7	18.2	17.9	18.0	17.8	14.2
SAM P12882	17.3	8.6	11.3	14.0	—	14.7	19.8	—	—	18.9	—	—	20.9	16.5	14.1
AM 117496	—	—	—	13.0	—	—	19.5	—	—	18.9	—	—	—	—	—
AM 117497	17.5	9.0	12.4	16.6	—	—	19.5	—	—	21.4	—	—	20.1	16.5	14.2
S. tindalei															
AM 117493	17.2	7.5	9.6	12.5	11.8	12.6	14.7	13.9	14.1	16.2	14.7	14.6	17.4	13.9	12.1
AM 117499	18.2	8.1	9.3	12.8	12.1	13.0	15.3	13.6	14.6	16.8	15.0	14.3	17.0	14.4	12.5
AM 117492	16.8	—	—	12.7	—	—	14.7	—	—	17.2	16.6	15.8	17.5	—	12.9

L: length; AW: width anteriorly; PW: width posteriorly.

TABLE 5
Comparative Measurements of Cheek Teeth of *S. andersoni*

Dimension	Marcus, 1962 $\bar{x}$	Marcus, 1962 O.R.	Callabonna P13673 Left	Callabonna P13673 Right	Dimension	Tedford, 1966 O.R.	Callabonna P13673 Left
P_3 length	15.09	14.4–16.3	14.2	14.2	P^3 length	14.6–15.9	15.35
Width anteriorly	6.44	6.2–7.0	5.4	5.4	Width anteriorly	7.3–8.2	7.35
Width posteriorly	7.03	6.6–7.6	—	7.2	Width posteriorly	9.4–10.4	8.80
M_1 length	11.80	11.4–11.9	9.2	9.0	M^1 length	11.0–11.4	10.3
Width protolophid	8.48	8.2–8.9	—	—	Width protoloph	10.7–11.2	10.7
Width hypolophid	8.74	8.5–8.9	8.6	8.6	Width metaloph	10.9–11.8	10.9
M_2 length	13.28	12.5–13.8	10.0	11.0	M^2 length	12.4–13.0	11.4
Width protolophid	9.94	9.6–10.2	9.5	—	Width protoloph	11.2–12.8	12.3
Width hypolophid	9.92	9.7–10.2			Width metaloph	11.0–12.8	12.35
M_3 length	13.80	12.6–14.3	11.0	—	M^3 length	13.1–13.6	13.1
Width protolophid	11.10	10.8–11.4	10.9	—	Width protoloph	11.2–13.0	12.35
Width hypolophid	10.70	10.5–11.2	—	—	Width metaloph	10.9–12.4	11.75
M_4 length	13.0	12.7–13.5	11.5	—	M^4 length	12.8–12.8	13.0
Width protolophid	10.95	10.6–11.3	—	—	Width protoloph	10.7–11.0	11.9
Width hypolophid	10.07	9.7–10.4	—	—	Width metaloph	9.5–9.8	10.2
Mandible at M_{2-3}							
Depth	27.70	26.4–30.3	29.6	28.0			
Width	14.42	13.0–15.4	16.5	15.4			

$\bar{x}$: Mean; O.R.: observed range.

TABLE 6
Measurements of Atlas and Axis Vertebrae of *Sthenurus*

Measurements	*S. stirlingi* SAM P22533	*S. stirlingi* AMNH 117496	*S. tindalei* AMNH 117493	*S. tindalei* AMNH 117499
Atlas				
Anteropost. length across neural arch at center line	22.7	20.5	19.2	—
Dorsoventral diam. neurapophyses to neural spine	40.5	30.5	36.0	—
Max. width across condylar articulation	61.8	51.5	52.8	—
Max. width across postzygapophyses	48.3	a41	45.3	—
Transverse width across diapophysis	120.3	a98	a87	—
Axis				
Length of odontoid process	11.8	8.6	9.2	—
Diam. of odontoid process	13.0	10.8	10.7	—
Max. width across prezygapophyses	49.4	40.4	42.5	—
Transverse diam. of centrum	30.0	24.4	25.0	—
Dorsoventral diam. of centrum	27.3	12.8	13.8	—
Anteropost. length of centrum	34.2	29.0	31	—
Max. diam. ventral surface centrum to dorsal neural crest	59.0	—	—	—
Max. anteropost. length neural crest	35.2	—	—	45.5
Max. width across postzygapophyses	a52	41.0	—	—
Max. width across transverse processes	a66	—	—	—

a: Approximate measurement.

TABLE 7
Measurements of Cervical Vertebrae of *Sthenurus*

Measurements	Cervical 3			Cervical 4			Cervical 5				Cervical 6				Cervical 7				
Specimens:	A	B	C	A	B	D	E	A	B	F	E	A	B	C	E	A	B	D	C
Anteropost. length centrum	17.1	14.7	19.3	13.0	14.2	9.1	11.2	12.7	14.2	15.3	11.1	16.2	14.6	18.5	11.9	15.3	16.5	12.1	18.0
Dorsoventral diam. centrum anteriorly	16.3	12.3	15.3	16.1	12.4	13.2	8.7	15.9	12.3	12.4	9.2	16.3	12.3	17.6	9.3	18.7	13.0	13.5	16.8
Dorsoventral diam. centrum posteriorly	16.6	13.0	15.4	16.8	12.7	13.4	9.5	16.8	12.5	13.2	9.9	17.7	13.0	16.0	10.4	17.3	13.0	15.0	18.2
Transverse diam. centrum anteriorly	31.9	24.3	28.0	33.2	25.0	25.5	17.2	30.8	23.8	26.4	19.0	30.8	24.5	31.8	19.5	35.1	26.4	30.7	32.3
Transverse diam. centrum posteriorly	33.6	26.2	29.3	33.3	25.5	25.5	19.8	35.0	25.8	26.0	19.3	34.3	28.4	—	20.0	36.5	29.7	32.1	32.7
Transverse diam. across postzygapophyses	56.1	43.1	a51	58.6	49.3	—	33.0	62.7	—	—	34.0	56.1	—	55.8	34.8	58.3	a43	a45	a57
Transverse diam. across pleurapophyses	89.4	a78	a69	91.6	a74	—	—	90.2	—	—	34.2	96.4	—	61.5	34.3	95.5	a80	—	—
Height neural spine above ventral surface of centrum	60.2	—	46.2	55.0	—	—	—	57.6	—	—	—	54.0	—		32.2	a50	—	—	—

Letters refer to the following taxa and specimens: *S. stirlingi:* A, SAM P22533; B, AMNH 117496; D, AMNH 117495. *S. tindalei:* C, AMNH 117499; F, AMNH 117491. *S. andersoni:* E, SAM P13763. a: Approximate measurement.

TABLE 8
Measurements of Thoracic Vertebrae of *Sthenurus*

	Thoracic 1				Thoracic 2			Thoracic 3		Thoracic 4				Thoracic 5		
Measurements Specimens:	A	B	E	F	A	B	E	A	E	A	C	D	E	B	C	D
Max. length of centrum	24.0	23.0	14.9	a22	27.9	22.9	17.0	24.5	17.5	26.5	18.4	26.4	19.0	27.7	19.8	25.3
Dorsoventral diam. centrum anteriorly	19.3	16.0	10.3	19.1	20.6	15.1	10.3	23.5	10.0	24.6	18.5	—	10.0	19.2	20.3	18.2
Transverse diam. centrum anteriorly	31.1	22.5	20.0	20.1	24.0	22.6	15.8	23.9	16.2	24.1	22.8	21.7	16.2	22.8	22.1	23.1
Dorsoventral diam. centrum posteriorly	21.2	17.3	10.2	21.0	23.2	17.7	10.0	24.5	10.1	25.7	20.4	27.4	10.4	23.2	22.2	18.8
Transverse diam. centrum posteriorly	31.4	30.0	21.2	34.7	34.0	34.7	21.2	37.8	a20	37.8	36.2	27.7	22.9	34.5	29.5	30.2
Transverse width across diapophyses	99.2	79.0	54.0	a90	76.0	69.0	—	73.4	—	69.0	46.2	a52	—	40.1	41.9	a40
Transverse width across postzygapophyses	37.5	31.5	25.9	43.5	33.6	—	—	38.5	—	29.6	25.0	—	—	a21	—	—
Ant. edge prezygapophyses to post. edge of postzygapophyses	35.0	29.8	21.0	35.8	34.8	—		38.5	—	40.4	27.0	28.0	—	36.7	—	—
Height neural spine above ventral surface of centrum	96.5	85.4	52.0	—	99.3	—	—	78.0	—	75.3	54.4	—	—	66.0	—	—

Letters refer to the following taxa and specimens: *S. stirlingi:* A, SAM P22533; B, AMNH 117496; C, AMNH 117495. *S. tindalei:* D, AMNH 117493; F, AMNH 117499. *S. andersoni:* E, SAM P13763.

TABLE 8—(*Extended*)

Measurements	Specimens:	Thoracic 5		Thoracic 6		Thoracic 7			Thoracic 8		Thoracic 10		Thoracic 11			Thoracic 12	Thoracic 13	
		E	F	D	F	D	E	F	D	E	F	D	A	C	D	D	D	F
Max. length of centrum		20.8	26.4	23.5	a29	25.5	22.4	28.0	26.3	26.3	30.0	29.0	31.8	26.9	31.3	33.2	35.0	35.2
Dorsoventral diam. centrum anteriorly		11.3	—	18.5	—	20.7	—	a27	22.5	15.9	27.3	23.2	—	27.2	25.0	25.5	28.3	33.2
Transverse diam. centrum anteriorly		16.3	25.8	22.2	—	23.2	—	a27	26.1	19.5	25.6	26.1	31.8	27.7	26.0	28.1	28.7	30.0
Dorsoventral diam. centrum posteriorly		11.9	26.6	19.4	26.6	22.5	—	28.3	23.7	16.4	30.0	24.5	—	29.7	25.5	28.8	31.7	36.2
Transverse diam. centrum posteriorly		24.0	a32	29.2	a35	30.0	—	35.4	35.2	30.0	a38	35.0	37.1	38.4	42.0	42.8	34.7	a36
Transverse width across diapophyses		—	—	38.7	—	36.5	—	a56	39.5	—	a52	43.1	—	46.5	48.4	53.0	51.0	—
Transverse width across postzygapophyses		—	a37	22.1	—	23.8	—	a28	26.1	—	a30	26.1	—	31.6	34.3	34.8	27.7	—
Ant. edge prezygapophyses to post. edge of postzygapophyses		—	—	32.7	—	40.3	—	—	43.6	—	—	43.6	—	40.0	40.5	47.2	56.1	—
Height neural spine above ventral surface of centrum		—	—	55.7	—	60.8	—	—	60.3	—	—	60.3	—	69.5	61.0	68.5	77.2	—

TABLE 9

Measurements of Lumbar Vertebrae of *Sthenurus*

	Lumbar 1		Lumbar 2			Lumbar 3		Lumbar 4				Lumbar 5		Lumber 6				
Measurements Specimens:	A	B	C	A	B	C	A	C	A	D	B	C	B	C	A	D	B	E
Max. length of centrum	42.8	40.5	31.0	45.0	43.8	35.0	44.1	38.0	53.6	50.1	46.7	36.5	42.2	38.9	51.3	42.0	39.6	43.2
Dorsoventral diam. centrum anteriorly	43.0	34.5	21.2	38.5	33.2	22.2	41.6	22.6	40.5	33.2	33.4	22.0	30.7	23.6	37.0	35.5	31.7	36.7
Transverse diam. centrum ant.	39.0	36.5	30.5	47.8	39.2	33.9	56.0	37.3	60.7	53.6	46.8	39.1	37.6	39.4	63.2	—	49.7	48.3
Dorsoventral diam. centrum posteriorly	41.5	36.3	21.9	42.9	33.3	21.9	41.1	21.3	37.5	31.4	31.5	23.0	33.1	23.4	39.7	36.0	33.7	37.9
Transverse diam. centrum post.	48.8	39.0	34.8	49.2	44.0	32.7	60.3	39.7	65.2	56.5	48.2	39.3	50.0	42.1	66.8	54.7	53.3	52.7
Transverse width across metapophyses	91.5	58.2	—	80.0	46.5	—	72.3	—	—	—	45.1	—	45.0	—	60.6	—	44.2	43.4
Transverse width across postzygapophyses	39.3	27.2	—	31.9	25.0	23.3	31.3	—	40.0	—	28.0	—	—	—	34.2	—	42.1	41.6
Transverse width across diapophyses	—	42.9	—	52.5	47.5	—	56.0	—	48.7	—	46.7	—	—	—	—	—	—	—
Height of neural spine above ventral surface of centrum	—	84.5	—	121.6	92.5	—	126.3	—	135.0	—	96.0	—	—	—	97.7	—	64.4	—

Letters refer to the following taxa and specimens: *S. stirlingi:* A, SAM P22533; D, AMNH 117496. *S. tindalei:* B, AMNH 117493; E, AMNH 117491. *S. andersoni:* C, SAM P13763.

TABLE 10
Measurements of Caudal Vertebrae of *Sthenurus*

	Caudal 1		Caudal 2			Caudal 3				Caudal 4	
Measurements Specimens:	A	B	A	B	C	A	D	B	C	A	D
Max. length of centrum	30.2	36.2	27.8	37.9	35.5	28.1	40.7	39.8	35.2	32.0	42.5
Dorsoventral diam. centrum anteriorly	20.9	28.8	19.2	30.2	—	19.9	30.9	25.6	25.4	19.7	30.0
Transverse diam. centrum anteriorly	22.6	35.0	24.9	36.0	—	23.5	40.2	35.5	31.6	23.0	37.9
Dorsoventral diam. centrum posteriorly	19.2	29.3	19.7	29.5	24.7	20.4	31.5	27.0	25.5	18.8	30.0
Transverse diam. centrum posteriorly	30.3	38.0	23.9	36.7	35.3	24.0	41.2	36.2	32.4	22.6	40.9
Transverse width across diapophyses	57.9	—	65.6	80	69	—	100	85.7	68.0	—	97
Transverse width across postzygapophyses	—	33.6	24.6	36.2	—	—	—	36.4	27	—	31.5
Ant. edge prezygapophyses to post. edge postzygapophyses	—	54.5	42.4	53.7	—	—	—	54.9	50.8	40.3	59.1

	Caudal 4		Caudal 5				Caudal 6			
Measurements Specimens:	B	C	A	D	B	C	A	D	B	E
Max. length of centrum	40.4	33.7	36.7	50.0	44.3	38.5	52.0	62.5	55.6	46.7
Dorsoventral diam. centrum anteriorly	27.6	25.0	19.6	30.0	26.8	22.6	18.6	30.4	27.2	25.0
Transverse diam. centrum anteriorly	34.7	30.0	24.1	36.0	35.0	30.0	23.2	37.3	35.5	30.9
Dorsoventral diam. centrum posteriorly	27.8	25.1	19.0	30.2	27.2	22.6	17.8	—	—	—
Transverse diam. centrum posteriorly	37.0	30.7	27.2	41.4	37.5	33.7	21.4	—	—	—
Transverse width across diapophyses	77	72.2	40.8	87	73.9	72.9	—	—	—	—
Transverse width across postzygapophyses	30.5	29	42.9	24.4	24.3	23	—	—	—	—
Ant. edge prezygapophyses to post. edge postzygapophyses	55.1	51.9	—	60.3	54.4	48.0	—	—	—	—

	Caudal 7			Caudal 8				Caudal 9			
Measurements Specimens:	A	D	B	C	A	D	B	A	D	C	F
Max. length of centrum	52.6	72.7	61	56.0	51.1	76.9	56	47.8	77.5	59.0	65.7
Dorsoventral diam. centrum anteriorly	17.9	30.9	28.2	24.5	17.2	31.5	—	15.7	33.3	—	27.2
Transverse diam. centrum anteriorly	21.7	41.9	36.3	33.0	—	40.8	—	17.9	43.3	—	34.6
Dorsoventral diam. centrum posteriorly	17.6	—	—	—	—	—	—	14.5	—	—	—
Transverse diam. centrum posteriorly	19.7	—	—	—	19.8	—	—	17.8	—	—	—

Letters refer to the following taxa and specimens: *S. andersoni:* A, SAM P13673. *S. stirlingi:* B, AMNH 117496; D, SAM P22533; E, AMNH 117495. *S. tindalei:* C, AMNH 117493; F, AMNH 117491.

TABLE 10—(*Continued*)

Measurements	Specimens:	Caudal 10 A	Caudal 10 D	Caudal 10 C	Caudal 11 A	Caudal 11 D	Caudal 11 E	Caudal 11 C	Caudal 12 A	Caudal 12 D	Caudal 12 C	Caudal 13 A	Caudal 13 D	Caudal 13 C
Max. length of centrum		44.4	76.8	59.0	40.3	69.3	52.4	57.8	35.2	65.0	56.5	29.8	58.3	53.5
Dorsoventral diam. centrum anteriorly		14.7	33.3	—	14.0	29.0	23.3	—	11.4	26.6	—	10.8	17.2	—
Transverse diam. centrum anteriorly		17.4	42.7	—	15.5	33.5	28.0	—	14.0	31.6	—	12.0	25.5	—
Dorsoventral diam. centrum posteriorly		13.8	—	—	12.7	—	—	—	10.9	—	—	—	—	—
Transverse diam. centrum posteriorly		16.0	—	—	—	—	—	—	13.0	—	—	11.0	—	—

TABLE 11
Measurements of Scapula, Humerus, and Radius of *Sthenurus*

Measurements	*S. stirlingi* SAM P22533	*S. stirlingi* AMNH 117497	*S. stirlingi* AMNH 117494	*S. tindalei* AMNH 117495	*S. tindalei* AMNH 117493	*S. andersoni* AMNH 117499	*S. andersoni* SAM P13673
Scapula							
Anteropost. diam. glenoid cavity	40.5	29.0	a42	21.4	28.7	38.0	19.5
Transverse diam. glenoid cavity	26.1	17.5	30.0	16.1	17.8	21.8	11.9
Anteropost. diam. from ant. edge coracoid process to post. border scapula above glenoid cavity	60.2	46.2	67.3	31.4	45.1	59.4	—
Anteropost. diam. from scapular notch to post. border scapula	44.2	33.5	—	26.0	29.3	39.9	—
Humerus							
Greatest length	256.5	194.5	—	—	184.0	238.0	151.8
Min. anteropost. diam. shaft	21.0	16.3	—	—	14.4	18.6	10.4
Min. transverse diam. shaft	23.0	16.7	—	—	15.0	19.4	10.5
Transverse diam. trochlea	46.5	39.5	45.0	—	34.1	52.0	24.1
Max. transverse diam. distal end	82.0	67.2	—	—	54.0	77.0	38.4
Min. anteropost. diam. trochlea	13.8	11.7	23.5	—	9.2	19.2	13.2
Head to distal pectoralis crest	142.0	116.8	—	—	90.0	131.5	79.0
Head to distal deltoid crest	113.3	88.4	—	—	73.5	102.7	56.5
Radius							
Max. length less distal epiphysis	273.0	—	—	205	—	—	176.6
Max. length with distal epiphysis	—	229.5	—	14.3	—	—	—
Anteropost. diam. shaft at midpoint	19.5	15.9	—	14.3	—	—	9.4
Transverse diam. shaft at midpoint	14.9	10.8	—	10.0	—	—	—

TABLE 12
Measurements of Ulna of *Sthenurus*

Measurements	*S. stirlingi*			*S. tindalei*		*S. andersoni*	
	SAM P22533	AMNH 117496	AMNH 117497	AMNH 117495	AMNH 117493	AMNH 117499	SAM P13673
Max. length less distal epiphysis	310.0	—	—	233.5	233.0	—	—
Max. length with distal epiphysis	323.5	264.5	—	—	—	278.5	200.0
Length of olecranon from coronoid process	63.4	41.0	48.9	38.0	39.7	42.8	28.0
Dorsoventral diam. post. end olecranon	22.3	15.3	17.7	16.5	15.9	15.4	12.0
Transverse diam. post. end olecranon	16.0	13.5	12.2	12.0	12.1	12.1	8.9
Dorsoventral diam. at semilunar notch	26.4	17.4	20.0	15.5	15.8	17.1	12.5
Transverse diam. across anconeal process	20.7	13.0	15.5	13.0	12.0	13.9	8.2
Transverse diam. across coronoid–radial facet	36.2	27.3	29.9	22.0	22.0	26.7	17.8
Dorsoventral diam. shaft distal to radial facet	27.9	18.8	21.1	19.5	18.5	18.5	13.0
Transverse diam. shaft distal to radial facet	14.5	11.0	11.1	11.0	11.3	12.3	7.9
Dorsoventral diam. shaft at midpoint	19.5	12.8	14.4	11.1	10.0	12.0	7.7
Transverse diam. shaft at midpoint	10.1	7.1	8.8	7.3	7.2	6.8	6.2
Dorsoventral diam. of styloid process	17.4	13.2	—	—	—	13.0	8.6

TABLE 13
Measurements of Metacarpals I-III of *Sthenurus*

Measurements	*S. stirlingi*				*S. tindalei*		*S. andersoni*
	SAM P22533	AMNH 117496	AMNH 117494	AMNH 117497	AMNH 117493	AMNH 117491	SAM P13673
Metacarpal I							
Maximum length	23.2	16.4	—	21.1	—	—	18.2
Dorsoventral diam. shaft prox. end	6.5	5.6	—	7.7	—	—	5.5
Transverse diam. shaft prox. end	6.9	5.3	—	7.7	—	—	4.3
Dorsoventral diam. shaft midshaft	6.3	4.2	—	5.5	—	—	—
Transverse diam. shaft midshaft	6.3	3.1	—	5.5	—	—	—
Dorsoventral diam. shaft distal end	6.0	5.2	—	7.7	—	—	—
Transverse diam. shaft distal end	7.5	6.7	—	7.7	—	—	—
Metacarpal II							
Maximum length	62.9	51.7	—	51.1	43.8	—	32.9
Dorsoventral diam. shaft prox. end	14.5	12.7	—	12.3	11.0	—	8.8
Transverse diam. shaft prox. end	12.0	10.6	—	10.0	9.5	—	6.7
Dorsoventral diam. shaft midshaft	11.4	9.4	—	9.0	7.5	—	5.9
Transverse diam. shaft midshaft	11.0	8.4	—	8.8	7.4	—	5.6
Dorsoventral diam. shaft distal end	12.0	10.8	—	11.1	8.4	—	7.2
Transverse diam. shaft distal end	16.5	14.7	—	14.4	12.4	—	8.7
Metacarpal III							
Maximum length	64.4	53.3	65.3	54.4	45.2	51.0	34.8
Dorsoventral diam. shaft prox. end	15.0	13.7	15.7	13.3	10.8	11.9	8.2
Transverse diam. shaft prox. end	13.5	11.5	13.7	12.2	10.8	11.8	7.0
Dorsoventral diam. shaft midshaft	11.2	9.2	10.6	10.0	8.2	7.6	8.0
Transverse diam. shaft midshaft	11.1	8.6	12.2	9.9	8.1	8.2	6.0
Dorsoventral diam. shaft distal end	12.1	10.5	13.0	10.0	8.4	9.5	—
Transverse diam. shaft distal end	16.8	15.1	18.3	15.5	11.5	14.3	9.4

TABLE 14
Measurements of Metacarpals IV and V of *Sthenurus*

Measurements	*S. stirlingi*				*S. tindalei*		
	SAM P22533	AMNH 117496	AMNH 117494	AMNH 117497	AMNH 117493	AMNH 117499	AMNH 117491
Metacarpal IV							
Maximum length	50.4	40.6	51.9	40.0	35.2	—	39.5
Dorsoventral diam. shaft prox. end	13.1	11.2	14.7	10.1	9.7	—	10.9
Transverse diam. shaft prox. end	11.6	9.3	12.9	10.1	9.2	—	9.8
Dorsoventral diam. shaft midshaft	8.9	7.4	9.1	7.7	6.8	—	6.7
Transverse diam. shaft midshaft	8.9	6.8	10.1	7.7	6.8	—	7.0
Dorsoventral diam. shaft distal end	10.2	9.5	11.4	10.0	8.0	—	9.2
Transverse diam. shaft distal end	14.3	12.2	14.5	12.0	10.0	—	11.5
Metacarpal V							
Maximum length	27.9	21.0	—	21.1	—	—	20.5
Dorsoventral diam. shaft prox. end	7.5	7.5	—	7.7	—	—	6.1
Transverse diam. shaft prox. end	8.8	6.2	—	6.7	—	—	5.5
Dorsoventral diam. shaft midshaft	4.8	4.5	—	5.6	—	—	4.1
Transverse diam. shaft midshaft	4.8	5.0	—	6.6	—	—	4.5
Dorsoventral diam. shaft distal end	8.0	6.1	—	6.6	—	—	6.1
Transverse diam. shift distal end	6.2	7.3	—	7.7	—	—	7.1

TABLE 15
Measurements of Phalanges of Digit III of the Manus of *Sthenurus*

Measurements	*S. stirlingi*				*S. tindalei*	
	SAM P22533	AMNH 117496	AMNH 117494	AMNH 117497	AMNH 117493	AMNH 117491
Proximal phalanx digit III						
Maximum length	35.4	29.0	41.2	27.7	28.0	29.7
Dorsoventral diam. prox. end	13.5	12.1	15.1	12.2	10.3	11.0
Transverse diam. prox. end	20.4	17.4	21.5	17.7	14.7	16.0
Dorsoventral diam. distal end	11.2	9.0	12.5	10.0	8.3	9.3
Transverse diam. distal end	16.7	13.0	17.3	14.4	12.3	13.5
Medial phalanx digit III						
Maximum length	29.6	24.0	—	24.4	—	24.0
Dorsoventral diam. prox. end	13.7	10.9	14.5	11.1	9.5	10.9
Transverse diam. prox. end	19.2	15.2	19.5	14.4	13.5	15.2
Dorsoventral diam. distal end	13.0	9.9	—	10.0	—	9.9
Transverse diam. distal end	16.1	12.2	—	13.3	—	12.5
Distal phalanx digit III						
Maximum length	67.2	—	70.0	65.6	53.3	—
Dorsoventral diam. prox. end	15.6	14.7	16.2	12.2	10.9	—
Transverse diam. prox. end	18.4	—	19.7	15.5	12.9	—

TABLE 16
Measurements of Phalanges of Digit IV of the Manus of *Sthenurus*

Measurements	*S. stirlingi* SAM P22533	AMNH 117496	AMNH 117494	AMNH 117497	*S. tindalei* AMNH 117493	AMNH 117491
Proximal phalanx digit IV						
Maximum length	30.3	24.1	34.4	23.3	27.8	25.3
Dorsoventral diam. prox. end	11.5	11.0	—	10.0	10.5	9.9
Transverse diam. prox. end	17.3	15.7	18.4	15.4	15.1	14.4
Dorsoventral diam. distal end	9.2	7.1	—	7.8	7.9	6.5
Transverse diam. distal end	14.0	10.8	—	11.1	11.2	10.2
Medial phalanx digit IV						
Max. length	24.0	18.7	25.6	18.8	—	18.8
Dorsoventral diam. prox. end	11.8	10.0	10.9	10.0	9.4	10.0
Transverse diam. prox. end	15.7	13.0	15.8	12.2	13.3	13.0
Dorsoventral diam. distal end	9.5	7.5	10.1	8.8	—	7.5
Transverse diam. distal end	13.2	10.0	14.3	10.1	—	10.0
Distal phalanx digit IV						
Maximum length	50.4	45.2	—	50.0	45.3	42.7
Dorsoventral diam. prox. end	12.5	10.1	14.3	10.0	10.7	10.3
Transverse diam. prox. end	14.8	12.0	16.0	12.2	12.5	12.9

TABLE 17
Measurements of Phalanges of Digit V of the Manus of *Sthenurus*

Measurements	*S. stirlingi* SAM P22533	AMNH 117496	AMNH 117494	AMNH 117497	*S. tindalei* AMNH 117491
Proximal phalanx digit B					
Maximum length	19.6	14.0	21.2	13.3	15.3
Dorsoventral diam. prox. end	7.7	6.3	9.5	6.6	6.6
Transverse diam. prox. end	11.1	8.8	12.0	8.8	8.5
Dorsoventral diam. distal end	5.7	4.2	6.6	4.4	4.3
Transverse diam. distal end	8.3	5.8	10.4	6.6	6.3
Medial phalanx digit V					
Maximum length	15.0	9.7	14.3	9.9	9.8
Dorsoventral diam. prox. end	7.2	5.4	8.6	5.5	—
Transverse diam. prox. end	8.7	6.6	10.0	6.6	—
Dorsoventral diam. distal end	5.7	4.7	6.8	5.5	—
Transverse diam. distal end	8.5	6.0	7.7	6.7	—
Distal phalanx digit V					
Maximum length	21.3	16.1	22.7	21.1	—
Dorsoventral diam. prox. end	6.9	6.3	10.0	6.7	—
Transverse diam. prox. end	8.0	6.1	8.8	6.0	—

TABLE 18
Measurements of Pelvis of *Sthenurus*

Measurements	*S. stirlingi*				*S. tindalei*	
	SAM P22533	AMNH 117496	AMNH 117497	AMNH 117495	AMNH 117493	AMNH 117499
Length ant. end ilium to post. border ischium	410.1	—	352.0	280.5	a287	350.0
Greatest depth ilium	56.0	54.9	60.6	44.2	50.3	53.1
Length ant. edge acetabulum to ant. end ilium	237.5	—	203.0	152.0	a153	183.0
Length ant. edge acetabulum to post. border ischium	178.4	144.6	158.0	a140	146.2	172.8
Diam. of acetabulum measured at right angles to long axis of acetabular fossa	61.5	55.3	45.3	63.4	57.0	58.7
Long diam. of obturator foramen	100.2	77.4	91.0	—	71.6	86.8
Greatest diam. of obturator normal to long diam.	70.8	—	45.5	—	61.4	68.8
Length of pubic symphysis	85.0	a65	82.5	—	86.4	—
Lateromedial length of ilium at distal end	83.7	—	67.7	55.0	a47	65.8

a: Approximate measurement.

TABLE 19
Measurements of Femur, Tibia, and Fibula of *Sthenurus*

Measurements	*S. andersoni*	*S. stirlingi*					*S. tindalei*		
	SAM P13673	SAM P22533	AMNH 117496	AMNH 117497	AMNH 117494	SAM P13940	AMNH 117495	AMNH 117493	AMNH 117499
Femur									
Length greater trochanter to lateral condyle	235.8	347.0	296.5	296.0	—	325.0	228.5	—	319.0
Length head to medial condyle	217.5	283.0	261.0	261.0	—	277.0	238.0	—	281.0
Greatest diam. of head	31.0	47.2	44.7	45.6	—	43.7	47.8	—	50.5
Anteropost. diam. shaft at adductor tubercle	29.7	42.1	36.5	42.2	—	40.9	34.8	35.3	37.8
Trans. diam. shaft at adductor tubercle	29.0	42.1	38.8	39.5	—	43.8	33.4	37.4	39.8
Anteropost. diam. medial condyle	47.7	77.7	69.3	69.5	—	76.1	63.1	64.3	72.4
Trans. width medial condyle	23.8	37.8	33.0	33.4	—	39.4	30.0	31.8	35.5
Anteropost. diam. lateral condyle	53.1	83.8	78.0	77.7	82.5	84.3	63.0	75.2	81.0
Trans. width lateral condyle	23.8	39.1	34.0	37.7	37.5	38.5	30.0	35.0	34.3
Trans. condylar width	53.5	88.9	78.2	76.7	—	83.9	74.6	77.1	81.0
Tibia									
Length intercondyloid eminence to ant. border astragalus facet	418.0	590.0	521.0	517.0	—	550.0	412	478.0	494
Trans. diam. prox. end	52.4	91.2	80.5	80.0	—	84.6	56.6	77.8	82.7
Anteropost. diam. midshaft	21.0	33.4	36.0	30.2	—	36.5	24.6	27.2	34.0
Trans. diam. midshaft	23.6	35.0	31.0	29.5	—	34.6	24.9	27.8	31.5
Anteropost. diam. distal end	27.5	49.9	35.9	37.8	—	41.0	38.1	37.1	—
Trans. diam. distal end	32.0	53.0	45.0	45.6	—	47.0	46.1	46.2	—
Fibula									
Max. length	—	558.0	—	504.0	—	—	—	—	—
Anteropost. length of tibial groove prox. end	—	37.1	35.0	33.4	36.9	—	—	32.5	—
Transverse diam. prox. end	—	31.4	28.2	31.2	30.7	—	—	23.0	—
Anteropost. diam. distal end	—	27.7	24.0	23.2	28.5	24.6	23.0	—	27.5
Transverse diam. distal end	—	14.7	14.0	14.5	14.9	13.0	12.7	—	13.8

TABLE 20
Measurements of Tarsals of *Sthenurus*

Measurements	*S. stirlingi*							*S. tindalei*			*S. andersoni*
	SAM P13937	SAM P13938	SAM P22533	AMNH 117496	AMNH 117494	AMNH 117495	AMNH 117497	AMNH 117493	AMNH 117499	AMNH 117491	SAM P13673
Astragalus											
Greatest length	43.0	44.5	45.0	43.1	45.9	42.7	39.0	42.7	—	40.5	28.6
Greatest width	51.0	47.0	52.5	48.9	52.7	44.4	48.2	45.7	—	47.4	29.0
Greatest length head	38.8	39.7	42.0	43.2	43.1	37.1	35.3	38.6	—	37.8	—
Greatest width of head measured perpendicular to line of greatest length	39.0	38.0	36.0	38.2	40.0	38.7	39.2	32.1	—	32.2	—
Calcaneum											
Greatest length	89.1	89.4	94.4	85.0	97.5	71.5	87.2	87.8	91.6	91.3	65.6
Greatest width from sustenaculum to lateral process	41.0	42.5	44.1	40.3	44.6	40.8	45.0	39.6	47.3	40.8	—
Greatest width across cuboid facet	31.5	34.0	33.5	34.5	38.3	31.4	34.4	32.0	34.1	30.9	—
Dorsoventral diam. neck immediately post. to sustenaculum	32.5	32.2	35.5	31.2	35.8	33.3	31.8	31.7	33.8	35.5	—
Trans. diam. neck immediately post. to sustenaculum	20.0	19.2	19.1	19.4	21.2	17.5	19.7	17.5	20.9	19.1	—
Trans. diam. posterior border	38.8	39.8	42.0	38.9	42.1	26.5	35.5	34.0	39.1	38.5	23.5
Dorsoventral diam. post. border	35.4	35.2	39.4	36.6	38.0	31.0	36.1	31.7	36.9	32.0	21.7
Cuboid											
Greatest length	19.0	19.9	22.4	21.1	22.0	18.6	19.8	18.8	23.1	20.2	10.7
Greatest transverse diam.	36.6	37.0	39.0	37.7	42.2	37.0	37.6	37.5	41.1	34.6	26.7
Greatest dorsoventral diam. at ant. border	38.4	38.4	37.0	35.7	38.9	32.9	36.0	34.5	39.9	34.5	25.4
Navicular											
Anteropost. length	16.4	—	16.3	13.8	16.9	12.5	14.2	15.0	—	—	11.5
Greatest trans. diam.	11.0	—	12.0	11.3	12.7	10.0	11.5	10.3	—	—	—
Dorsoventral diam.	23.5	—	26.8	24.2	27.0	22.2	24.2	23.4	—	—	18.5
Ectocuneiform											
Anteroposterior length	—	—	19.2	17.9	19.6	17.9	17.0	19.6	20.2	—	—
Greatest dorsoventral diam.	—	—	34.4	31.2	31.9	27.8	31.9	28.1	31.3	—	—

TABLE 21
Measurements of Metatarsals of *Sthenurus*

Measurements	*S. andersoni*	*S. stirlingi*								*S. tindalei*	
	SAM P13673	SAM P13937	SAM P13938	SAM P13939	SAM P22533	AMNH 117496	AMNH 117494	AMNH 117495	AMNH 117497	AMNH 117493	AMNH 117491
Metatarsal III											
Greatest dorsoventral diam. prox. end	—	—	—	—	14.7	—	13.9	13.0	12.6	—	—
Transverse diam. prox. end	—	—	—	—	7.0	—	6.9	5.8	6.8	—	—
Metatarsal IV											
Greatest length	133.3	177.5	180.0	167.3	179.3	167.0	188.4	163.5	165.0	157.0	168.1
Dorsoventral diam. prox. end	22.2	33.5	35.0	32.0	38.5	33.8	36.9	33.4	32.4	34.3	34.0
Transverse diam. prox. end	24.0	—	32.0	32.2	36.4	35.3	36.9	38.4	34.0	30.5	32.2
Dorsoventral diam. distal end	18.4	27.9	27.3	25.8	29.4	24.6	29.2	25.3	26.0	26.3	26.6
Transverse diam. distal end	28.0	39.2	38.9	37.2	39.2	36.3	42.8	35.9	35.5	36.2	37.1
Metatarsal V											
Greatest length	94.2	80	—	—	132.5	81	109	79	111.7	—	—
Dorsoventral diam. prox. end	14.3	16.7	17.1	—	19.5	17.7	18.9	24.6	14.1	16.3	16.4
Transverse diam. prox. end	7.5	16.0	16.1	—	16.8	14.7	18.3	15.0	15.8	17.3	16.6
Dorsoventral diam. distal end	2.7	—	—	—	5.2	—	5.4	—	2.5	—	—
Transverse diam. distal end	3.1	—	—	—	5.0	4.4	—	—	1.7	—	—

TABLE 22

Measurements of Phalanges of Metatarsal IV of *Sthenurus*

Measurements	*S. andersoni*	*S. stirlingi*						*S. tindalei*		
	SAM P13673	SAM P13937	SAM P13938	SAM P22533	AMNH 117496	AMNH 117494	AMNH 117497	AMNH 117493	AMNH 117499	AMNH 117491
Proximal phalanx										
Greatest length	44.0	57.5	57.1	62.5	56.3	66.8	57.8	54.0	59.3	59.0
Dorsoventral diam. prox. end	17.5	23.4	23.7	25.5	22.5	25.7	22.1	22.5	23.3	24.8
Transverse diam. prox. end	27.2	35.5	37.6	40.0	35.0	42.6	34.1	36.6	39.7	38.1
Dorsoventral diam. distal end	12.3	17.0	17.4	19.6	16.4	19.3	17.6	17.6	18.5	17.7
Transverse diam. distal end	24.6	35.5	35.2	35.6	32.6	38.9	32.8	34.8	36.1	33.3
Median phalanx										
Greatest length	38.0	52.6	52.5	57.2	51.4	58.0	52.0	52.6	—	—
Dorsoventral diam. prox. end	16.0	21.7	21.9	24.1	21.7	23.2	21.5	19.4	—	—
Transverse diam. prox. end	26.2	34.7	36.7	38.3	36.6	38.4	34.4	34.2	—	—
Dorsoventral diam. distal end	12.2	16.4	17.6	20.4	17.5	20.0	18.8	15.0	—	—
Transverse diam. distal end	18.0	27.4	28.4	29.8	26.1	30.0	26.3	27.2	—	—
Distal phalanx										
Greatest length	32.7	47.6	46.3	47.2	42.8	49.1	45.5	42.6	45.3	48.4
Dorsoventral diam. prox.	28.7	22.7	23.1	23.4	21.5	25.9	23.5	20.0	22.4	23.2
Transverse diam. prox.	17.4	25.4	24.6	25.1	24.2	28.0	23.7	21.2	24.7	26.9

TABLE 23

Sthenurus Species from Lake Callabonna Ranked According to Sex and Dental Age

	Sex	P2	P3	M1	M2	M3	M4
S. stirlingi							
AMNH 117498	M	–	–	L+	L+	L	L
AMNH 117494	M	–	–				
SAM P12882	M	–	IV	L+	L+	L	L
SAM P22533	M	–	II	M	E	B	U
AMNH 117495	?M	III	–	B	U	U	U
AMNH 117496	F	–	IV	L+	L+	L	L
AMNH 117497	F	–	III	L	M	M	E
S. tindalei							
AMNH 117491	M	–	IV	L+	L+	L	M
AMNH 117499	M	–	III	L+	L+	L	M
AMNH 117493	F	–	II	L	M	E	U
AMNH 117492	F	–	II	L	M	E	U
S. andersoni							
SAM P13673	?	–	IV	L+	L+	L	L

TABLE 24

Differences in Mean Head, Foreleg, and Hind Leg Lengths for Male and Female _M. giganteus_ of Known Age Expressed as a Percentage of Male Parameter (After Poole et al., 1984) Along with the Molar Indexes (M.I.; After Kirkpatrick, 1964)

Age		Head			Foreleg			Hind leg		
(months)	M.I.	Male	Female	%	Male	Female	%	Male	Female	%
15	0.65	152.2	143.3	5.85	161.2	146.1	9.37	396.0	371.4	6.21
18	0.90	163.1	152.0	6.8	178.2	157.4	11.67	429.1	395.9	7.74
21	1.14	171.3	158.4	7.5	191.4	165.9	13.32	454.3	414.2	8.83
24	1.39	177.6	163.4	8.0	201.9	172.6	14.51	474.0	428.5	9.60
30	1.88	186.9	170.6	8.72	217.4	182.4	16.10	502.9	449.1	10.7
36	2.37	193.3	175.5	9.21	228.3	189.2	17.13	523.1	463.4	11.4

TABLE 25

Summary of Molar Morphology in Macropodinae (from Sanson, 1980) Along with the Character States Found in the Callabonna Sthenurines.

Character	*Wallabia, Dorsopsis, Dendrolagus, Thylogale, Setonix*	*Macropus, Megaleia*	*S. stirlingi*	*S. tindalei*	*S. andersoni*
Broad dietary preference	Browse	Graze			
Link structure	Weak	Strong	Weak	Weak	Absent
Striae pattern on links	Longitudinal when present	Transverse	Transverse	Longitudinal	Longitudinal
Wear on midlinks	Midlink enamel rarely breeched	Midlink enamel breeched in worn condition	Would be breeched only in old individuals	Breeched only in old animals	Breeched only in old individuals
P^3 development	Well developed	Reduced or vestigial	Well developed	Well developed	Well developed
P^3 permanency	Retained throughout life	P^3 often or always lost	Retained in adult	Retained in adult	Retained in adult
Striae pattern on lophs	Longitudinal only	Longitudinal with superimposed transverse on upper lingual and lower labial margins	Longitudinal only	Longitudinal	Longitudinal
Dentine–enamel boundaries	Indicate longitudinal movement only	Longitudinal and transverse movement	Longitudinal only	Longitudinal	Longitudinal
Anterior cingulum	Narrow	Broad	Narrow on anterior teeth	Narrow on anterior teeth	Narrow on anterior teeth
Number of teeth in occlusion in adult	Whole tooth row	Restricted to a few teeth at a time	Whole tooth row, but more wear on anterior teeth	Whole tooth row but more wear on anterior teeth	Whole tooth row but more wear on anterior teeth
Plane along oclusal surface of lower cheek teeth	Flat	Curved (in a reverse curve of Spee)	Slightly curved (in a reverse curve of Spee)	Slightly curved (in a reverse curve of Spee)	Slightly curved (in a reverse curve of Spee)
Molar progression	None	Some to rapid	None	None	None

TABLE 26

Comparison of Skeletal Proportions of Extant Macropodines and Callabonna Sthenurines

		Proportions of skeletal elements expressed as percentage of total length of each assemblage													
		Vertebral column					Forelimb and girdle				Hind limb and girdle				
	N	Cervical	Thoracic	Lumbar	Sacral	Caudal	Scapula	Humerus	Radius ulna	Manus	Ilium	Ischio pubis	Femur	Tibia	Pes
Dendrolagus lumholtzi	1	6	16	13	3	62	20	28	33	19	16	10	24	27	22
Macropus rufus	2	8	18	13	3	58	19	28	39	15	12	9	17	41	22
		8	18	14	4	57	18	24	42	16	11	9	17	39	24
Macropus giganteus	2	8	16	15	3	59	18	29	35	19	13	10	19	35	24
		9	19	13	3	56	20	27	37	16	13	9	17	38	22
Sthenurus stirlingi	1	8	20	15	4	53	18	27	32	24	14	11	17	36	22
Sthenurus tindalei	1	7	19	15	4	54	18	25	33	23	11	11	19	25	24

TABLE 27
Ratios of Skeletal Proportions of Extant Macropodines and Callabonna Sthenurines

	Forelimb/ vert. column	Hind limb/ vert. column	Humerus/ulna	Femur/tibia	Forelimb/ hind limb
Dendrolagus lumholtzi	0.29	0.45	0.86	0.89	0.70
Macropus rufus	0.40	0.74	0.72	0.43	0.57
	0.31		0.56		0.42
Macropus giganteus	0.32	0.64	0.83	0.54	0.57
	0.38	0.67	0.72	0.45	0.52
Sthenurus stirlingi	0.41	1.18	0.86	0.48	0.38
Sthenurus tindalei	0.36	1.12	0.76	0.55	0.33

APPENDIX

FOSSIL VERTEBRATE LOCALITIES AT LAKE CALLABONNA

The following information on fossil vertebrate localities at Lake Callabonna is brought together to aid future investigations in that area. Where accurate information is available, these sites are plotted on the geological map (fig. 2); other sites can only be approximately located.

John Ragless, 1885: Mr. John Ragless, lessee of Callabonna Station, sent "some teeth and portions of the lower jaw" of *Diprotodon* to the South Australian Museum 8 years before the major work on the station by the Museum. These remains were found by his son, Mr. Frederick B. Ragless, "in a watercourse at a depth of five feet, about two miles east of the margin of Lake Callabonna and about twelve miles northeast of the place" where the 1893 discoveries were made (Stirling, 1894: 186). These directions place the site on the lower reaches of Callabonna Creek at approximately grid coordinate 312325, Callabonna 1:250,000 sheet.

South Australian Museum, 1893: Two principal sites were worked. The first site was exploited by Mr. Henry Hurst and his brother George and coworkers on behalf of the South Australian Museum from February to mid-August. Reports and photographs by the collectors are on file in the South Australian Museum. The Government Geologist, H. Y. L. Brown, described the work at the time of his visit (June 1893) and his report and some of his photographs were printed in 1894. This site is essentially the same as SIAM site 1, as established by identification of the 1893 photographs in the field. In August 1893 A. H. C. Zietz took over the work on behalf of the South Australian Museum and remained in the field until November. He shifted the collecting to near the expedition camp site, which has been established by contemporary photographs and the discovery of camp litter (in 1953) 0.75 mile farther south as indicated on figure 2. The available records do not allow allocation of specific remains to each site, but together these sites yielded *Genyornis newtoni* (holotype specimen), *Diprotodon australis, D.* cf. *minor, Phascolonus gigas, Macropus* cf. *titan, Sthenurus andersoni,* and *S. stirlingi.* Stirling (1894: 209) reported that "at least 100 distinct animals" representing *Diprotodon* species were obtained.

Two other sites were discovered in the course of the 1893 work, but, as far as is known, no material was collected there. One of these lies 8 miles northwest of the site worked by the Hursts (Brown, 1894) "at the springs lying in the lake bed" (Stirling, 1894: 207); the other lay 3 miles northwest of the Hursts' locality (Brown, 1894). Stirling (1894: 207) further reported that bones "were observed on the surface in a very weathered condition all along the track" connecting these outlying sites. The SIAM work corroborates these observations.

Australian Museum, 1946: Mr. Harold O. Fletcher, Curator Emeritus of Fossils at the Australian Museum, visited Lake Callabonna in the company of Mr. Frank Forster, Stock Inspector of Tibooburra (New South Wales), and Mr. George Alder of Waka Station near Broken Hill (New South Wales) who had knowledge of the bone occurrence. Mr. Alder led the party to the vicinity of the mound springs in "the centre of the lake," 5 miles from the shore (Fletcher, 1948). As described, this site would correspond to the western chain of springs in figure 2 in the vicinity of which the 1893 and SIAM expeditions also observed *Diprotodon* skeletons. The Australian Museum party apparently only collected a few bones of *Diprotodon.*

University of California–South Australian Museum, 1953: An effort to relocate the fossil sites of the 1893 expedition led to success in late May and June 1953 by a party consisting of R. A. Stirton, R. H. Tedford (University of California), P. Lawson (South Australian Museum), and G. D. Woodard (University of Adelaide). This group relocated the camp site of 1893 and collected *Diprotodon* remains from near the camp and in the flats 0.75 mile north of camp (i.e., at the two 1893 sites). Stirton (1954) wrote a popular account of this work. Three partial skeletons of *Diprotodon* and remains of eight other individuals were collected. An upper molar of a small macropodid and fragments of other, but unidentifiable, taxa were obtained. Photographs

and field notes by R. A. Stirton and R. H. Tedford are available at UCMP.

Smithsonian Institution–American Museum of Natural History–South Australian Museum, 1970 (acronym: SIAM): The party consisted of C. Ray and F. Pearce (Smithsonian), R. Tedford and R. Emry (AMNH), and N. Pledge and P. Lawson (South Australian Museum). A documentary motion picture of part of the expedition work was made by the Film Unit of the office of the Premier of South Australia (copy on file at AMNH). The following sites were worked from 5 July through 15 September, 1970:

1) Lake Callabonna, site 1, grid coord. 3112–3085, lat. 29°50′S, long. 140°10′E. Southern portion of lake floor; localities excavated on low samphire-covered rises in middle of central channel carrying water from southeast portion of lake northward; active springs 100 yd to SE; 6 mi SW of deserted Callabonna homestead. This is essentially the same site worked by the Hurst party in 1893 and exactly the same as one worked by the University of California–South Australian Museum, 1953.

Geology: Excavations reveal 2 ft of superficial sand (Holocene) disconformably overlying laminated clays 2.5 ft thick (fig. 3) that contain fossil vertebrate, plant, and invertebrate remains resting on more than 2 ft of interbedded sand and clay (Millyera Formation, Pleistocene). Measured section: R. Tedford, field notes, 20 July 1970.

Fossils: Three partial skeletons of *Diprotodon* and isolated bones of a medium-sized macropodid were obtained.

2) Lake Callabonna, site 2, grid coord. 3115–3090, lat. 29°50′S, long. 140°10′E. Southern portion of lake floor; northeast edge of central island overlooking channel containing site 1; 6.25 mi SW of deserted Callabonna homestead.

Geology: Green-gray and brown clayey fine sand with gypsum rosettes and thin travertine lenses of Holocene deposits overlying Eurinilla Formation (fig. 3). Base 21 ft above floor of adjacent present-day channel. White sand lenses at base contain bird bones; eggshell in situ (Holocene, C-14: 2000–2300 yr BP). Measured section: R. Tedford, field notes, 17 July 1970.

Fossils: Four cormorant (*Phalacocorax*) partial skeletons, various bird bones, partial eggs, eggshell fragments, guano, fish spines, and otoliths from upper level.

3) Lake Callabonna, site 3, grid coord. 3105–3090, lat. 29°50′S, long. 140°10′E. Southern portion of lake floor, western tip of prominent low bluff overlooking northern end of present-day channel containing site 1, 6 mi SW of deserted Callabonna homestead.

Geology: Fossil vertebrates from green-gray laminated clays above and below layer of large selenite crystals, lower 4 ft of bluff (fig. 3). *Diprotodon* skeletal material from various levels in this interval (Millyera Formation, Pleistocene). Measured section: R. Tedford, field notes, 13 July 1970.

Fossils: Parts of four *Diprotodon* skeletons, one (SIAM 12) from above selenite layer.

4) Lake Callabonna, site 4, grid coord. 3090–3155, lat. 29°45′S, long. 140°9′E. Southern portion of lake, 4 mi N of sites 1–3, on deflated lake floor, 6.5 mi WNW of deserted Callabonna homestead.

Geology: Fossil vertebrates from Millyera Formation laminated green-gray, blue, and ochrous claystones with fine sand partings, up to 4 ft thick overlain by widespread selenite unit and underlain by 3–4 ft laminated fine sands that in turn rest on black claystones of Namba Formation (Millyera Formation, C-14: 39,900 yr BP).

Fossils: This site produced a diverse fauna, including partial skeletons of *Diprotodon,* remains of six individuals (one of which, SIAM 63, represents the small morph "*D.* cf. *minor*"); *Phascolonus,* five individuals; *Sthenurus tindalei,* four individuals; *S. stirlingi,* six individuals; *Dromaius,* three individuals; *Geryornis,* six individuals, plus charophytes, pollen, and macroplant material, beetle wing cases, molluscs, and ostracods.

Five additional sites where vertebrate remains were exposed at the lake surface were noticed during reconnaissance in 1970. No collections were made at these sites, but they are recorded here to stimulate future investigation (see fig. 2):

5) Lake Callabonna, site A, grid coord. 3112–3100, 0.75 mi N of SIAM site 3, *Diprotodon* partial skeletons exposed on lake floor. R. Tedford, field notes, 27 July 1970.

6) Lake Callabonna, site B, grid coord.

3072–3165, 1.3 mi NW of SIAM site 4, scattered skeletal remains exposed on lake floor, including those of *Diprotodon, Protemnodon, Sthenurus, Genyornis,* and a smaller bird. R. Tedford, field notes, 7 July 1970.

7) Lake Callabonna, site C, grid coord. 3060–3170, 2.1 mi NW of SIAM site 4, trackway site (Tedford, 1973), *Diprotodon* and macropodid(?) trackways in marl below the selenite unit, a few scattered skeletons of *Diprotodon.* R. Tedford, field notes, 9–10 July and 15 September 1970.

8) Lake Callabonna, site D, grid coord. 3034–3167, 3.3 mi WNW of SIAM site 4, articulated *Diprotodon* skeletons scattered over several acres of lake floor, a few bones of large macropodids seen but no skeletons. R. Tedford, field notes, 8 July 1970.

9) Lake Callabonna, site E, grid coord. 3007–3187, 5.1 mi NW of SIAM site 4, exposures of 21–24 ft of Millyera Formation in valley west of southernmost moundspring group shown on Callabonna 4-mi sheet. Section includes green-gray clays with thin marls below selenite bench-forming unit and green-gray laminated clays above selenite, all intruded by artesian springs including extinct and active systems. *Diprotodon* remains noted below selenite; a more diverse fauna above selenite in flats immediately west of mound spring including *Diprotodon, Phascolonus, Macropus, Sthenurus,* small macropodid, and *Genyornis.* R. Tedford, field notes, 8 July 1970.

Museum of Victoria, 1983: T. Rich and party from the Museum of Victoria, Monash University, and the Australian Museum (Sydney) assisted by a unit of Royal Australian Electrical and Mechanical Engineers, Australian Army, spent 8 days at SIAM site 4, collecting four partial *Diprotodon* skeletons selected from 30 individuals exposed on the lake floor. They failed to find remains of the other taxa collected at this site by the SIAM party in 1970. Two other sites near SIAM site 1 were located and a partial *Diprotodon* skeleton was collected from one of these (RAEME site 1). A documentary motion picture of this work was made by Channel 10 (Melbourne). T. Rich and P. Rich, field notes, 12–29 September 1983.